Development of medial coronoid disease in Labrador retrievers: Diagnostic and pathogenic studies

Seng Fong Lau

Development of medial coronoid disease in Labrador retrievers: Diagnostic and pathogenic studies
Seng Fong Lau
PhD thesis, Utrecht University, The Netherlands

ISBN: 978-90-393-5962-4

Cover: K.F. Siew
Layout and printing: K.F. Siew and Creo Creation

Correspondence and reprint requests: lausengfong@hotmail.com

Development of medial coronoid disease in Labrador retrievers: Diagnostic and pathogenic studies

Ontwikkeling van het afwijkend mediaal coronoïd bij Labrador retrievers: Diagnostische en pathogenetische studies
(met een samenvatting in het Nederlands)

Perkembangan penyakit medial koronoid dalam baka Labrador retrievers: Kajian diagnostik dan patogenik
(Ringkasan dalam Bahasa Malaysia)

Proefschrift

ter verkrijging van de graad van doctor aan de Universiteit Utrecht
op gezag van de rector magnificus, prof. dr. G.J. van der Zwaan,
ingevolge het besluit van het college voor promoties
in het openbaar te verdedigen op
maandag 28 oktober 2013
des middags te 4.15 uur

door
Seng Fong Lau
geboren op 22 december 1979 te Sarikei, Maleisië

Promotoren: Prof. dr. G.Voorhout
Prof. dr. H.A.W. Hazewinkel

Co-promotoren: Dr. C.F. Wolschrijn
Dr. M.A. Tryfonidou

Financial support by Malaysia Ministry of Higher Education (MOHE), Universiti Putra Malaysia (UPM) and Boehringer Ingelheim for the publication of this thesis is gratefully acknowledged.

Table of contents

Chapter 1

Aims and scope of the thesis

Introduction

Disease of the medial coronoid process of the canine elbow joint was first reported in 1974 as a developmental skeletal disease causing forelimb lameness in dogs (Tirgari, 1974). Medial coronoid disease was initially described as ununited coronoid process, and in later years as fragmented medial coronoid process (Henry, 1984). In this thesis, the term medial coronoid disease is used, since this term encompasses pathological change of both the articular cartilage and the subchondral bone of the medial coronoid process (Moores et al., 2008; Fitzpatrick et al., 2009). The Labrador retriever was chosen as representative dog breed because of its popularity as companion and working dog, and because the breed is susceptible to medial coronoid disease, with the incidence of medial coronoid disease being as high as 50% in dogs presented with forelimb lameness (Ubbink et al., 1998; Fitzpatrick et al., 2009).

Aims and scope of the thesis

Labrador retrievers referred to the Utrecht University Clinic of Companion Animals between 2008 and 2012 with forelimb lameness and three litters of purpose-bred Labrador retrievers originating from a medial coronoid disease (MCD)-affected dam and two MCD-affected sires were studied in order to;

1. Investigate breed-specific features of advanced and incipient MCD on radiography, computed tomography, and surgical/necropsy examination.

2. Elucidate the pathogenesis of the disease in order to provide foundation for the interpretation of the molecular genetic studies performed by others, with a view to improve disease diagnosis.

The general introduction of this thesis **(Chapter 2)** provides an overview of different aspects of MCD, such as disease background, postnatal development of the normal elbow joint, gross and functional anatomy of the normal elbow joint, suggested disease etiopathogeneses, and techniques used to investigate and diagnose the disease. The study reported in **Chapter 3** investigated the breed-specific diagnostic and surgical features of MCD in 31 Labrador retrievers grouped by age at first complaint of lameness (≤12 months and >12 months) that had been referred to the University Clinic for Companion Animals at Utrecht University from 2008 until early 2012. In the same study, sclerotic lesions of

the ulna from MCD-affected dogs were investigated and quantitatively measured by means of computed tomography (CT). In the study described in **Chapter 4**, the development of MCD was studied in purpose-bred Labrador retrievers, to establish the earliest age at which MCD develops and to identify radiographic or CT features of incipient MCD. It was also attempted to investigate whether ulnar subtrochlear sclerosis is a primary cause or a secondary consequence of MCD. The study described in **Chapter 5** investigated the potential of the collagenase-generated biomarker of osteoarthritis, Col2-3/4$C_{long\ mono,}$ in plasma and synovial fluid as a marker of incipient MCD. In the study described in **Chapter 6**, changes in articular cartilage and subchondral bone of the medial coronoid process (MCP) in growing Labrador retrievers with incipient MCD were investigated by using equilibrium partitioning of an ionic contrast agent with micro-CT (EPIC-microCT). In the study reported in **Chapter 7**, radiographic images were taken every fortnight from the age 6–7 weeks until 16–17 weeks in MCD-prone Labrador retrievers, to investigate whether limb angulation and disparity have a role in MCD development. The aim of the studies described in **Chapter 8** was to investigate early micro-morphological changes in the MCP of young Labrador retrievers with or without MCD, in an attempt to elucidate the pathogenesis of MCD in the Labrador retrievers. In the same chapter, the reorganization of articular cartilage and subchondral bone was studied in Labrador retrievers before MCD developed. The findings and results of all the studies are discussed in **Chapter 9** from a diagnostic and etiopathogenic perspective. A summary is presented in **Chapter 10**.

References

Fitzpatrick, N., Smith, T.J., Evans, R.B., Yeadon, R., 2009. Radiographic and arthroscopic findings in the elbow joints of 263 dogs with medial coronoid disease. Veterinary Surgery 38, 213-223.

Henry, W.B., Jr, 1984. Radiographic diagnosis and surgical management of fragmented medial coronoid process in dogs. Journal of the American Veterinary Medical Association 184, 799-805.

Moores, A.P., Benigni, L., Lamb, C.R., 2008. Computed tomography versus arthroscopy for detection of canine elbow dysplasia lesions. Veterinary Surgery 37, 390-398.

Tirgari, M., 1974. Clinical radiographical and pathological aspects of arthritis of the elbow joint in dogs. Journal of Small Animal Practice 15, 671-679.

Ubbink, G.J., van de Broek, J., Hazewinkel, H.A., Rothuizen, J., 1998. Cluster analysis of the genetic heterogeneity and disease distributions in purebred dog populations. Veterinary Record 142, 209-213.

Chapter 2

General introduction

Medial coronoid disease in dogs

Medial coronoid disease (MCD) is known as one of the most frequently diagnosed heritable disorders of dogs and usually affects young, large breed dogs (Flückiger, 1992; Boulay, 1998; Janutta et al., 2006; Burton et al., 2008; Temwichitr et al., 2010; Lavrijsen et al., 2012). It has been described under a well-known umbrella disease i.e. elbow dysplasia (ED) together with entities such as ununited anconeal process (UAP), osteochondrosis (OC) or osteochondritis dissecans (OCD) of the humeral trochlea, and radioulnar joint incongruity (RUI).

This disease of the medial coronoid process (MCP) was first called *"ununited medial coronoid process"* of the canine elbow joint and was described as the presence of an ossified bone loosely attached to the medial coronoid process of the ulna (Tirgari, 1974). In later years, it became known as *"fragmented medial coronoid process"* (FMCP; Henry, 1984). The term "medial coronoid disease" was introduced in 2008 as being a more representative term for FMCP, as it encompasses lesions of both articular cartilage and subchondral bone (Moores et al., 2008; Fitzpatrick et al., 2009). The prevalence of MCD was found to be 11-50% in Labrador retrievers presenting with forelimb lameness (Ubbink et al., 1998; Meyer-Lindenberg et al., 2002; Fitzpatrick et al., 2009), and 6% in a recent screened cohort of 2693 Dutch Labrador retrievers (Lavrijsen et al., 2012). The first clinical signs of MCD usually occur between 4 and 8 months of age, although lameness has been reported as early as 3 months (Olsson, 1983; Voorhout and Hazewinkel, 1987; Fitzpatrick et al., 2009); but there are also cases described where clinical signs become apparent much later in life (Henry, 1984; van Bruggen et al., 2010). The dogs that are brought to veterinary clinics have usually developed an advanced stage of the disease because the early, mild signs of lameness are easily overlooked by the owner or confused with "growing pains". Common clinical signs of MCD are lameness, stiff or stilted gait due to shortened steps, and slight abduction of the affected forelimb. In most cases, joint effusion, crepitus, and pain reaction during joint manipulation can be detected during physical examination (Olsson, 1983).

Despite a number of reports in the veterinary literature (Flückiger, 1992; Boulay, 1998; Remy et al., 2004; Janutta et al., 2006; Meyer-Lindenberg et al., 2006; Burton et al., 2008; Moores et al., 2008; Fitzpatrick et al., 2009; Lappalainen et al., 2009; Vermote et al., 2009; Temwichitr et al., 2010; Lavrijsen et al., 2012), little is known about the etiology of the disease. This chapter reviews what is known about of the development of the MCP, the etiopathogenesis of MCD, and the investigation techniques used to study and diagnose MCD.

Postnatal development of the medial coronoid process of the ulna

Investigation of the postnatal development of the MCP of the ulna has revealed no evidence of a secondary ossification center (Fox et al., 1983; Guthrie et al., 1992; Breit et al., 2004; Wolschrijn and Weijs, 2004; Breit et al., 2005; Wolschrijn and Weijs, 2005; Breit et al., 2006; Wolschrijn et al., 2008). At birth, the MCP is completely cartilaginous but subsequently ossifies, starting at the base and proceeding to the apex of the MCP. This developmental process involves the unique properties of both cartilage and bone, beginning with chondrocytes differentiation, matrix calcification, vascular invasion, and finally ossification. Anatomical studies of MCP development have shown that ossification of the cartilaginous template of the MCP at the humeral contact area in immature MCPs always ossified centrally first, then followed by the tip, and the medial and lateral borders of the MCP (Fig. 1). The MCP has been found to mature later in large breed dogs (more than 15 kg) at an age of approximately 20 weeks than in small breed dogs (less than 10 kg) at an age of approximately 16 weeks (Breit et al., 2004; Breit et al., 2006).

In a histological study, Guthrie *et al.* (1992) reported that the articular cartilage of the MCP is not of uniform thickness and is thickest at the apex (in a 3-week-old Labrador retriever). Collagen fibrils within the cartilaginous MCP are not established before the age of 3 weeks. In the same study, the authors noted the absence of cartilage canals in articular cartilage from a 8-week-old Labrador retriever (Guthrie et al., 1992). However, in a later study, performed with Golden retrievers, cartilage canals were detected up to 13 weeks of age (Wolschrijn et al., 2008). Micro-computed tomography (microCT) revealed that bone density (reflected by high bone volume fraction and low trabecular separation) increased from 8 weeks onward, accompanied by a well-defined orientation of the trabecular alignment toward the humero-ulnar articular surface and the attachment of the annular ligament which indicates that functional adaptation of the MCP to weight bearing occurs at this young age in large breed dogs (Wolschrijn and Weijs, 2004). At 18 weeks of age, the subchondral bone layer of the humeral articular side of the MCP reached a completely smooth appearance, reflecting remodeling of the bone in response to high compressive loading perpendicularly on the humero-ulnar joint (Muller-Gerbl et al., 1989; Wolschrijn and Weijs, 2005). Complete ossification of the MCP occurs as early as 20-22 weeks of age (Fig. 2; Olsson, 1983; Breit et al., 2004).

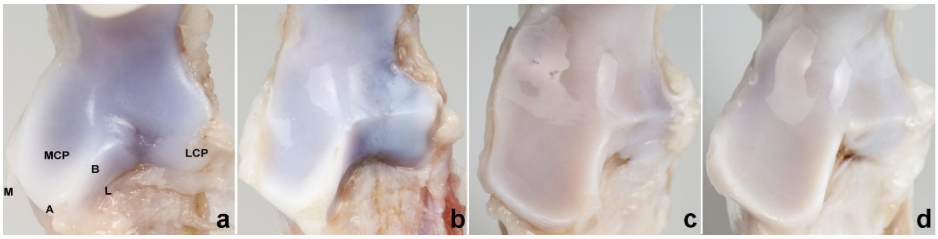

Fig. 1. *Proximal ulna of left elbow obtained from Labrador retrievers at (a) 5, (b) 12, (c) 18, (d) 25 weeks of age, showing the base (B) of the medial coronoid process (MCP) and tip or apex (A) of the MCP. LCP, lateral coronoid process; L, lateral border of the MCP; M, medial border of the MCP. The articular cartilage transforms from blue-white to more opaque and yellowish as it ages, which might related to dehydration and age-related pigment deposition (Van der Korst et al., 1968).*

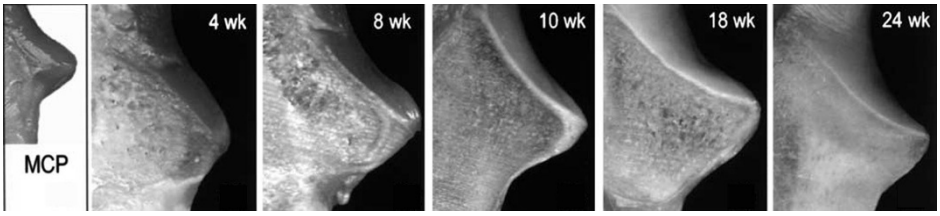

Fig. 2. *Sagittal sections showing developmental stages of the medial coronoid process (MCP) in Rottweilers by age in weeks (wk). (Pictures courtesy of S. Breit)*

Gross and functional anatomy of the elbow joint

The elbow joint comprises the humeroradial, humeroulnar, and proximal radioulnar joints. All these joints share a common joint capsule. The humeroradial and humeroulnar joints serve as hinge joints, which allow the extension and flexion of the radius and ulna over the humerus. The normal range of extension and flexion of the elbow joint in adult Labrador retrievers is 164-167° and 34-38°, respectively (Jaegger et al., 2002). The proximal radioulnar joint (Fig. 3) serves as pivot joint, allowing pronation and supination of the antebrachium. In a recent study of the contact mechanics of normal canine elbow joints, the peak contact pressure (PCP) was found to be increased and the contact area decreased in both the medial and lateral coronoid process during both pronation and supination, instead of shifting of pressure between the two compartments. In the same study, an increased PCP was found in the medial compartment during 115° flexion of the joint (Cuddy et al., 2012).

The trochlear notch of the ulna articulates with the humeral trochlea and extends to form two prominences distally, the MCP and the lateral coronoid process (LCP). Both coronoid processes, especially the MCP, are important in increasing the total surface area of the elbow joint for weight bearing (Fox et al., 1983; Preston et al., 2000). The

humeroradial joint is reported to be involved in at least 75%-80% of the weight bearing of the elbow, with the remaining 20-25% loading on the MCP and LCP (Berzon and Quick, 1980; Sjöström, 1998). However, in an in vitro study to simulate conditions obtained from dogs with a mean body weight of 20 kg during the mid-stance phase at a trot, force distribution across the elbow joint suggested that the mean force acting on the radius and ulnar might be equally divided (Mason et al., 2005).

Five ligaments (medial and lateral collateral, annular, oblique, and olecranon) connect the bones (Fig. 4). The medial and lateral collateral ligaments are attached proximally at the medial and lateral epicondyles of the distal humerus, respectively. Distally, the ligaments are divided into two crura: the cranial crus of both ligaments are attached to the radius and the caudal crus of both ligaments are attached to the ulna (Constantinescu and Constantinescu, 2009). The annular ligament runs transversely around the radius and is attached to the apex of the MCP and the lateral coronoid process. The annular ligament plays an important role in regulating the normal articulation between the bones (Miller et al., 1993). The oblique ligament originates from the proximal edge of the supratrochlear foramen and crosses obliquely at the cranial surface of the elbow joint. As with the collateral ligaments, it divides into a cranial portion, which inserts onto the proximal medial border of the radius, and a caudal portion, which fuses with the cranial portion of the medial collateral ligament (Miller et al., 1993; Oliveira et al., 2003; Villamonte-Chevalier et al., 2012). The olecranon ligament joins the medial border of the olecranon fossa to the medial aspect of the olecranon, just distal to the olecranon tuberosity (Constantinescu and Constantinescu, 2009).

The major muscle groups of the elbow joint are the brachial and antebrachial groups. The biceps brachii and brachialis muscles cross over the cranial aspect of the elbow, whereas the long and lateral heads of the triceps brachii muscle and anconeus muscle cover the lateral aspect of the joint. The medial head of the triceps and the tensor fasciae antebrachii muscle run on the medial aspect of elbow (Fig. 4; Constantinescu and Constantinescu, 2009). Given the anatomy of the joint, the following forces can be expected to act on the MCP: a vertical downward force from the humeral condyle, a horizontal compressive force from the radial head, and a cranial tensile force from the attached annular ligament and during contraction of the biceps brachii and brachialis muscles groups (Wolschrijn and Weijs, 2004; Burton et al., 2010; Hulse et al., 2010; Villamonte-Chevalier et al., 2012).

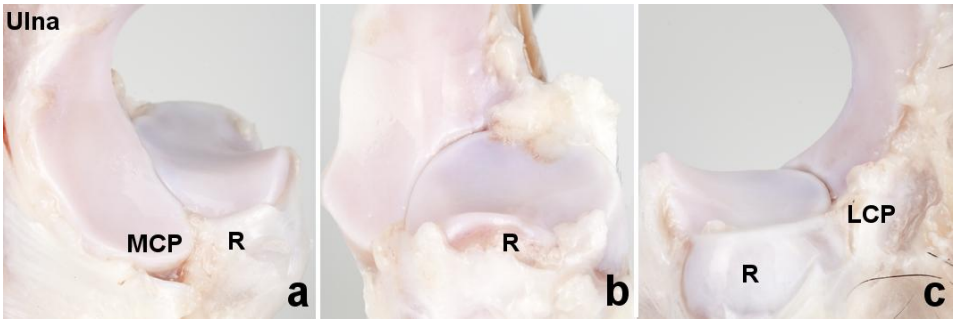

Fig. 3. *Gross anatomy of the radioulnar joint of a left elbow obtained from a 27-week-old Labrador retriever. (a) Medial view of the joint showing the close contact of the lateral aspect of the medial coronoid process (MCP) with the radial head (R). (b) Frontal view and (c) Lateral view with lateral coronoid process (LCP) visible.*

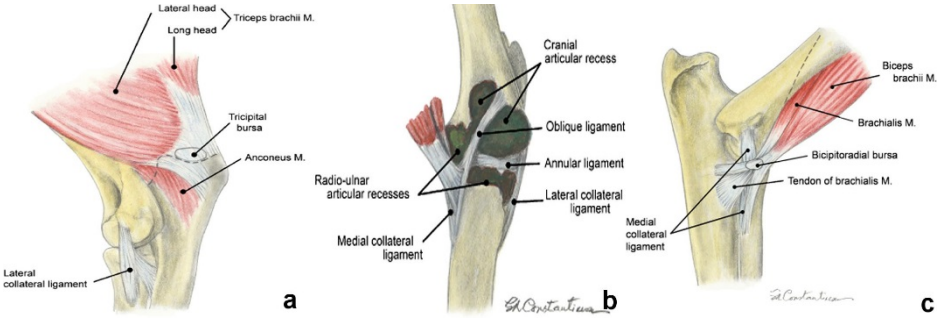

Fig. 4. *Muscles and ligaments of the elbow joint of a dog. (a) Lateral view. (b) Frontal view. (c) Medial view (Pictures courtesy of G.M. Constantinescu).*

Etiopathogenesis of medial coronoid disease (MCD)

Although MCD has been recognized as a heritable disease for more than 30 years, its mode of inheritance is still unclear (Grøndalen and Grøndalen, 1981; Guthrie and Pidduck, 1990; Ubbink et al., 1998; Everts et al., 2000; Ubbink et al., 2000; Temwichitr et al., 2010). The heritability (h^2) of ED, including MCD, is reported to vary between 0.17 and 0.77 in Labrador retrievers; 0.77 for male and 0.45 for female dogs (Grøndalen and Grøndalen, 1981; Guthrie and Pidduck, 1990; Lavrijsen et al., 2012). A simple, autosomal recessive mode of inheritance has been ruled out (Padgett et al., 1995; Evert et al., 2000), and instead the disease is suggested to have a multifactorial and polygenic origin (Guthrie and Pidduck, 1990; Mäki et al., 2004). The incidence of MCD can be reduced by selective-breeding programs (Swenson et al., 1997). Salg *et al.* (2006) hypothesized that it is possible that

disturbance of one or more collagen genes in an indirect manner (disturbance in expression or alteration in post-translational modification) may cause MCD. Despite extensive research, the causative genes have not yet been identified and more disease- and breed-specific research is recommended. Apart from this, several hypotheses regarding the etiopathogenesis have been proposed.

a. Disturbance of endochondral ossification

Cartilage serves as a template for endochondral ossification. During endochondral ossification, chondrocytes undergo proliferation, differentiation, maturation, and apoptosis. Deregulation of this process may lead to skeletal malformation (Shum and Nuckolls, 2002). The first theory related MCD to other development diseases like OCD and UAP was by Tirgari and Olsson (Tirgari, 1974; Olsson, 1981). The term *"ununited medial coronoid process"* was introduced as the disease was believed to be caused by osteochondrosis (OC; Tirgari, 1974; Tirgari, 1980; Olsson, 1981). OC is defined as a focal disturbance of endochondral ossification of articular cartilage in growing animals, by which an area of retained cartilage that extends into subchondral bone fails to ossify (Reiland et al., 1978; Olsson, 1981; Ekman and Carlson, 1998; Ytrehus et al., 2007). The presence of retained cartilage is thought to serve as a weak starting point for fissures to develop in the articular cartilage layer.

The occurrence of osteochondrotic lesions has been associated with chondronecrosis, caused by a failure of blood supply to growing cartilage (Carlson et al., 1995; Ekman and Carlson, 1998; Ytrehus et al., 2004; Olstad et al., 2008). A histological study of fragmentation of the MCP in a 20-week-old Golden retriever revealed focally thickened cartilage and evidence of chondronecrotic lesions at the osteochondral junction (similar as in figure 5; Wolschrijn et al., 2005). Another report also demonstrated discrete foci of chondrocytes embedded in cartilage matrix, i.e., cartilage island within the subchondral bone area of the diseased MCPs obtained from dogs older than 24 weeks of age. These lesions were hypothesized to reflect either a disturbance of ossification or a repair process, by which the body attempts to 'fill in' microcracks in subchondral bone (Goldhammer et al., 2009). However, histological studies of MCPs from dogs with advanced disease argue against OC being a primary cause of MCD (Crouch et al., 2000; Danielson et al., 2006).

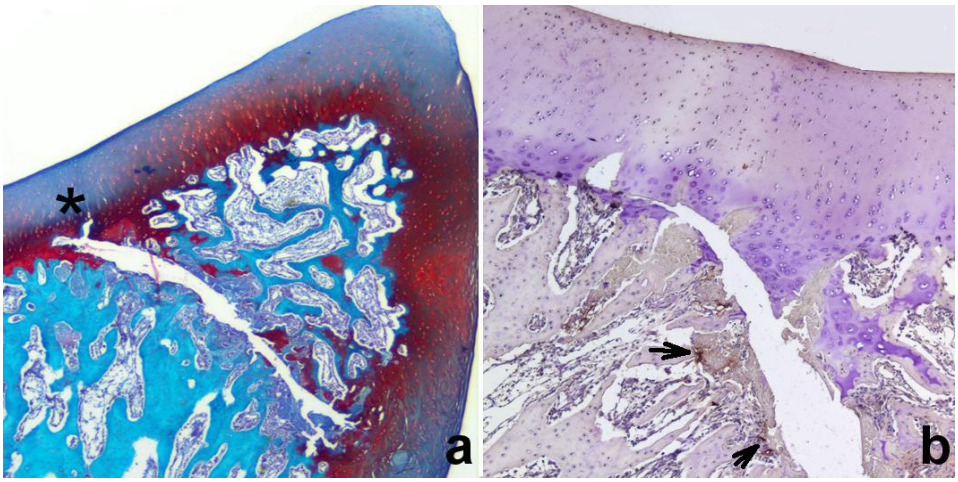

Fig. 5. *Lateral aspect of the medial coronoid process (MCP) of a left ulna taken from a 25-week-old Labrador retriever affected by medial coronoid disease. (a) Intact articular cartilage surface overlying a fissure in the subchondral bone layer with focally thickened articular cartilage (*). (Safranin O, x 2). (b) Enlarged view of the focally thickened articular cartilage (*) in (a), showing brown staining (arrows) surrounding the fissure, indicating the presence of vascular endothelial cells (von Willebrand factor and hematoxylin counterstained, x 4).*

b. Abnormalities of subchondral bone

In the 1990s and 2000s, results from histological studies were more supportive of MCD to be caused by abnormalities of the underlying subchondral bone. Danielson *et al.* (2006) reported the size of fatigue microcracks increased by an increase of disease severity and damage being more severe at the fragmented site than at the rest of the bone. The results were consistent with a fibrous non-union, which indicated fatigue microcracks of the MCP causing MCD, rather than by OC (Crouch et al., 2000; Danielson et al., 2006; Gemmill and Clements, 2007). The loss of osteocytes with more pronounced osteoporosis of the fragmented MCP has also been reported (Danielson et al., 2006; Goldhammer et al., 2009). Later studies with dual-energy x-ray absorptiometry (DEXA) showed the mean bone mineral density of the MCP to be lower in MCD-positive animals than in controls. In both groups, bone mineral density was 50% lower at the axial border of the MCP than at the abaxial border. This suggests that the abaxial border might be more resistant to compressive loading than the axial border, and that this difference might predisposes the axial border of the MCP to develop microcracks (Burton et al., 2010).

The opposite, i.e., an increase in bone density at the MCP and ulnar trochlear notch, is also suggested to contribute to the development of MCD (Smith et al., 2009).

Subtrochlear notch sclerosis (STS), which is characterized by increased radiopacity adjacent to the ulnar trochlear notch and caudal to the coronoid process, is an important indicator in diagnosing MCD radiographically (Burton et al., 2007; Fitzpatrick et al., 2009). Although there is a lot of evidence that there is a relationship between STS and MCD (Burton et al., 2008; Fitzpatrick et al., 2009, Smith et al., 2009; Lavrijsen et al., 2012), it is still debated whether STS is the cause of MCD or the result of secondary degenerative changes. It was postulated as a cause of MCD with the explanation that increased stiffness of subchondral bone would cause the overlying articular cartilage layer to become more vulnerable to injury (Dequeker et al., 1995; Temwichitr et al., 2010).

c. Abnormal mechanical loading

Abnormal mechanical loading has been suggested to be an important cause of MCD. Possible causes of this impairment of mechanical loading are changes in joint alignment and spaces that result in RUI because of a disparity in the length of the radius and ulna (Preston et al., 2001; Davidson et al., 2008; Fitzpatrick et al., 2009), underdevelopment of the ulnar trochlear notch (Wind, 1986; Wind and Packard, 1986), or physiological incongruity during loading (Preston et al., 2000; House et al., 2009). Numerous studies have investigated the most efficient way to detect RUI in an early stage, since RUI is believed to be a major factor contributing to MCD development (Murphy et al., 1998; Mason et al., 2002; Blond et al., 2005; Gemmill et al., 2005; Holsworth et al., 2005; Kramer et al., 2006; Samoy et al., 2006; Gemmill and Clements, 2007; Bottcher et al., 2009). Although RUI in conjunction with MCD is typical finding in Bernese Mountain dogs (in 50% of the cases of ED; Lavrijsen et al., 2012), RUI has been reported in Labrador retrievers in a much lower frequency (Gemmill et al., 2005). Labrador retrievers with MCD are believed not to have significant RUI at the medial coronoid region at the time of diagnosis (Kramer et al., 2006). Other possible causes or factors contributing to MCD development include changes in the magnitude and topographic distribution of loading, pressure or forces within the joint, such as tensile forces originating from the annular ligament (Wolschrijn and Weijs, 2004), and shear stress between the contact area of the proximal radial head and the axial border of the MCP during pronation and supination (Hulse, 2010). Both Fitzpatrick and Yeadon (2009) and Hulse *et al.* (2010) suggested that biceps brachii/brachialis muscle complex in relation to the bony anatomy might lead to rotational instability, and give rise to shear planes between the radial head and the radial incisure of the MCP. This may result in micro-damage or even fragmentation of the MCP. It has been shown that contact mechanics and alignment of normal dog elbows in three dimensions vary significantly, depending on the position of the elbow (Cuddy et al., 2012).

Several studies have investigated the role of the shape of the MCP (Breit et al., 2004; Breit et al., 2006), trochlear notch (Wind, 1986; Wind and Packard, 1986; Collins et al., 2001), and the articular contact areas (Eckstein et al., 1995; Preston et al., 2001; Fujita et al., 2003; Breit et al., 2005) in the development of MCD. Compared between the different breeds, there is also high variability between growth in the length and width of the MCP. Large breed dogs are believed to have a less pronounced growth in length of the MCP in comparison to the width of the MCP during growth of the elbow joint, resulting in a more obtuse shape of the MCP in comparison with small breed dogs (Breit et al., 2006). Hence, loading and forces acting on the MCP might be larger in large breed dogs than expected. A difference in the rate of ossification between small and large breed dogs is suggested to predispose large breed dogs to MCD: ossification of the MCP is completed significantly earlier in small breed dogs than in large breed dogs, and slow maturation of the MCP is believed to be a cause of MCD in larger dogs (Breit et al., 2004).

d. Others

In addition to the above-mentioned potential causes of MCD, environmental factors, such as diet and exercise (Sallander et al., 2006), and trauma (Hadley et al., 2009) cannot be ruled out as playing a role in MCD development.

Diagnostic techniques

a. Radiography

Radiography has always been the first-line screening tool for examining dogs with suspected MCD, since it is easy to access, is cheaper than computed tomography (CT) and arthroscopy, and is less invasive than the latter (Mason et al., 2002; Gemmill and Clements, 2007). The sensitivity of radiography to diagnose MCD, however, is estimated to range from only 10% to 62% (Wosar et al., 1999; Haudiquet et al., 2002). Negative radiographic findings cannot rule out MCD (Carpenter et al., 1993; Wosar et al., 1999; Punke et al., 2009). The radiographic diagnosis of MCD is challenging because the radial head is superimposed over the MCP and the close proximity of the ulnar trochlear notch and humeral condyle. Radiography typically detects advanced disease, with diagnostic criteria often being based on secondary changes caused by degenerative joint changes, such as osteophytosis at the proximal anconeal process and cranioproximal radial head, and the medial part of humeral condyle, and STS, and blunting or blurring of the cranial edge of the MCP (Keller et al., 1997; Hornof et al., 2000; Mason et al., 2002). In some cases, the primary lesion (i.e., fragmentation of MCP) can be seen concomitantly with other components of ED, such as indentation of the medial part of humeral condyle in the case

of OCD-like lesions, UAP, and the presence of RUI (Hornof et al., 2000; Meyer-Lindenberg et al., 2002; Lavrijsen et al. 2012). Differences in positioning the limb during radiographic examination also has been studied and reported in order to optimize the visualization of the lesion of MCD (Voorhout and Hazewinkel, 1987; Miyabayashi et al., 1995; Wosar et al., 1999; Hornof et al., 2000; Haudiquet et al., 2002). Multiple views, including mediolateral view with the elbow joint maximally extended and antebrachium supinated at 15° (Voorhout and Hazewinkel, 1987), and mediocaudal-laterocranial oblique radiographs (Miyabayashi et al., 1995) has been described.

Apart from the use of radiography for diagnostic purpose, radiography also plays an important role in the screening of potential breeding animals for ED (including MCD), employing 1, 2, or up to 4 radiographic views per elbow (Hazewinkel et al., 1988; Keller et al., 1997; Wosar et al., 1999). The International Elbow Working Group (IEWG) protocol is used in screening programs, to register signs of secondary degenerative changes, as well as the primary lesions (Tellhelm, 2011), and is similar to the protocol recommended by Lang *et al.* (1998).

Elbow dysplasia scoring		Radiographic findings
0	Normal elbow joint	● Normal elbow joint ● No evidence of incongruence, sclerosis, or osteophytosis
1	Mild arthrosis	● Presence of osteophytes < 2 mm high ● Minor sclerosis of the base of the coronoid process
2	Moderate arthrosis or suspect primary lesion	● Presence of osteophytes of 2 - 5 mm high ● Obvious sclerosis of the base of the coronoid process ● Step of 3-5 mm between radius and ulna (RUI) ● Indirect signs for a primary lesion (UAP, FCP/ Coronoid disease, OCD)
3	Severe arthrosis or evident primary lesion	● Presence of osteophytes of > 5 mm high ● Step of > 5 mm between radius and ulna (obvious RUI) ● Obvious presence of a primary lesion (UAP, FCP, OCD)

Table 1. *Elbow dysplasia (ED) evaluation according to the guidelines used in the International Elbow Working Group (IEWG) Elbow Screening Scheme (Tellhelm, 2011).*

b. Computed tomography

Computed tomography (CT) is a more accurate tool for diagnosing MCD. Comparing plain film radiography, xeroradiography, linear tomography, arthrography, and CT, the latter was reported to have the highest accuracy (86.7%), sensitivity (88.2%), and negative predictive value (84.6%) in detecting MCD (Carpenter et al., 1993). Its ability of interpreting the images in different reconstructive views and planes allows CT to be superior to radiography because there is no distraction of superimposed images. Displaced mineralized fragments

of the MCP, signs of RUI, and the presence of STS are easy to detect using CT (Reichle and Snaps, 1999; Reichle et al., 2000; Gemmill, 2004; Holsworth et al., 2005; Gemmill et al., 2006; Kramer et al., 2006; Samoy et al., 2006; Wagner et al., 2007). Maximal supination and pronation of the antebrachium leads to a significant variation in measurements of the radioulnar joint space; hence, a neutral position of the antebrachium during scanning is critical to detect RUI (House et al., 2009).

Both radiography and CT cannot be used to assess cartilage integrity and the animals are not in weight bearing position during the examination (De Rycke et al., 2002; Mason et al., 2002). These disadvantages mean that it is not possible to detect or assess pathological changes in cartilage and make it more difficult to determine the congruity of the elbow joints. The criteria used in CT to diagnose MCD are similar to those used in radiography. According to a study of CT in dogs positive for fragmentation of MCP, the most common signs are periarticular osteophytosis (97%), STS at the area of the MCP (86%), and fragmentation of MCP (66%; Groth et al., 2009).

c. Arthrotomy/Arthroscopy

Arthrotomy and arthroscopy serve as both diagnostic and treatment tools in MCD (Van Ryssen and van Bree, 1997; Hazewinkel et al., 1998; Meyer-Lindenberg et al., 2003; Wagner et al., 2007; Fitzpatrick et al., 2009; Punke et al., 2009; Vermote et al., 2009). Both techniques allow removal of loose bodies in the elbow joint and the lesions in which the overlying cartilage is frayed can be treated by curettage. Arthroscopy is preferred because of its shorter convalescence period and minimally invasive nature (van Bree and Van Ryssen, 1995; Meyer-Lindenberg et al., 2003). Arthroscopy has a sensitivity of 94% and a specificity of 81.9% for diagnosing elbow pathology (Wagner et al., 2007). It has a higher diagnostic value than radiography or CT because of its high specificity, reproducibility, and the ability to visualize cartilage lesions. However, arthrotomy and arthroscopy are more invasive than radiography and CT, and post-operative potential complications such as joint infections, wound dehiscence, and damage to the cartilage need to be taken into consideration. Recognition of MCD lesions during the surgical procedures is limited by several technical problems. For instance, the limited window of view might not allowed sufficient inspection of the medial compartment of the joint, and vision might be obscured by severe protrusion of synovial villi and hemorrhages. These limitations, together with joint manipulation during the surgical procedure, complicate the assessment of joint congruency (Van Ryssen and van Bree, 1997; Meyer-Lindenberg et al., 2003). The use of arthroscopy is limited by the need for expensive equipment and specialized training of personnel (van Bree and Van Ryssen, 1995).

d. Other diagnostic techniques

Bone scintigraphy (Fig. 6) is a useful diagnostic tool to localize occult causes of lameness (Schwarz et al., 2004; van Bruggen et al., 2010; Peremans et al., 2011) and has been used to detect and localize subtle pathological changes in the elbow joints of dogs, before changes could be detected by radiography or CT. Although scintigraphy appears to have a high sensitivity in detecting elbow joint disease, its diagnostic specificity is low (Schwarz et al., 2004). In addition, image resolution is rather poor compared with that of other techniques, and use of bone scintigraphy tends to be restricted by the limited availability of the modality and other issues, such as the handling of radiopharmaceuticals, which requires license application, personnel training, appropriate radiation isolation facilities, and extra documentation.

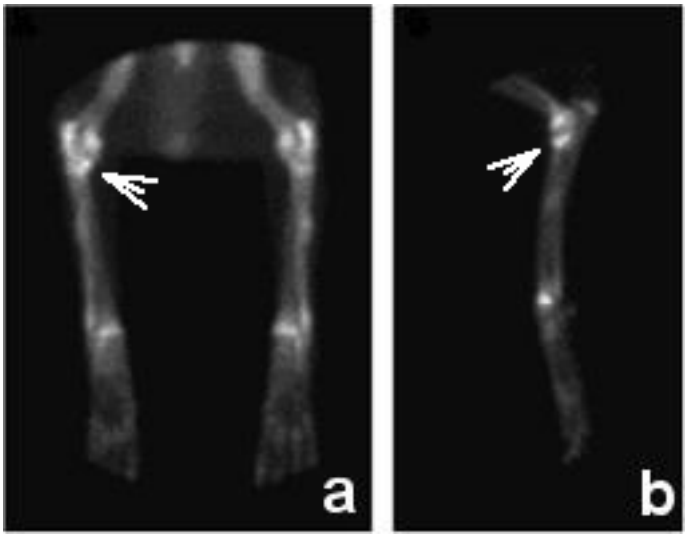

Fig. 6. *Scintigraphic study of a patient with an abnormal medial coronoid process (MCP) confirmed at surgery. Note the area of increased radioactivity in the region of the MCP (arrow): (a) caudomedial view and (b) lateral view (Pictures courtesy of L.W.L. van Bruggen).*

Magnetic resonance imaging (MRI; Fig. 7) has the same multiplanar advantage as CT, although CT has a better resolution for imaging bone. MRI of the elbow joints has been performed with 0.2 to 3.0-Tesla magnetic field (Janach et al., 2006; Baeumlin et al., 2010; Wucherer et al., 2012). It is the only diagnostic tool that allows tissue differentiation at the osteochondral junction (Probst et al., 2008). MRI is reported to have an accuracy of 91% in identifying both non-displaced, mineralized or non-mineralized fragments of the MCP (Snaps et al., 1997; Reichle and Snaps, 1999; Snaps et al., 1999). However, MRI has

technical and field strength-dependent resolution limitations because of the relatively small size of the elbow joint and the thin surface of articular cartilage in dogs. The combination of micro-single photon emission tomography and MRI was used recently to study the functional and anatomical predilection sites in elbow joint disease (Peremans et al., 2011).

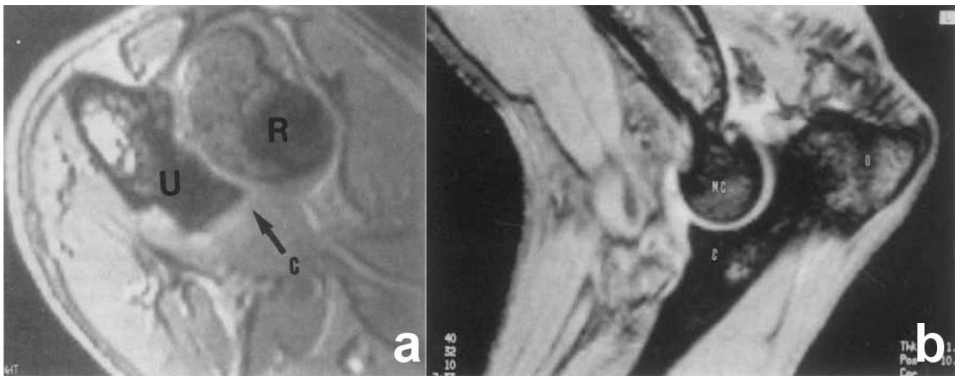

Fig. 7. *(a) Dorsal plane image of the elbow (GE FISP sequence). This plane allows a precise visualization of the articulation between the medial coronoid process (the arrow pointing the coronoid process, C) of the ulna (U) and the radial head (R). (b) Sagittal plane image of the elbow (GE FISP sequence). Sagittal slice passing through the medial coronoid process of the ulna. This plane shows clearly the articulation between the medial coronoid process (C) and the medial aspect of the humeral condyle (MC); 0: olecranon of the ulna (Pictures courtesy of F.R. Snaps).*

Although the ultrasonographic appearance (Fig. 8) of the canine elbow has been reported (Kramer et al., 1997; Knox IV et al., 2003; Lamb and Wong, 2005; Seyrek-Intas et al., 2009), the technique is used less often to diagnose MCD because of its inability to clearly distinguish the architecture of bones and cartilage, caused by the high acoustic impedance of bony tissue and the anatomical complexity of the elbow joint. Its selective usage in imaging tendons and ligaments is more common.

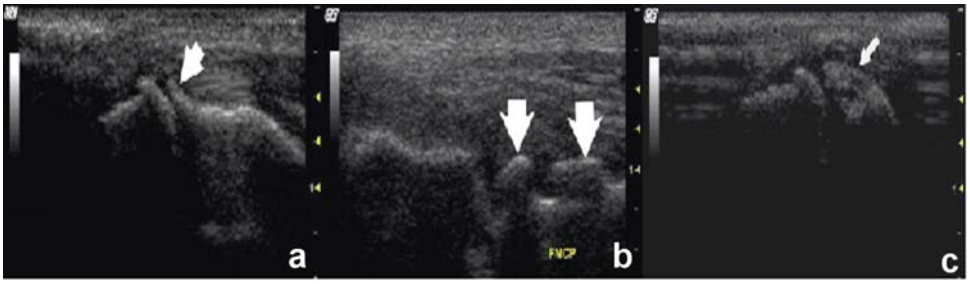

Fig. 8. *(a) Ultrasound image of a normal medial coronoid process. Note the sharp margins of the coronoid process (arrow). (b) Ultrasound image of irregular margins of the medial coronoid process (arrows), consistent with a fragment of the medial coronoid, which was confirmed on arthroscopy. (c) Ultrasound image of the medial coronoid process with incomplete calcification (Pictures courtesy of C.R. Cook).*

MicroCT is gaining popularity in osteoarthritis research, but the technique cannot be used in the clinic because of the size of the animals and the long scanning time (e.g. Scanning time for a bone length about 4 cm can take approximately 90 minutes). It has been used to study the postnatal development of MCP ex vivo (Wolschrijn and Weijs, 2004; Wolschrijn and Weijs, 2005; Wolschrijn et al., 2005). MicroCT has the ability to evaluate bony structures in three dimensions at micron level and its advantage over histology are the fast, automated image acquisition and the fact that specimen is not completely destroyed. Radial incisure fragmentation (RIF) has been described in a microCT study of MCPs obtained from clinical patients diagnosed with MCD, in which abnormal torsional loading was considered to precede fragmentation (Fitzpatrick et al., 2011). This ex vivo technique applied together with a contrast agent, i.e. Equilibrium Partitioning of an Ionic Contrast agent with microCT (EPIC-microCT), was used in our study to investigate changes in articular cartilage and subchondral bone in the MCP of juvenile Labrador retrievers with early-stage MCD. With this technique, negatively charged contrast molecules diffuse into the cartilage at sites where glycosaminoglycans (GAGs) depletion has occurred, and after yielding an equilibrium distribution of the ionic contrast agent that is inversely related to the density of negatively charged GAGs, detection of the x-ray radiation attenuation via microCT can be performed (Palmer et al., 2006). The morphology and biochemical composition of articular cartilage can be assessed precisely through this technique.

Conclusion

Despite numerous studies, breed-specific information about the diagnostic features and etiopathogenesis of MCD is lacking. The ability to recognize the lesions early is essential in order to start treatment before severe osteoarthritis develops, so as to optimize treatment outcomes. Radiography alone is not adequate to detect early MCD because radiographic signs are usually caused by secondary lesions, which could give rise to false-negative results if diagnosis is based solely on radiographic findings. CT is becoming increasingly available in veterinary practice, and the ability to recognize the early lesions is undoubtedly a benefit for the patient. The appearance of early MCD, without complicating secondary changes, might provide clues about the origin of the disease and subsequently enable us to learn more about the pathogenesis of MCD. This was the motivation to design studies to investigate the early development of MCD.

References

Baeumlin, Y., Rycke, L.D., Van Caelenberg, A., van Bree, H., Gielen, I., 2010. Magnetic resonance imaging of the canine elbow: An anatomy study. Veterinary Surgery 39, 566-573.

Berzon, J.L., Quick, C.B., 1980. Fragmented coronoid process: anatomical, clinical, and radiographic considerations with case analyses. Journal of the American Animal Hospital Association 16, 241-251.

Blond, L., Dupuis, J., Beauregard, G., Breton, L., Moreau, M., 2005. Sensitivity and specificity of radiographic detection of canine elbow incongruence in an in vitro model. Veterinary Radiology & Ultrasound 46, 210-216.

Bottcher, P., Werner, H., Ludewig, E., Grevel, V., Oechtering, G., 2009. Visual estimation of radioulnar incongruence in dogs using three-dimensional image rendering: an in vitro study based on computed tomographic imaging. Veterinary Surgery 38, 161-168.

Boulay, J.P., 1998. Fragmented medial coronoid process of the ulna in the dog. Veterinary Clinics of North America: Small Animal Practice 28, 51-74.

Breit, S., Künzel, W., Seiler, S., 2004. Variation in the ossification process of the anconeal and medial coronoid processes of the canine ulna. Research in Veterinary Science 77, 9-16.

Breit, S., Kunzel, W., Seiler, S., 2005. Postnatal modelling of the humeroantebrachial contact areas of radius and ulna in dogs. Anatomia Histologia Embryologia 34, 258-264.

Breit, S., Kunzel, W., Seiler, S., 2006. On the weight-bearing function of the medial coronoid process in dogs. Anatomia Histologia Embryologia 35, 7-12.

Burton, N.J., Comerford, E.J., Bailey, M., Pead, M.J., Owen, M.R., 2007. Digital analysis of ulnar trochlear notch sclerosis in Labrador retrievers. Journal of Small Animal Practice 48, 220-224.

Burton, N.J., Dobney, J.A., Owen, M.R., Colborne, G.R., 2008. Joint angle, moment and power compensations in dogs with fragmented medial coronoid process. Veterinary and Comparative Orthopaedics and Traumatology 21, 110-118.

Burton, N.J., Perry, M.J., Fitzpatrick, N., Owen, M.R., 2010. Comparison of bone mineral density in medial coronoid processes of dogs with and without medial coronoid process fragmentation. American Journal of Veterinary Research 71, 41-46.

Burton, N.J., Toscano, M.J., Barr, F.J., Owen, M.R., 2008. Reliability of radiological assessment of ulnar trochlear notch sclerosis in dysplastic canine elbows. Journal of Small Animal Practice 49, 572-576.

Carlson, C.S., Cullins, L.D., Meuten, D.J., 1995. Osteochondrosis of the articular-epiphyseal cartilage complex in young horses: evidence for a defect in cartilage canal blood supply. Veterinary Pathology 32, 641-647.

Carpenter, L.G., Schwarz, P.D., Lowry, J.E., Park, R.D., Steyn, P.F., 1993. Comparison of radiologic imaging techniques for diagnosis of fragmented medial coronoid process of the cubital joint in dogs. Journal of the American Veterinary Medical Association 203, 78-83.

Collins, K.E., Cross, A.R., Lewis, D.D., Zapata, J.L., Goett, S.D., Newell, S.M., Rapoff, A.J., 2001. Comparison of the radius of curvature of the ulnar trochlear notch of Rottweilers and Greyhounds. American Journal of Veterinary Research 62, 968-973.

Constantinescu, G.M., Constantinescu, I.A., 2009. A clinically oriented comprehensive pictorial review of canine elbow anatomy. Veterinary Surgery 38, 135-143.

Cook, C.R., Cook, J.L., 2009. Diagnostic imaging of canine elbow dysplasia: a review. Veterinary Surgery 38, 144-153.

Crouch, D.T., Cook, J.L., Lewis, D.D., Kreeger, J.M., Tomlinson, J.L., 2000. The presence of collagen types II and X in medical coronoid processes of 21 dogs. Veterinary and Comparative Orthopaedics and Traumatology 13, 178-184.

Cuddy, L.C., Lewis, D.D., Kim, S.E., Conrad, B.P., Banks, S.A., Horodyski, M.B., Fitzpatrick, N., Pozzi, A., 2012. Contact mechanics and three-dimensional alignment of normal dog elbows. Veterinary Surgery 41, 818-828.

Danielson, K.C., Fitzpatrick, N., Muir, P., Manley, P.A., 2006. Histomorphometry of fragmented medial coronoid process in dogs: a comparison of affected and normal coronoid processes. Veterinary Surgery 35, 501-509.

Davidson, P.T., Bullock-Saxton, J., Lisle, A., 2008. Anthropometric measurements of the scapula, humerus, radius and ulna in Labrador dogs with and without elbow dysplasia. Australian Veterinary Journal 86, 425-428.

De Rycke, L.M., Gielen, I.M., van Bree, H., Simoens, P.J., 2002. Computed tomography of the elbow joint in clinically normal dogs. American Journal of Veterinary Research 63, 1400-1407.

Dequeker, J., Mokassa, L., Aerssens, J., 1995. Bone density and osteoarthritis. The Journal of Rheumatology. Supplement 43, 98-100.

Eckstein, F., Lohe, F., Hillebrand, S., Bergmann, M., Schulte, E., Milz, S., Putz, R., 1995. Morphomechanics of the humero-ulnar joint: I. Joint space width and contact areas as a function of load and flexion angle. Anatomical Record 243, 318-326.

Ekman, S., Carlson, C.S., 1998. The pathophysiology of osteochondrosis. Veterinary Clinics of North America: Small Animal Practice 28, 17-32.

Everts, R.E., Hazewinkel, H.A., Rothuizen, J., van Oost, B.A., 2000. Bone disorders in the dog: a review of modern genetic strategies to find the underlying causes. Veterinary Quartery 22, 63-70.

Fitzpatrick, N., Garcia-Nolen, T., Daryani, A., Watari, S., Hayashi, K., 2011. Structural analysis of canine medial coronoid disease by microCT: radial incisure versus tip fragmentation. In: Scientific Presentation Abstracts of American College of Veterinary Surgeons Veterinary Symposium, Chicago, Illinois, E26.

Fitzpatrick, N., Smith, T.J., Evans, R.B., Yeadon, R., 2009. Radiographic and arthroscopic findings in the elbow joints of 263 dogs with medial coronoid disease. Veterinary Surgery 38, 213-223.

Fitzpatrick, N., Yeadon, R., 2009. Working algorithm for treatment decision making for developmental disease of the medial compartment of the elbow in dogs. Veterinary Surgery 38, 285-300.

Flückiger, M., 1992. Elbow dysplasia in the dog. Schweizer Archiv für Tierheilkunde 134, 261-271.

Fox, S.M., Bloomberg, M.S., Bright, R.M., 1983. Developmental anomalies of the canine elbow. Journal of the American Animal Hospital Association 19, 605-615.

Fujita, Y., Schulz, K.S., Mason, D.R., Kass, P.H., Stover, S.M., 2003. Effect of humeral osteotomy on joint surface contact in canine elbow joints. American Journal of Veterinary Research 64, 506-511.

Gemmill, T., 2004. Completing the picture: use of CT to investigate elbow dysplasia. Journal of Small Animal Practice 45, 429-430.

Gemmill, T.J., Clements, D.N., 2007. Fragmented coronoid process in the dog: is there a role for incongruency? Journal of Small Animal Practice 48, 361-368.

Gemmill, T.J., Hammond, G., Mellor, D., Sullivan, M., Bennett, D., Carmichael, S., 2006. Use of reconstructed computed tomography for the assessment of joint spaces in the canine elbow. Journal of Small Animal Practice 47, 66-74.

Gemmill, T.J., Mellor, D.J., Clements, D.N., Clarke, S.P., Farrell, M., Bennett, D., Carmichael, S., 2005. Evaluation of elbow incongruency using reconstructed CT in dogs suffering fragmented coronoid process. Journal of Small Animal Practice 46, 327-333.

Goldhammer, M.A., Smith, S.H., Fitzpatrick, N., Clements, D.N., 2009. A comparison of radiographic, arthroscopic and histological measures of articular pathology in the canine elbow joint. The Veterinary Journal 186, 96-103.

Grøndalen, J., Grøndalen, T., 1981. Arthrosis in the elbow joint of young rapidly growing dogs. V. A pathoanatomical investigation. Nordisk Veterinaermedicin 33, 1-16.

Groth, A.M., Benigni, L., Moores, A.P., Lamb, C.R., 2009. Spectrum of computed tomographic findings in 58 canine elbows with fragmentation of the medial coronoid process. Journal of Small Animal Practice 50, 15-22.

Guthrie, S., Pidduck, H.G., 1990. Heritability of elbow osteochondrosis within a closed population of dogs. Journal of Small Animal Practice 31, 93-96.

Guthrie, S., Plummer, J.M., Vaughan, L.C., 1992. Post natal development of the canine elbow joint: a light and electron microscopical study. Research in Veterinary Science 52, 67-71.

Hadley, H.S., Wheeler, J.L., Manley, P.A., 2009. Traumatic fragmented medial coronoid process in a Chihuahua. Veterinary and Comparative Orthopaedics and Traumatology 22, 328-331.

Haudiquet, P.R., Marcellin-Little, D.J., Stebbins, M.E., 2002. Use of the distomedial-proximolateral oblique radiographic view of the elbow joint for examination of the medial coronoid process in dogs. American Journal of Veterinary Research 63, 1000-1005.

Hazewinkel, H.A.W., Kantor, A., Meij, B. P., Voorhout, G., 1988. Fragmented coronoid process and osteochondritis dissecans of the medial humeral condyle. Tijdschrift voor Diergeneeskunde 113 Supplement 1, 41S-46S.

Hazewinkel, H.A.W., Meij, B. P., Theyse, L.F.H., 1998. Surgical treatment of elbow dysplasia. Veterinary Quartery 20 Supplement 1, 29-31.

Henry, W.B. Jr, 1984. Radiographic diagnosis and surgical management of fragmented medial coronoid process in dogs. Journal of the American Veterinary Medical Association 184, 799-805.

Holsworth, I.G., Wisner, E.R., Scherrer, W.E., Filipowitz, D., Kass, P.H., Pooya, H., Larson, R.F., Schulz, K.S., 2005. Accuracy of computerized tomographic evaluation of canine radio-ulnar incongruence in vitro. Veterinary Surgery 34, 108-113.

Hornof, W.J., Wind, A.P., Wallack, S.T., Schulz, K.S., 2000. Canine elbow dysplasia. The early radiographic detection of fragmentation of the coronoid process. Veterinary Clinics of North America: Small Animal Practice 30, 257-266.

House, M.R., Marino, D.J., Lesser, M.L., 2009. Effect of limb position on elbow congruity with CT evaluation. Veterinary Surgery 38, 154-160.

Hulse, D., Young, B., Beale, B., Kowaleski, M., Vannini, R., 2010. Relationship of the biceps-brachialis complex to the medial coronoid process of the canine ulna. Veterinary and Comparative Orthopaedics and Traumatology 23, 173-176.

Jaegger, G., Marcellin-Little, D.J., Levine, D., 2002. Reliability of goniometry in Labrador retrievers. American Journal of Veterinary Research 63, 979-986.

Janach, K.J., Breit, S.M., Künzel, W.W.F., 2006. Assessment of the geometry of the cubital (elbow) joint of dogs by use of magnetic resonance imaging. American Journal of Veterinary Research 67, 211–218

Janutta, V., Hamann, H., Klein, S., Tellhelm, B., Distl, O., 2006. Genetic analysis of three different classification protocols for the evaluation of elbow dysplasia in German shepherd dogs. Journal of Small Animal Practice 47, 75-82.

Keller, G.G., Kreeger, J.M., Mann, F.A., Lattimer, J.C., 1997. Correlation of radiographic, necropsy and histologic findings in 8 dogs with elbow dysplasia. Veterinary Radiology & Ultrasound 38, 272-276.

Knox IV, V.W., Sehgal, C.M., Wood, A.K.W., 2003. Correlation of ultrasonographic observations with anatomic features and radiography of the elbow joint in dogs. American Journal of Veterinary Research 64, 721-726.

Kramer, M., Gerwing, M., Hach, V., Schimke, E., 1997. Sonography of the musculoskeletal system in dogs and cats. Veterinary Radiology & Ultrasound 38, 139-149.

Kramer, A., Holsworth, I.G., Wisner, E.R., Kass, P.H., Schulz, K.S., 2006. Computed tomographic evaluation of canine radioulnar incongruence in vivo. Veterinary Surgery 35, 24-29.

Lamb, C.R., Wong, K., 2005. Ultrasonographic anatomy of the canine elbow. Veterinary Radiology & Ultrasound 46, 319-325.

Lang, J., Busato, A., Baumgartner, D., Flückiger, M., Weber, U.T., 1998. Comparison of two classification protocols in the evaluation of elbow dysplasia in the dog. Journal of Small Animal Practice 39, 169-174.

Lappalainen, A.K., Molsa, S., Liman, A., Laitinen-Vapaavuori, O., Snellman, M., 2009. Radiographic and computed tomography findings in Belgian shepherd dogs with mild elbow dysplasia. Veterinary Radiology & Ultrasound 50, 364-369.

Lavrijsen, I.C., Heuven, H.C., Voorhout, G., Meij, B.P., Theyse, L.F., Leegwater, P.A., Hazewinkel, H.A., 2012. Phenotypic and genetic evaluation of elbow dysplasia in Dutch Labrador retrievers, Golden retrievers, and Bernese Mountain Dogs. The Veterinary Journal 193, 486-492.

Mäki, K., Janss, L., Groen, A., Liinamo, A., Ojala, M., 2004. An indication of major genes affecting hip and elbow dysplasia in four Finnish dog populations. Heredity 92, 402-408.

Mason, D.R., Schulz, K.S., Fujita, Y., Kass, P.H., Stover, S.M., 2005. In vitro force mapping of normal canine humeroradial and humeroulnar joints. American Journal of Veterinary Research 66, 132-135.

Mason, D.R., Schulz, K.S., Samii, V.F., Fujita, Y., Hornof, W.J., Herrgesell, E.J., Long, C.D., Morgan, J.P., Kass, P.H., 2002. Sensitivity of radiographic evaluation of radio-ulnar incongruence in the dog in vitro. Veterinary Surgery 31, 125-132.

Meyer-Lindenberg, A., Fehr, M., Nolte, I., 2006. Co-existence of ununited anconeal process and fragmented medial coronoid process of the ulna in the dog. Journal of Small Animal Practice 47, 61-65.

Meyer-Lindenberg, A., Langhann, A., Fehr, M., Nolte, I., 2002. Prevalence of fragmented medial coronoid process of the ulna in lame adult dogs. The Veterinary Record 151, 230-234.

Meyer-Lindenberg, A., Langhann, A., Fehr, M., Nolte, I., 2003. Arthrotomy versus arthroscopy in the treatment of the fragmented medial coronoid process of the ulna (FCP) in 421 dogs. Veterinary and Comparative Orthopaedics and Traumatology 16, 204-210.

Miller, M.E., Christensen, G.C., Evans, H.E., 1993. Ligaments and joints of the thoracic limb. Miller's Anatomy of the Dog, Third Ed. W.B. Saunders Co. Philadelphia. London. Toronto. Montreal. Sydney. Tokyo, pp. 73-74.

Miyabayashi, T., Takiguchi, M., Schrader, S.C., Biller, D.S., 1995. Radiographic anatomy of the medial coronoid process of dogs. Journal of the American Animal Hospital Association 31, 125-132.

Moores, A.P., Benigni, L., Lamb, C.R., 2008. Computed tomography versus arthroscopy for detection of canine elbow dysplasia lesions. Veterinary Surgery 37, 390-398.

Muller-Gerbl, M., Putz, R., Hodapp, N., Schulte, E., Wimmer, B., 1989. Computed tomography-osteoabsorptiometry for assessing the density distribution of subchondral bone as a measure of long-term mechanical adaptation in individual joints. Skeletal Radiology 18, 507-512.

Murphy, S.T., Lewis, D.D., Shiroma, J.T., Neuwirth, L.A., Parker, R.B., Kubilis, P.S., 1998. Effect of radiographic positioning on interpretation of cubital joint congruity in dogs. American Journal of Veterinary Research 59, 1351-1357.

Oliveira, D., Martinez Baraldi Artoni, S., Marcos Orsi, A., Roque Rodriguez, A.I., 2003. Morphometric study of the medial collateral and oblique ligaments of the elbow joint of the dog (Canis familiaris). International Journal of Morphology 21, 23-28.

Olsson, S.-E., 1981. Pathophysiology morphology, and clinical signs of osteochondrosis in the dog. In: Pathophysiology in Small Animal Surgery, First Ed. Lea & Febiger, Philadelphia, USA, pp. 604-617.

Olsson, S.-E., 1983. The early diagnosis of fragmented coronoid process and osteochondritis dissecans of the canine elbow joint. Journal of the American Animal Hospital Association 19, 616-626.

Olstad, K., Ytrehus, B., Ekman, S., Carlson, C.S., Dolvik, N.I., 2008. Epiphyseal cartilage canal blood supply to the tarsus of foals and relationship to osteochondrosis. Equine Veterinary Journal 40, 30-39.

Padgett, G.A., Mostosky, U.V., Probst, C.W., Thomas, M.W., Krecke, C.F., 1995. The inheritance of osteochondritis dissecans and fragmented coronoid process of the elbow joint in Labrador retrievers. Journal of the American Animal Hospital Association 31, 327-330.

Palmer, A.W., Guldberg, R.E., Levenston, M.E., 2006. Analysis of cartilage matrix fixed charge density and three-dimensional morphology via contrast-enhanced micro-computed tomography. Proceedings of the National Academy of Sciences of the United States of America 103, 19255-19260.

Peremans, K., Vermeire, S., Dobbeleir, A., Gielen, I., Samoy, Y., Piron, K., Vandermeulen, E., Slegers, G., van Bree, H., De Spiegeleer, B., Dik, K., 2011. Recognition of anatomical predilection sites in canine elbow pathology on bone scans using micro-single photon emission tomography. The Veterinary Journal 188, 64-72.

Preston, C.A., Schulz, K.S., Kass, P.H., 2000. In vitro determination of contact areas in the normal elbow joint of dogs. American Journal of Veterinary Research 61, 1315-1321.

Preston, C.A., Schulz, K.S., Taylor, K.T., Kass, P.H., Hagan, C.E., Stover, S.M., 2001. In vitro experimental study of the effect of radial shortening and ulnar ostectomy on contact patterns in the elbow joint of dogs. American Journal of Veterinary Research 62, 1548-1556.

Probst, A., Modler, F., Kunzel, W., Mlynarik, V., Trattnig, S., 2008. Demonstration of the articular cartilage of the canine ulnar trochlear notch using high-field magnetic resonance imaging. The Veterinary Journal 177, 63-70.

Punke, J.P., Hulse, D.A., Kerwin, S.C., Peycke, L.E., Budsberg, S.C., 2009. Arthroscopic documentation of elbow cartilage pathology in dogs with clinical lameness without changes on standard radiographic projections. Veterinary Surgery 38, 209-212.

Reichle, J.K., Park, R.D., Bahr, A.M., 2000. Computed tomographic findings of dogs with cubital joint lameness. Veterinary Radiology & Ultrasound 41, 125-130.

Reichle, J.K., Snaps, F., 1999. The elbow. Clinical Techniques in Small Animal Practice 14, 177-186.

Reiland, S., Ordell, N., Lundeheim, N., Olsson, S.-E., 1978. Heredity of osteochondrosis, body constitution and leg weakness in the pig. A correlative investigation using progeny testing. Acta Radiologica.Supplementum 358, 123-137.

Remy, D., Neuhart, L., Fau, D., Genevois, J.P., 2004. Canine elbow dysplasia and primary lesions in German shepherd dogs in France. Journal of Small Animal Practice 45, 244-248.

Salg, K.G., Temwitchitr, J., Imholz, S., Hazewinkel, H.A.W., Leegwater, P.A.J., 2006. Assessment of collagen genes involved in fragmented medial coronoid process development in Labrador retrievers as determined by affected sibling-pair analysis. American Journal of Veterinary Research 67, 1713-1718.

Sallander, M.H., Hedhammar, A., Trogen, M.E., 2006. Diet, exercise, and weight as risk factors in hip dysplasia and elbow arthrosis in Labrador retrievers. Journal of Nutrition 136, 2050S-2052S.

Samoy, Y., Van Ryssen, B., Gielen, I., Walschot, N., van Bree, H., 2006. Review of the literature: elbow incongruity in the dog. Veterinary and Comparative Orthopaedics and Traumatology 19, 1-8.

Schwarz, T., Johnson, V.S., Voute, L., Sullivan, M., 2004. Bone scintigraphy in the investigation of occult lameness in the dog. Journal of Small Animal Practice 45, 232-237.

Seyrek-Intas, D., Michele, U., Tacke, S., Kramer, M., Gerwing, M., 2009. Accuracy of ultrasonography in detecting fragmentation of the medial coronoid process in dogs. Journal of the American Veterinary Medical Association 234, 480-485.

Shum, L., Nuckolls, G., 2002. The life cycle of chondrocytes in the developing skeleton. Arthritis Research 4, 94-106.

Sjöström, L., 1998. Ununited anconeal process in the dog. Veterinary Clinics of North America: Small Animal Practice 28, 75-86.

Smith, T.J., Fitzpatrick, N., Evans, R.B., Pead, M.J., 2009. Measurement of ulnar subtrochlear sclerosis using a percentage scale in Labrador retrievers with minimal radiographic signs of periarticular osteophytosis. Veterinary Surgery 38, 199-208.

Snaps, F.R., Balligand, M.H., Saunders, J.H., Park, R.D., Dondelinger, R.F., 1997. Comparison of radiography, magnetic resonance imaging, and surgical findings in dogs with elbow dysplasia. American Journal of Veterinary Research 58, 1367-1370.

Snaps, F.R., Park, R.D., Saunders, J.H., Balligand, M.H., Dondelinger, R.F., 1999. Magnetic resonance arthrography of the cubital joint in dogs affected with fragmented medial coronoid processes. American Journal of Veterinary Research 60, 190-193.

Swenson, L., Audell, L., Hedhammar, A., 1997. Prevalence and inheritance of and selection for hip dysplasia in seven breeds of dogs in Sweden and benefit: cost analysis of a screening and control program. Journal of the American Veterinary Medical Association 210, 207-214.

Tellhelm, B., 2011. Grading primary ED-lesions and elbow osteoarthrosis according to the IEWG protocol. Proceedings of the 26th Annual Meeting of International Elbow Working Group. Amsterdam, Holland. pp. 14-15.

Temwichitr, J., Leegwater, P.A., Hazewinkel, H.A., 2010. Fragmented coronoid process in the dog: a heritable disease. The Veterinary Journal 185, 123-129.

Tirgari, M., 1974. Clinical radiographical and pathological aspects of arthritis of the elbow joint in dogs. Journal of Small Animal Practice 15, 671-679.

Tirgari, M., 1980. Clinical, radiographical and pathological aspects of ununited medial coronoid process of the elbow joint in dogs. Journal of Small Animal Practice 21, 595-608.

Ubbink, G.J., van de Broek, J., Hazewinkel, H.A., Rothuizen, J., 1998. Cluster analysis of the genetic heterogeneity and disease distributions in purebred dog populations. The Veterinary Record 142, 209-213.

Ubbink, G.J., van de Broek, J., Hazewinkel, H.A., Wolvekamp, W.T., Rothuizen, J., 2000. Prediction of the genetic risk for fragmented coronoid process in Labrador retrievers. The Veterinary Record 147, 149-152.

van Bree, H., Van Ryssen, B., 1995. Arthroscopy in the diagnosis and treatment of front leg lameness. Veterinary Quartery 17 Supplement 1 S32-S34.

van Bruggen, L.W., Hazewinkel, H.A., Wolschrijn, C.F., Voorhout, G., Pollak, Y.W., Barthez, P.Y., 2010. Bone scintigraphy for the diagnosis of an abnormal medial coronoid process in dogs. Veterinary Radiology & Ultrasound 51, 344-348.

Van der Korst, J., Skoloff, L., Miller, E., 1968. Senescent pigmentation of cartilage and degenerative joint disease. Archives of Pathology 86, 40-47.

Van Ryssen, B., van Bree, H., 1997. Arthroscopic findings in 100 dogs with elbow lameness. The Veterinary Record 140, 360-362.

Vermote, K.A., Bergenhuyzen, A.L., Gielen, I., van Bree, H., Duchateau, L., Van Ryssen, B., 2009. Elbow lameness in dogs of six years and older. Veterinary and Comparative Orthopaedics and Traumatology 23, 43-50.

Villamonte-Chevalier, A., Soler, M., Sarria, R., Agut, A., Latorre, R., 2012. Anatomical study of fibrous structures of the medial aspect of the canine elbow joint. The Veterinary Record 171, 596-596.

Voorhout, G., Hazewinkel, H.A.W., 1987. Radiographic evaluation of the canine elbow joint with special reference to the medial humeral condyle and the medial coronoid process. Veterinary Radiology 28, 158-165.

Wagner, K., Griffon, D.J., Thomas, M.W., Schaeffer, D.J., Schulz, K., Samii, V.F., Necas, A., 2007. Radiographic, computed tomographic, and arthroscopic evaluation of experimental radio-ulnar incongruence in the dog. Veterinary Surgery 36, 691-698.

Wind, A.P., 1986. Elbow incongruity and developmental elbow diseases in the dog: part I. Journal of the American Veterinary Medical Association 22, 711-724.

Wind, A.P., Packard, M.E., 1986. Elbow incongruity and developmental elbow diseases in the dog: part II. Journal of the American Veterinary Medical Association 22, 725-730.

Wolschrijn, C.F., Gruys, E., van der Wiel, C.W., Weijs, W.A., 2008. Cartilage canals in the medial coronoid process of young Golden retrievers. The Veterinary Journal 176, 333-337.

Wolschrijn, C.F., Weijs, W.A., 2004. Development of the trabecular structure within the ulnar medial coronoid process of young dogs. The Anatomical Record. Part A, Discoveries in Molecular, Cellular, and Evolutionary Biology 278, 514-519.

Wolschrijn, C.F., Weijs, W.A., 2005. Development of the subchondral bone layer of the medial coronoid process of the canine ulna. The Anatomical Record. Part A, Discoveries in Molecular, Cellular, and Evolutionary Biology 284, 439-445.

Wosar, M.A., Lewis, D.D., Neuwirth, L., Parker, R.B., Spencer, C.P., Kubilis, P.S., Stubbs, W.P., Murphy, S.T., Shiroma, J.T., Stallings, J.T., Bertrand, S.G., 1999. Radiographic evaluation of elbow joints before and after surgery in dogs with possible fragmented medial coronoid process. Journal of the American Veterinary Medical Association 214, 52-58.

Wucherer, K.L., Ober, C.P., Conzemius, M.G., 2012. The use of delayed gadolinium enhanced magnetic resonance imaging of cartilage and T2 mapping to evaluate articular cartilage in the normal canine elbow. Veterinary Radiology & Ultrasound 53, 57-63.

Ytrehus, B., Carlson, C.S., Ekman, S., 2007. Etiology and pathogenesis of osteochondrosis. Veterinary Pathology 44, 429-448.

Ytrehus, B., Ekman, S., Carlson, C.S., Teige, J., Reinholt, F.P., 2004. Focal changes in blood supply during normal epiphyseal growth are central in the pathogenesis of osteochondrosis in pigs. Bone 35, 1294-1306.

Chapter 3

Radiographic, computed tomographic, and arthroscopic findings in Labrador retrievers with medial coronoid disease

S.F. Lau[1]; L.F.H. Theyse[2]; G. Voorhout[1]; H.A.W. Hazewinkel[2]

[1] Division of Diagnostic Imaging, Faculty of Veterinary Medicine, Utrecht University, Yalelaan 108, 3584CM, Utrecht, The Netherlands

[2] Department of Clinical Sciences of Companion Animals, Faculty of Veterinary Medicine, Utrecht University, Yalelaan 108, 3584CM, Utrecht, The Netherlands

Submitted to Veterinary Surgery

Abstract

Objective:

To describe the radiographic, computed tomographic (CT), and arthroscopic findings in Labrador retrievers diagnosed with medial coronoid disease (MCD) in different age groups, and to compare the ulnar subtrochlear sclerosis (STS) observed on radiographs with the ratio between the mean attenuation of the ulnar subtrochlear bone and the mean attenuation of the cortical bone measured on CT.

Methods:

31 patients (31 elbow joints) and six healthy Labrador retrievers (6 elbow joints) as a control population. Radiographic, CT, and intra-operative arthroscopic images (2008-2012) were evaluated. Statistical analysis was performed for the descriptive study, evaluate the difference of the findings between age groups, and investigate the correlation between radiographic and CT evaluated ulnar STS.

Results:

Ulnar STS (87.6%) was the most common radiographic findings in age group when first complaint of lameness at ≤12 months and blurring of the cranial edge of the medial coronoid process (MCP; 66.7%) was the most common radiographic findings in age group when first complaint of lameness at >12 months. Fragmentation of the MCP (≤12 months, 93.8% and >12 months, 66.7%) was the most common findings on CT in both age groups. A displaced fragment (68.8%) was the most common arthroscopic finding in dogs ≤12 months, whereas osteochondromalacia (53.3%) was the most common findings in dogs >12 months. Sensitivity of radiography and CT in detecting MCD in dogs ≤12 months was 93.8% and in dogs >12 months was 73.3% and 66.7%, respectively. Radiographic evaluated ulnar STS was strongly correlated with CT evaluated ulnar STS.

Conclusion:

Our results demonstrated a wide range of radiographic, CT, and arthroscopic findings in Labrador retrievers. In order to understand the development of the STS, additional studies investigating the intramedullary bone cavity at the ulnar subtrochlear notch are critical. We conclude that MCD can occur without there being relevant radiographic and CT findings and that a thorough physical examination and history remain essential to the diagnosis.

Introduction

The term medial coronoid disease (MCD) has been introduced as being more representative than the term fragmented medial coronoid process (FMCP), as it includes all pathological changes of articular cartilage and subchondral bone at its vicinity (Moores et al., 2008; Fitzpatrick et al., 2009). The prevalence of MCD was found to be 11-50% in Labrador retrievers presenting with forelimb lameness (Meyer-Lindenberg et al., 2002; Fitzpatrick et al., 2009), and 6% in a screened cohort of Dutch Labrador retrievers (Lavrijsen et al., 2012).

Because of its availability and easy access, radiography is the first-line tool for diagnosing MCD, despite its variable sensitivity, which ranges from 10% to 62% (Wosar et al., 1999; Haudiquet et al., 2002). A presumptive diagnosis of MCD is frequently based on the detection of secondary degenerative joint changes, such as periarticular osteophytosis at specific joint locations, ulnar subtrochlear sclerosis (STS), and blunting or blurring of the cranial edge of the medial coronoid process (MCP), rather than on the detection of the primary lesion (Carpenter et al., 1993; Keller et al., 1997; Hornof et al., 2000; Holsworth et al., 2005; Cook et al., 2009). In some cases, primary lesions, such as fragmentation of the MCP, medial compartment erosion of the humeral trochlea in the case of osteochondritis dissecans (OCD)-like lesions, and the presence of radioulnar incongruity (RUI), can be seen concomitantly with secondary changes (Hornof et al., 2000; Lavrijsen et al., 2012). Computed tomography (CT) is superior to radiography because it enables assessment of the MCP on transverse slices and multiplanar reconstructed images (Holsworth et al., 2005; Kramer et al., 2006; Samoy et al., 2006; Wagner, et al., 2007). Reichle *et al.* reported the most common CT finding to be abnormal shape of MCP (97%), sclerosis of the MCP (95%), followed by irregularity of the radial incisures (83%), osteophytosis (74%), fragmentation of the MCP (28%), fissures of the MCP (27%), and humeral trochlear subchondral lucency (16%; Reichle et al., 2000). However, neither CT nor radiography allows assessment of the integrity of articular cartilage, which can be achieved with arthroscopy. This technique has been described since 1993 (Van Ryssen et al., 1993), and has become very popular due to its minimally invasive diagnostic and therapeutic characteristics. Arthroscopy in 263 dogs revealed fragmentation of the MCP as the most common finding (64.1%), followed by contact lesions in the humeral trochlea (49.0%), and cartilage fissures (18.3%; Fitzpatrick et al., 2009). In addition, arthroscopy is claimed to be of greater diagnostic value than radiography and CT in detecting experimentally induced RUI (Wagner, et al., 2007).

The aim of the present study was to describe the radiographic, CT, and arthroscopic findings of the elbow joints of Labradors retrievers diagnosed with MCD, and to compare the findings in dogs when lameness first complaint at ≤12 months with those

when lameness first complaint at >12 months. We also investigated the correlation of the ratio between the mean attenuation of the ulnar subtrochlear bone and the mean attenuation of the cortical bone measured on CT with the ulnar STS observed on radiographic findings.

Materials and methods

Data collection

Labrador retrievers that were referred to the University Clinic for Companion Animals at Utrecht University from 2008 until early 2012 with forelimb lameness, and were suspected of MCD on basis of the results of clinical and radiographic examination, were included in the study. Once the dogs were scheduled for arthroscopy, CT of the elbow joints was done prior to arthroscopy, but CT-findings had no effect on the decision to perform arthroscopy. Clinical examination, radiography, CT, and arthroscopy were performed within 3 months. Healthy Labrador retrievers from a non-related study, that underwent an identical complete radiographic and CT evaluation, served as a control population. Their elbow joints were diagnosed to be healthy at necropsy and histological examination after the dogs were euthanized. The study was approved by the Ethics Committee of Utrecht University as required by Dutch law.

Radiographic assessment

Four radiographic views consisted of craniocaudal (CrCd), craniolateral-caudomedial oblique (CrL-CdMO), 90° flexed mediolateral (ML), and extended 15° supinated ML projections of all investigated elbow joints were obtained as described before (Voorhout and Hazewinkel, 1987). The radiographs were assessed by a panel of three specialists (one board certified radiologist and two board certified veterinary orthopedic surgeons), and the diagnosis was achieved by consensus. All three observers are active participants of the national screening program according to the International Elbow Working Group (IEWG) guidelines. During the radiographic evaluation, the observers were unaware of the dog's signalment and surgical findings. Radiographs were evaluated systematically for elbow dysplasia (ED) according to the guidelines of the IEWG (Tellhelm, 2011): grade 0 for elbows without evidence of a primary lesion, osteophytosis, and sclerosis; grade 1 for elbows with osteophytosis less than 2 mm in size, and/or presence of ulnar STS and/or blunting or blurring of the cranial edge of MCP; grade 2 for elbows with osteophytosis of 2 to 5 mm in size and/or obvious sclerosis in combination with suspected primary lesion of RUI, ununited anconeal process (UAP), fragmentation of the MCP and OCD-like lesion; and grade 3 for elbows with osteophytosis more than 5 mm in size and/or obvious primary lesion (RUI, UAP,

fragmentation of MCP, or OCD-like lesion). Grade 0 was considered free from MCD and grades 1 to 3 were considered MCD positive. Ulnar STS, which is characterized by the loss of the trabecular bone architecture and increased perceived density (Lappalainen et al., 2009), was assessed subjectively as negative, mild, or obvious. Blunting or blurring of the cranial edge of the MCP was characterized by the loss of a clearly defined cranial edge of the MCP on ML and extended supinated ML views. Similar to primary lesions, this criterion was scored as negative, suspect or obvious on radiographs.

Computed tomographic assessment

Dogs were anesthetized and positioned in dorsal recumbency on the scanner table with the forelimbs extended and the antebrachia parallel to each other during scanning (Fig. 1). Transverse views were made perpendicular to the antebrachia in 1 mm thick slices with 120 kV, 120 mA, and 1 sec scanning time. CT studies were evaluated by a board certified radiologist who was unaware of the signalment, and the clinical, radiographic, and arthroscopic findings. Series were reviewed in transverse slices, as well as in sagittal and dorsal reconstructions. The evaluation criteria included the following signs: periarticular osteophytosis; abnormal contour and structure of the MCP; cyst-like lesion at the radial incisure of the ulna and humeral trochlea; irregularity of the radial incisure of the ulna; and evidence of other primary lesions, such as fragmentation of MCP, RUI, and OCD-like lesions (Reichle et al., 2000). Joints were considered congruent when there was absence of a step defect between the proximal radius and ulna in the sagittal plane. In contrast with the radiographical diagnosis of MCD based on a combination of primary and secondary lesions, on CT, MCD was based solely on the evidence of a primary lesion (i.e. fragmentation of MCP)

Fig. 1. *Dog was positioned in dorsal recumbency on the computed tomographic scanning table.*

Arthroscopic assessment

Arthroscopy was performed to confirm the diagnosis and to treat MCD by removal of diseased bone and cartilage (Van Ryssen et al., 1993). All the arthroscopic procedures were performed by the same board certified veterinary orthopedic surgeon. The medial compartment of the elbow joint was checked thoroughly during surgery. Complete surgical records together with the captured arthroscopic images were reviewed to identify the different features of MCD: coronoid dysplasia characterized by osteomalacia and chondromalacia, fragmentation with a fragment in situ or displaced fragments, synovitis, and RUI. Pathological changes of the cartilage at the ulnar joint surface of the MCP and humeral trochlea were graded using a 5-point ordinal scale based on Modified Outerbridge Scores (Table 1; Schulz, 2003; Goldhammer et al., 2010). Osteomalacia and chondromalacia were defined as softening of the subchondral bone and cartilage (Fig. 2), which is easily removed by probing and curettage. Synovitis was assessed subjectively according to the appearance of the synovium, with erythematous discoloration of the synovial membrane and in more severe cases, a large number of villous protrusions.

MOS	Description of cartilage
0	Normal cartilage appearance
1	Chondromalacia (softening and swelling of the cartilage)
2	Partial thickness fibrillation and fissuring of the cartilage
3	Full thickness cartilage fissuring
4	Full thickness cartilage erosion with exposure of the subchondral bone

Table 1. *Modified Outerbridge Scoring (MOS) System (Schulz, 2003; Goldhammer et al., 2010) used to evaluate articular cartilage of the medial coronoid process and humeral trochlea during arthroscopy.*

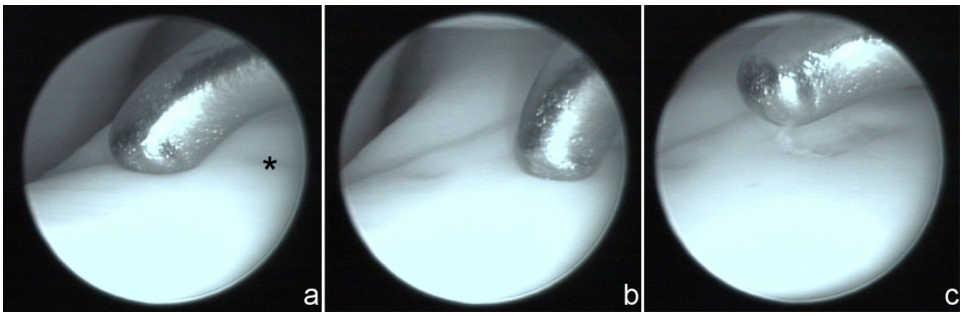

Fig. 2. *Appearance of chondromalacia (a) before probing of cartilage at (*), (b) probing, (c) after probing, indentation of the cartilage surface at the medial coronoid process.*

Study I: Radiographic, computed tomographic and arthroscopic findings in clinical patients with medial coronoid disease

Radiographic, CT, and arthroscopic findings were investigated and reported in clinical patients with medial coronoid disease grouped by age at first complaint of lameness. All the findings were compared statistically between two age groups in order to recognize the difference and the most common lesions found in MCD affected dogs in each age groups. Sensitivity of radiography, CT, and the combination of both diagnostic modalities in detecting MCD was calculated for both age groups.

Study II: Ulnar subtrochlear sclerosis investigation

Radiographs and CT images of elbow joints obtained from the patient group (*n*=9 elbows) diagnosed with MCD and ulnar STS without periarticular osteophytosis were selected and compared with those elbow joints obtained from healthy dogs (*n*=6 elbows), which were negative for sclerosis. Diagnosis of sclerosis was achieved in consensus within the 3 panelists in study I and converted into a binary score (present or absent). On the sagittal reconstructed CT images, a region of interest (ROI) was drawn at the ulnar subtrochlear bone area (Fig. 10c and f), excluding cortical bone. The mean attenuation (HU) was measured within the ROI. Another ROI was drawn at the cortical bone (Fig. 10c) and the mean attenuation of the cortical bone in this ROI was measured. The ratio between the mean attenuation of the ulnar subtrochlear bone and the mean attenuation of the cortical bone was calculated and used for analysis. The correlation between the radiographic binary score and the ratio of the CT mean attenuation was investigated as described in statistical analysis.

Statistical Analysis

SPSS for Windows (SPSS version 16.0, SPSS Inc.) was used for statistical analysis. In study I, descriptive statistics were used to describe the diverse spectrum of the lesions and the difference of the radiographic, computed tomographic, and arthroscopic findings in dogs when lameness first complaint at ≤12 months and dogs when lameness first complaint at >12 months of age were compared using the Mann-Whitney U test in a non-parametric value. Sensitivity of radiography, CT, and the combination of both techniques were reported by calculating the percentage of actual MCD positive cases which were correctly identified. In study II, the age distribution between the patient and healthy groups was compared by using Mann-Whitney U test before the correlation study. In order to investigate the biserial correlation between CT attentuation and ulnar STS (in binary), the Microsoft EXCEL add-in program (XLSTAT 2012, Addinsoft, Inc.) was used. Correlations and differences were considered significant when $P<0.05$. We used the following guidelines to interpret the strength of relationship between the variables: values between 0 and 0.3 indicate a weak relationship, 0.3 to 0.7 indicate a moderate relationship, and 0.7 to 1.0 indicate a strong relationship (Ratner, 2009).

Results

Clinical data

Thirty-one Labrador retrievers (*n*=31 elbows) with clinical lameness were identified and 16 dogs (51.6%) were ≤12 months of age when first complaint of lameness (Fig. 3). All dogs were presented with a history of persistent or intermittent lameness. Crepitation and joint effusion were detected in the affected joints during the physical examination and pain reactions were elicited by joint flexion and extension.

Of the 16 dogs (*n*=16 elbows) ≤12 months of age (mean ± SD age 7.9 ± 2.1 months, range, 5-12 months), 11 were male (eight intact and three neutered) and five female (four intact and one neutered). The dogs weighed 30.3 ± 4.9 kg (mean ± SD) with a range of 22-38 kg. Mean (± SD) duration of lameness was 2.4 ± 1.5 months (range, 1-5 months). In the 15 dogs (n=15 elbows) >12 months when first complaint of lameness (mean ± SD age 51.6 ± 26.4 months, range, 13-97 months), nine were male (five intact and four neutered) and six female (one intact and five neutered). The dogs weighed 34.4 ± 5.7 kg (mean ± SD) with a range of 24-42 kg. Mean (± SD) duration of lameness was 5.9 ± 3.5 months (range, 1-13 months).

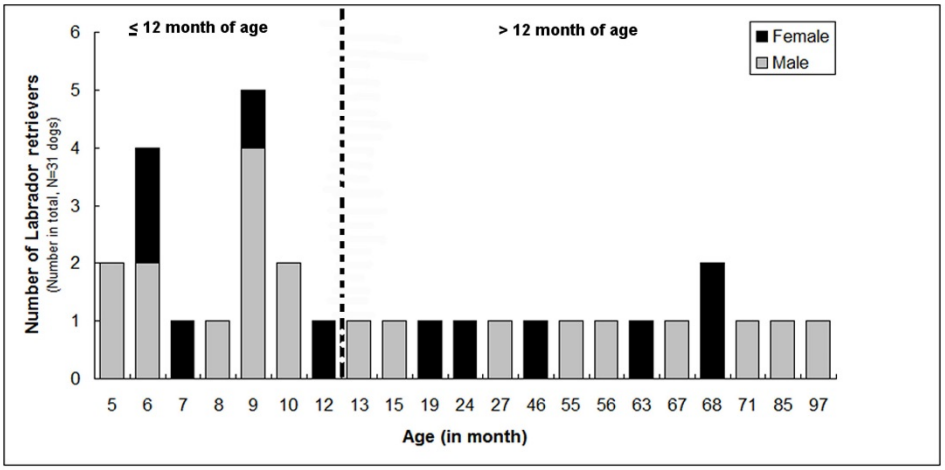

Fig. 3. *Age and gender distribution of 31 Labrador retrievers with arthroscopically confirmed medial coronoid disease (MCD).*

Healthy controls

Six healthy elbow joints from six age-matched Labrador retrievers (four males and two females) from a non-related study were compared with the joints of the MCD dogs younger than 12 months of age. The dogs were 6.5 ± 0.8 months (range, 5-7 months) old and weighed 27.2 ± 4.9 kg (range, 19-34 kg).

Study I: Radiographic, computed tomographic and arthroscopic findings in clinical patients with medial coronoid disease

Radiographic findings

In the 16 dogs ≤12 months, 1 of 16 (6.2%) elbow joints were scored as ED grade 0, 1 (6.2%) as ED grade 1, 12 (75.0%) as grade 2, and 2 (12.5%) as grade 3 (Fig. 4). Ulnar STS was the most common radiographic findings in this group and was present in 14 (87.6%) elbow joints, with 7 elbows (43.8%) showing mild sclerosis and 7 (43.8%) showing obvious sclerosis. Blunting or blurring of the cranial edge of the MCP was detected in 12 (75.0%) elbow joints. In 9 (56.3%) elbow joints, periarticular osteophytosis was detected, with the most common site being the medial edge of the MCP ('g' on IEWG score; Fig. 5), followed by the proximal surface of the anconeal process ('a' on IEWG score; Fig. 5). Radiographically, primary lesions such as obvious fragmentation of the MCP were detected in 1 (6.2%) elbow joints and 12 (75.0%) joints being considered suspect, based on the secondary degenerative changes. An OCD-like lesion was identified in 3 (18.8%) elbow joints on the humeral trochlea, and 2 (12.5%) elbow joints were diagnosed as showing RUI (Fig. 6).

In the 15 dogs >12 months, 4 of 15 (26.7%) elbow joints were scored as ED grade 0, 4 (26.7%) as ED grade 1, 5 (33.3%) as ED grade 2, and 2 (13.3%) as ED grade 3 (Fig. 4). Blunting or blurring of the cranial edge of the MCP was the most common radiographic finding in this group and was present in 10 (66.7%) elbow joints, followed by different degrees of ulnar STS found in 8 (53.3%) joints, with 6 (40.0%) interpreted as mild sclerosis and 2 (13.3%) as obvious sclerosis. Only 6 (40.0%) elbow joints showed evidence of periarticular osteophytosis, with the most common site being the medial edge of the MCP ('g' on IEWG score; Fig. 5), followed by the cranial aspect of the radial head ('b' on IEWG score; Fig. 5). Obvious fragmentation of the MCP was detected radiographically in 1 (6.7%) elbow joints and 6 (40.0%) being considered suspect. RUI was present in 2 (13.3%) elbows. No elbow joints showed evidence of OCD-like lesion (Fig. 6). Four elbow joints were interpreted as radiographically normal.

Based on the combination of the primary and secondary lesions, the sensitivity of radiography for detecting MCD in our study was 93.8% in dogs ≤12 months of age and 73.3% in dogs >12 months of age. Statistically, the degree of ulnar STS evaluated radiographically was significantly different (*P*=0.02) between dogs ≤ and dogs >12 months, with more severe ulnar STS scored in dogs ≤12 months. Although there was some degree of differences in other radiographic findings between both age groups, the differences were not significant (*P*=0.068-0.946).

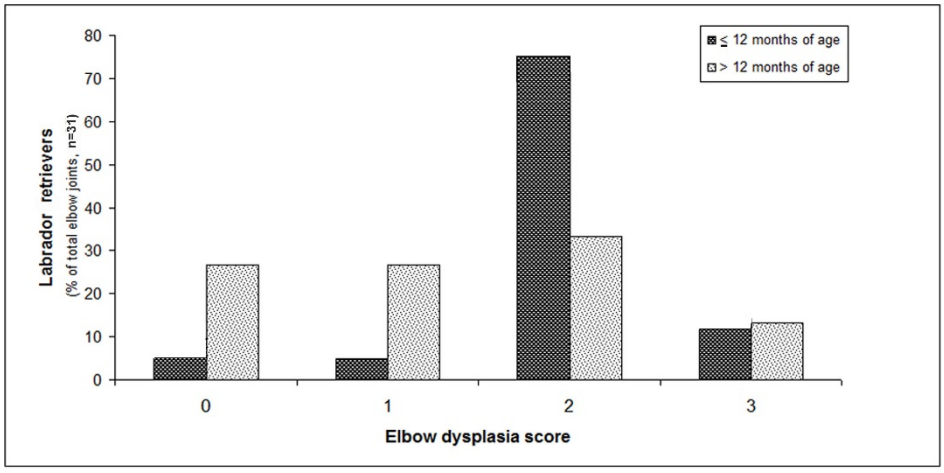

Fig. 4. *The distribution of elbow dysplasia (ED) scores in Labrador retrievers ≤ and >12 months.*

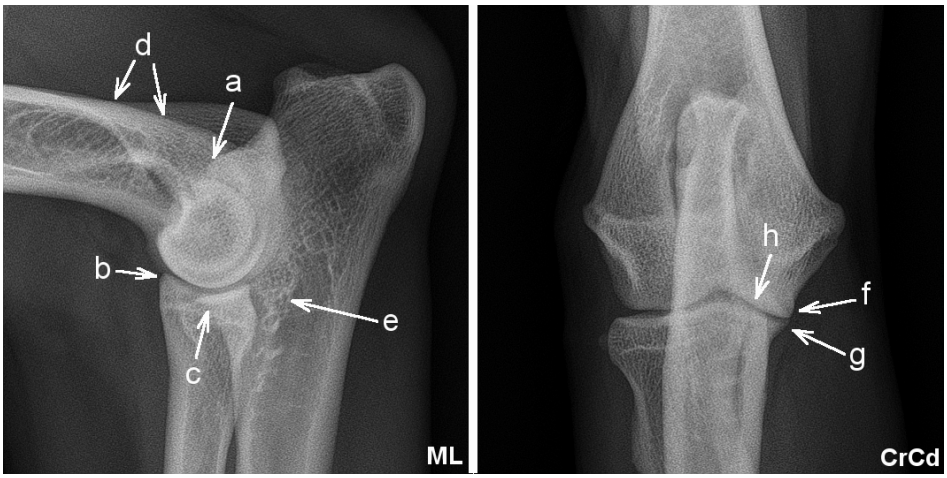

Fig. 5. *The mediolateral (ML) and craniocaudal (CrCd) views show the radiographic assessment locations for periarticular osteophytosis at the (a) proximal surface of the anconeal process, (b) the cranial aspect of the radial head, (c) the cranial edge of the medial coronoid process, (d) the caudal surface of the lateral condylar ridge, (f) the medial contour of the humeral trochlea, and (g) the medial contour of the medial coronoid process. The trochlear notch at the base of the coronoid process was assessed for sclerosis (e) and the subchondral bone of the humeral trochlea was assessed for an indentation (h).*

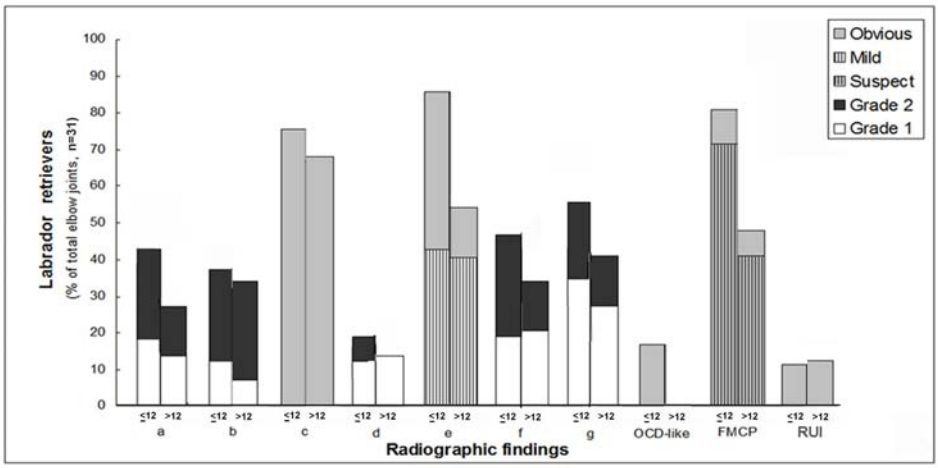

Fig. 6. *The distribution of scores (in %) for the screening sites and primary lesions that constitute medial coronoid disease (MCD) detected in Labrador retrievers aged ≤12 months and >12 months. At sites a, b, d, f and g, periarticular osteophytosis was scored with osteophytes <2 mm (grade 1), 2 to 5 mm (grade 2), or >5 mm (grade 3) in size. At site c, blurring or blunting in the cranial edge of the medial coronoid process (MCP); e, the presence of sclerosis; and OCD-like lesion (site h), the presence of an indentation*

of the subchondral bone on the humeral trochlea were scored. Primary lesions were scored 'suspect' based on secondary changes and lesions were scored 'obvious' if clearly identified on radiographs. OCD, osteochondritis dissecans; FMCP, fragmentation of MCP; RUI, joint incongruity.

Computed tomographic findings

In dogs ≤12 months of age (16 elbow joints), the most common CT finding was 'obvious' fragmentation of MCP, which was found in 15 (93.8%) elbow joints. Osteophytosis was detected in 12 (75.0%) elbow joints, with 5 (31.2%) joints being interpreted as grade 1, 5 (31.2%) as grade 2, and 2 (12.5%) as grade 3. Of the 16 elbow joints, 9 (56.2%) were considered to have sclerosis of the MCP, cyst-like lesions were found on the radial incisure of the ulna and humeral trochlea in 9 (56.2%) elbow joints, an OCD-like lesion was detected on the humeral trochlear in 8 (50.0%) elbow joints, and RUI was detected in 3 (18.8%) elbow joints. Change in MCP contour and structure was detected in 1 (6.2%) elbow joint (Fig. 8). CT images showed 'obvious' fragmentation of MCP in a dog that had negative radiographic findings (Fig. 7a).

In the dogs >12 months of age (15 elbow joints), the most common CT finding was 'obvious' fragmentation of MCP, which was found in 10 (66.7%) elbow joints and 1 (6.7%) joint being interpreted as 'suspect'. Osteophytosis was detected in 9 (60.0%) elbow joints: 5 (33.3%) grade 1, 3 (20.0%) with grade 2, and 1 (6.7%) with grade 3. Cyst-like lesions on the radial incisure of the ulna and humeral trochlea were detected in 4 (26.7%) elbow joints, and OCD-like lesions of the humeral trochlea were detected in 4 (26.7%) elbow joints. Changes in the MCP contour were detected in only 3 (20.0%) elbow joints on CT images. RUI was detected in 1 (6.7%) elbow joint, as was lucency at the MCP. Sclerotic lesions were not detected in the older dogs (Fig. 8). Of the four dogs that had negative radiographic findings, one showed evidence of 'suspect' fragmentation of MCP; the others had normal CT findings.

The sensitivity of CT in detecting MCD in our study was 93.8% in dogs ≤12 months of age and 66.7% in dogs >12 months of age, based on the evidence of fragmentation of MCP. Statistically, the degree of sclerosis detected at the MCP on CT was significantly different (P=0.001) between dogs ≤ and dogs >12 months, with more severe sclerosis at the MCP found in dogs ≤12 months. The differences of other CT findings were not significant (P=0.063-0.963).

Combination of both radiographic and computed tomographic findings

The sensitivity of the combination of both radiography and CT in detecting MCD was 100% in dogs ≤12 months and 80% in dogs >12 months.

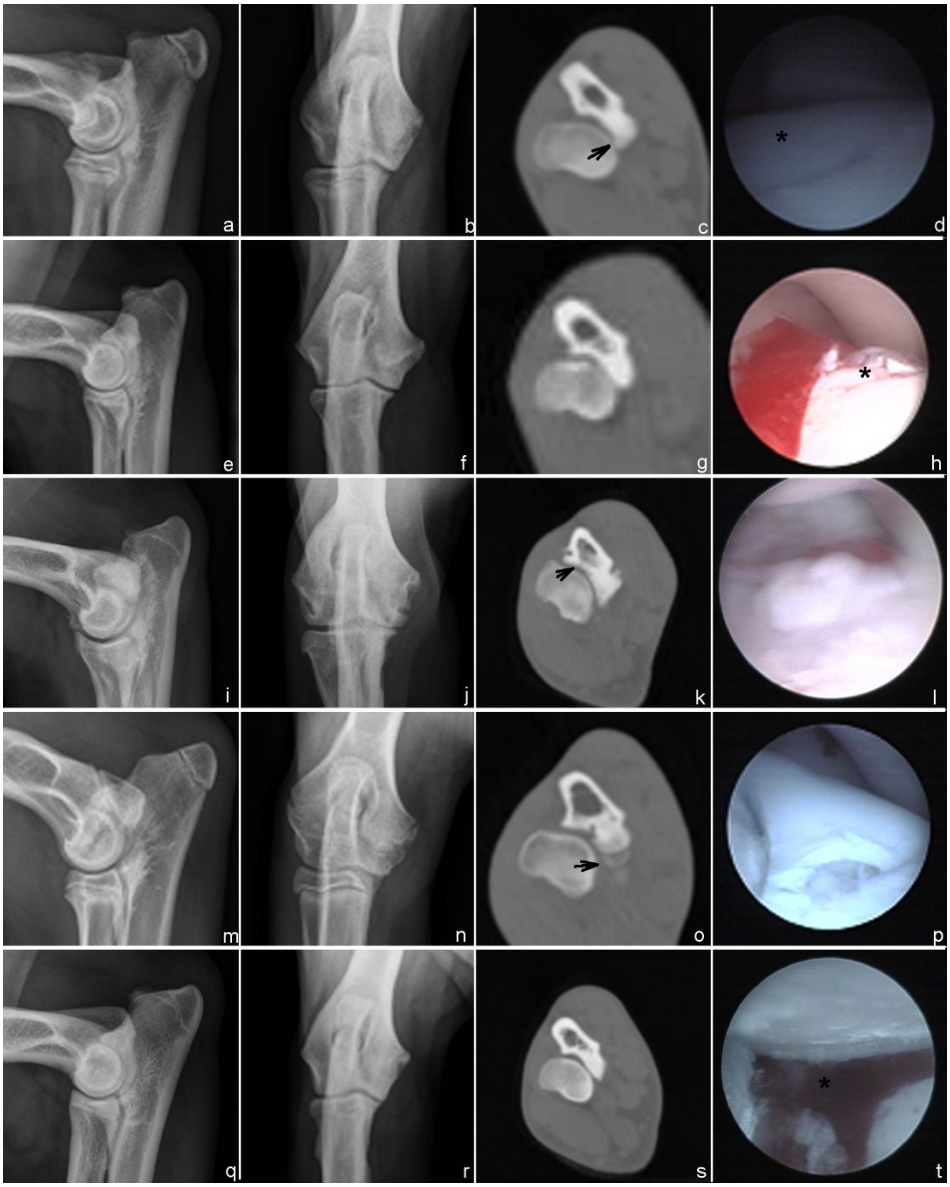

Fig. 7. *Radiographic images (mediolateral and craniocaudal projections), transverse view of the computed tomographic (CT) image matched with the arthroscopic image demonstrating a spectrum of findings. (a-d) Right elbow joint obtained from a 6-month-old neutered female Labrador retriever with normal radiographic findings; however, 'obvious' indications of fragmentation of the MCP (arrow) and joint incongruity (RUI) were identified on CT images. During arthroscopy, displaced bone fragment (*) was found with Modified Outerbridge grade 2 cartilage pathology at the medial coronoid process*

(MCP) and humeral trochlea, without evidence of RUI. (e-h) Right elbow joint obtained from a 68-month-old neutered female Labrador retriever with normal radiographic and CT findings. During arthroscopy, bone fragments (*) were found with Modified Outerbridge grade 4 cartilage pathology at the MCP and humeral trochlea, without evidence of RUI. (i-l) Right elbow joint obtained from a 15-month-old intact male Labrador retriever with Elbow Dysplasia (ED) grade 3 with obvious ulnar subtrochlear sclerosis (STS) and abnormal cranial edge of MCP on radiographic images. Primary lesions such as fragmentation of MCP and RUI were identified. On CT images, periarticular osteophytosis grade 3, abnormal MCP contour, cyst-like lesion on the radial incisure of the ulna (arrow), fragmentation of MCP, and RUI were identified. During arthroscopy, bone fragment was found with Modified Outerbridge grade 4 cartilage pathology at the MCP and humeral trochlea, without evidence of RUI. (m-p) Left elbow joint obtained from a 5-month-old neutered male Labrador retriever diagnosed ED grade 2 with obvious ulnar STS and 'suspect' fragmentation of MCP. On CT images, periarticular osteophytosis grade 2, abnormal MCP contour and lucency (arrow), cyst-like lesion at the ulnar radial incisure, and fragmentation of MCP were identified. Neither diagnostic technique showed evidence of RUI. During arthroscopy, a bone fragment was found with Modified Outerbridge grade 1 cartilage pathology at the MCP and grade 3 at the humeral trochlea, with concrete evidence of RUI. (q-t) Right elbow joint obtained from a 67-month-old intact male Labrador retriever with normal radiographic findings. The only finding on CT was abnormal MCP contour. During arthroscopy, bone fragment was found with Modified Outerbridge grade 4 at the MCP (*) and humeral trochlea.

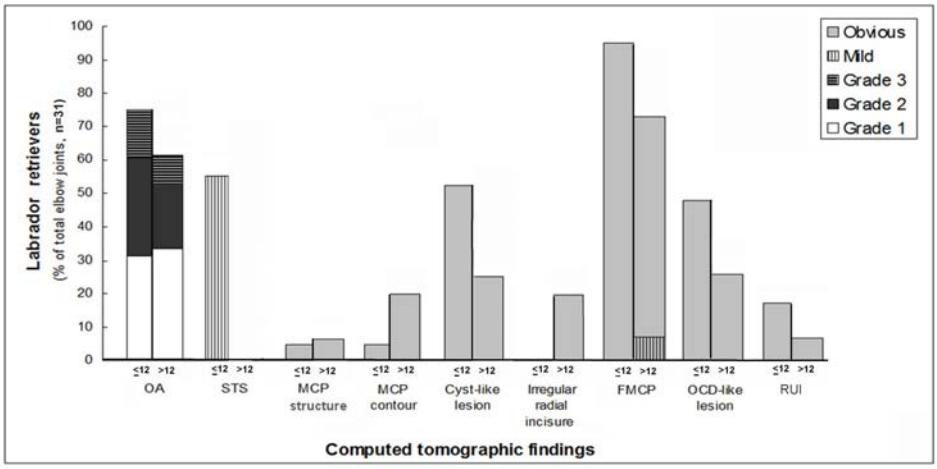

Fig. 8. *The distribution of lesions (in %) detected on computed tomography in Labrador retrievers ≤ and >12 months. OA, periarticular osteophytosis; STS, ulnar subtrochlear sclerosis; MCP, medial coronoid process; FMCP, fragmentation of medial coronoid process; OCD, osteochondritis dissecans; RUI, joint incongruity.*

Arthroscopic findings

All the Labrador retrievers presented with lameness were diagnosed with different features of MCD and synovitis during arthroscopy. In dogs ≤12 months, a displaced fragment was found in 11 (68.8%) elbow joints, fragment in situ in 3 (18.8%) elbow joints, and osteochondromalacia in 2 (12.5%) elbow joints. The median Modified Outerbridge score of the MCP was 2, and it was 4 for the humeral trochlea. Two (12.5%) of the elbow joints were diagnosed as having RUI during arthroscopy (Fig. 9).

In dogs >12 months, 8 (53.3%) elbow joints were found to have osteochondromalacia at arthroscopy, 6 (40.0%) a displaced fragment, and 1 (6.7%) a fragment in situ. The median Modified Outerbridge score of the MCP was 1 and it was 4 for the humeral trochlea. None of the dogs was diagnosed as having RUI during arthroscopy (Fig. 9).

Statistically, the different features of MCD were significantly different (*P*=0.04) between dogs ≤ and dogs >12 months, with higher incidence of displaced fragment found in dogs ≤12 months. The differences of other arthroscopic findings were not significant (*P*=0.063-0.963).

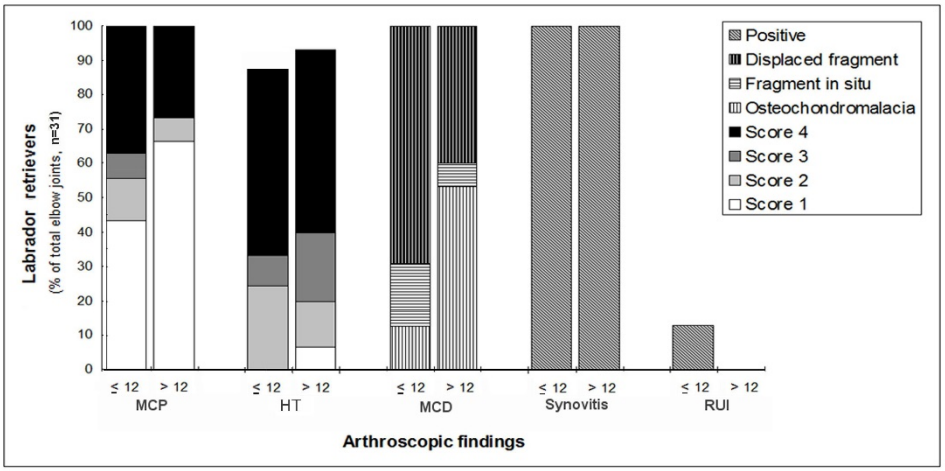

Fig. 9. *The distribution of lesions (in %) detected at arthroscopy in Labrador retrievers younger and older than 12 months. MCP, medial coronoid process; HT, humeral trochlea; MCD, medial coronoid disease; RUI, joint incongruity.*

Study II: Ulnar subtrochlear sclerosis investigation

The age distribution between the patient and healthy groups was not significantly different (*P*=0.202). Hence, both groups were comparable. The mean ± SD CT attenuation in the ROI was 972.7 ± 147.5 HU (range, 741-1189 HU) in the patient group and 587.2 ± 102.4 (range, 463-739 HU) in the healthy group. The ratio between the mean attenuation of the ulnar subtrochlear bone and cortical bone was 0.303 ± 0.060 (range, 0.237-0.390) in the patient group and 0.493 ± 0.060 in the healthy group (range, 0.400-0.604). Statistically, the ratio between the mean attenuation of the ulnar subtrochlear bone and cortical bone was strongly correlated with ulnar STS in binary scores (*r*=0.85, *P*<0.0001). On reconstructed CT images, ulnar STS could be seen at the intramedullary cavity distal to the ulnar trochlear notch (Fig. 10b and c).

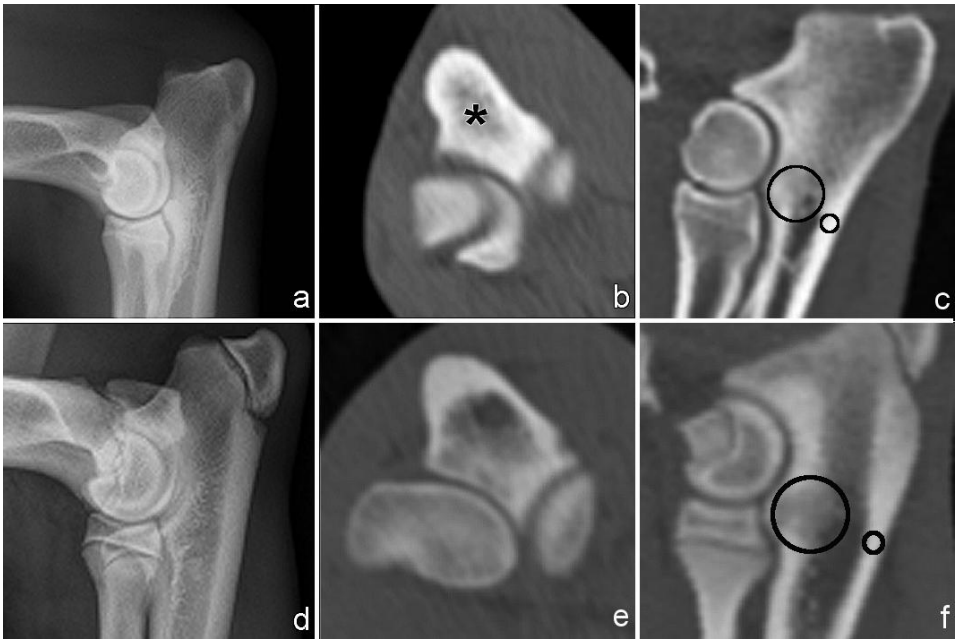

Fig. 10. *Ulnar subtrochlear sclerosis (STS) observed on radiographic and computed tomographic (CT) images. (a) Mediolateral view of an elbow obtained from a 56-month-old Labrador retriever with 'obvious' sclerosis; (b) on the CT transverse view (caudal to the most proximal part of the radial head), there was increased of opacity (*) at the intramedullary cavity. (c) Regions of interest (ROIs) were selected at the reconstructed sagittal view of CT for the attenuation (HU) measurement at the ulnar subtrochlear bone region and cortical bone. (d) Mediolateral view of an elbow obtained from a 6-month-old Labrador retriever without sclerosis; on the (e) CT transverse view (caudal to the most proximal part of the radial head), there was less opacity detected at the intramedullary cavity. (f)*

Regions of interest (ROIs) were selected at the reconstructed sagittal view of CT for the attenuation (HU) measurement at the ulnar subtrochlear bone region and cortical bone.

Discussion

The most common radiographic finding in dogs ≤12 months was ulnar STS (87.6%) and it appeared to be significantly more severe than in dogs >12 months (*P*=0.02). In contrast with the younger dogs, changes in the cranial edge of the MCP (66.7%) were the most common radiographic finding in the dogs >12 months of age; however, interpretation of this criterion based on two-dimensional radiographs is suboptimal. The abnormal MCP shapes detected radiographically are most likely due to periarticular osteophytosis, displaced bone fragments, and structural changes of the MCP. With CT, the lack of superimposed anatomy enables the observer to interpret morphological changes, such as fragmentation of MCP and osteophytosis at the apex of MCP, in greater detail than is possible with radiography.

The highest incidence of periarticular osteophytosis was detected at the IEWG screening site 'a', 'b' and 'g' in both age groups. Periarticular osteophytosis is an important component of the assessment criteria in IEWG ED screening schemes. On the basis of the guidelines of the IEWG, which take into consideration both primary and secondary lesions, the sensitivity of radiographs in detecting MCD in our study was higher (≤12 months, 93.8%; >12 months, 73.3%) than previously reported (16-62%; Haudiquet et al., 2002; Fitzpatrick et al., 2009).

The most common CT finding in our study was 'obvious' fragmentation of MCP (≤12 months, 93.8%; >12 months, 66.7%) in both age groups, with a low incidence of sclerosis of the MCP (≤12 months, 56.2%; >12 months, 0%). These findings are in contrast with previously reported CT findings, where sclerosis of the MCP (85%) and humeral trochlea (77%) was the most common finding, followed by fragmentation (44%; Moores et al., 2008). Groth *et al.* (2009) also reported a high incidence of sclerosis of the MCP (83%). These differences reveal the limitation of subjective evaluation of sclerosis, with a large inter-observer variation between different studies. High incidence of 'obvious' fragmentation of MCP recognized in both groups might be due to the fact that our study was breed-specific and fragmentation of the MCP was the most frequently diagnosed form of ED in Labrador retrievers (Lavrijsen et al., 2012). Of the 31 elbows from both groups of dogs, five were undiagnosed on CT: three were diagnosed with osteochondromalacia and the remaining two were diagnosed with fragmentation of MCP during arthroscopy. The failure to diagnose fragmentation of MCP can be explained by the fact that CT is not reliable for diagnosing MCD with fragments in situ or minimally displaced fragments (Carpenter et al., 1993; Van Ryssen et al., 1997; Moores et al., 2008; Groth et al., 2009).

Arthroscopically, fragmentation of MCP (68.8%) was the most common finding in dogs ≤12 months and osteochondromalacia (53.3%) in dogs >12 months. The features of MCD between both age groups were significantly difference (*P*=0.04). Due to the unknown etiopathogenesis of the MCD, it is uncertain whether this difference represents separate entities or different grades of the same process (Van Ryssen et al., 1997). All the cases diagnosed with OCD-like lesion on both radiography and CT showed different score on Modified Outerbridge Score. There were 7 out of 31 elbows scored 4 during surgery failed to showed indication of OCD-like lesion on both radiography and CT. This can be explained by the fact that with these techniques, the integrity of articular cartilage cannot be assessed. In our study, we did not attempt to define OCD-like lesions further into contact lesions, OC, or OCD (Hazewinkel et al., 2008). Periarticular osteophytosis, displaced fragments, and joint manipulation during the arthroscopic procedure may complicate the joint assessment, including joint congruence (Van Ryssen et al., 1997; Meyer-Lindenberg et al., 2003). Given the discrepancy between the radiographic, CT, and surgical findings, we must conclude that MCD can occur without there being relevant radiographic and CT findings and that a thorough physical examination and history remain essential to the diagnosis.

Combination of both radiography and CT was able to diagnose 100% and 80% of the MCD cases in dogs ≤ and dogs >12 months of age, respectively. It is obviously higher than based solely on radiography (≤12 months, 93.8%; >12 months, 73.3%) or CT (≤12 months, 93.8%; >12 months, 66.7%). However, the cost-effectiveness, time consumption and necessity to anaesthetize the animals for the CT examination make the combination of both techniques less practical. The CT diagnosis, based solely on the detection of fragmentation of MCP, showed similar sensitivity in comparison to radiographic diagnosis based mainly on the secondary lesions. Whether or not CT should be used as a first line diagnostic tool depends on clinician judgments.

The mechanism underlying the development of sclerosis is not known, despite its importance as indicator in the radiographic diagnosis of MCD. It was thought to occur most likely as a result of superimposition of periarticular osteophytosis and an increase in subchondral bone mineral density (Hornof et al., 2000; Burton et al., 2007; Smith et al., 2009). On CT images, sclerosis was mainly detected at the MCP (Reichle et al., 2000; Moores et al., 2008; Groth et al., 2009). However, in study II, we demonstrated the sclerosis of the intramedullary bone cavity by comparing ulnas with and without sclerosis and without interference from periarticular osteophytosis. The significant correlation between the ratio of the mean CT attenuation and subjective radiographic interpretation of ulnar STS supports the importance of investigating alterations of the intramedullary cavity of the ulnar subtrochlear region.

We chose to study Labrador retrievers because of the high incidence of MCD in this popular breed. We attempted to identify the common radiographic, CT, and arthroscopic findings for MCD, especially in dogs ≤12 months of age because early detection of imaging abnormalities is crucial in order to provide early treatment and to optimize treatment outcomes. However, our study was limited by the fact that most of the criteria used to describe the diagnostic findings were subjective and not validated. Moreover, observer experience and preference might influence the evaluation, which was performed once and thus inter-observer variation and intra-observer variation could not be established. Low number of cases unabled the investigation of specificity, positive predictive value and negative predictive value for each techniques.

We demonstrated a wide range of radiographic, computed tomographic and surgical variables in Labrador retrievers ≤12 and >12 months of age. Ulnar STS appeared to be the most common radiographically finding in Labrador retrievers ≤12 months of age. This further highlights the importance to further investigate the ulnar STS, especially at the intramedullary bone cavity at the ulnar subtrochlear notch. Radiographic and computed tomographic findings should not be used as sole criteria for surgical decision, but including the patient history and physical examination. The marked incidence of cartilage lesions especially in Labrador retrievers >12 months of age, which are radiographic and computed tomographic silent, require more sensitive diagnostic method to identify the lesions.

References

Burton, N.J., Comerford, E.J., Bailey, M., Pead, M.J., Owen, M.R., 2007. Digital analysis of ulnar trochlear notch sclerosis in Labrador retrievers. Journal of Small Animal Practice 48, 220-224.

Carpenter, L.G., Schwarz, P.D., Lowry, J.E., Park, R.D., Steyn, P.F., 1993. Comparison of radiologic imaging techniques for diagnosis of fragmented medial coronoid process of the cubital joint in dogs. Journal of the American Veterinary Medical Association 203, 78-83.

Cook C.R., Cook J.L., 2009. Diagnostic imaging of canine elbow dysplasia: A review. Veterinary Surgery 38, 144-153.

Fitzpatrick, N., Smith, T.J., Evans, R.B., Yeadon, R., 2009. Radiographic and arthroscopic findings in the elbow joints of 263 dogs with medial coronoid disease. Veterinary Surgery 38, 213-223.

Goldhammer, M.A., Smith, S.H., Fitzpatrick, N., Clements, D.N., 2009. A comparison of radiographic, arthroscopic and histological measures of articular pathology in the canine elbow joint. The Veterinary Journal 186, 96-103.

Groth, A.M., Benigni, L., Moores, A.P., Lamb, C.R., 2009. Spectrum of computed tomographic findings in 58 canine elbows with fragmentation of the medial coronoid process. Journal of Small Animal Practice 50, 15-22.

Haudiquet P.R., Marcellin-Little D.J., Stebbins M.E., 2002. Use of the distomedial-proximolateral oblique radiographic view of the elbow joint for examination of the medial coronoid process in dogs. American Journal of Veterinary Research 63, 1000-1005.

Hazewinkel, H.A.W., 2008. Elbow dysplasia: Definition and clinical diagnoses. Proceedings of the 23rd Annual Meeting of International Elbow Working Group. Dublin, 8-12.

Holsworth, I.G., Wisner, E.R., Scherrer, W.E., Filipowitz, D., Kass, P.H., Pooya, H., Larson, R.F., Schulz, K.S., 2005. Accuracy of computerized tomographic evaluation of canine radio-ulnar incongruence in vitro. Veterinary Surgery 34, 108-113.

Hornof, W.J., Wind, A.P., Wallack, S.T., Schulz, K.S., 2000. Canine elbow dysplasia. The early radiographic detection of fragmentation of the coronoid process. Veterinary Clinics of North America: Small Animal Practice 30, 257-266.

Keller, G.G., Kreeger, J.M., Mann, F.A., Lattimer, J.C., 1997. Correlation of radiographic, necropsy and histologic findings in 8 dogs with elbow dysplasia. Veterinary Radiology & Ultrasound 38, 272-276.

Kramer, A., Holsworth, I.G., Wisner, E.R., Kass, P.H., Schulz, K.S., 2006. Computed tomographic evaluation of canine radioulnar incongruence in vivo. Veterinary Surgery 35, 24-29.

Lavrijsen, I.C., Heuven, H.C., Voorhout, G., Meij, B.P., Theyse, L.F., Leegwater, P.A., Hazewinkel, H.A., 2012. Phenotypic and genetic evaluation of elbow dysplasia in Dutch Labrador retrievers, Golden retrievers, and Bernese Mountain Dogs. The Veterinary journal 193, 486-492.

Lappalainen A.K., Molsa S., Liman A., Laitinen-Vapaavuori, O., Snellman, M., 2009. Radiographic and computed tomography findings in Belgian Shepherd dogs with mild elbow dysplasia. Veterinary Radiology & Ultrasound 50, 364-369.

Meyer-Lindenberg, A., Langhann, A., Fehr, M., Nolte, I., 2002. Prevalence of fragmented medial coronoid process of the ulna in lame adult dogs. The Veterinary Record 151:230-234.

Meyer-Lindenberg, A., Langhann, A., Fehr, M., Nolte, I., 2003. Arthrotomy versus arthroscopy in the treatment of the fragmented medial coronoid process of the ulna (FCP) in 421 dogs. Veterinary and Comparative Orthopaedics and Traumatology 16, 204-210.

Moores A.P., Benigni L., Lamb C.R., 2008. Computed tomography versus arthroscopy for detection of canine elbow dysplasia lesions. Veterinary Surgery 37, 390-398.

Ratner B., 2009. The correlation coefficient: Its values range between +1/−1, or do they? Journal of Targeting Measurement and Analysis for Marketing 17, 139-142.

Reichle, J.K., Park, R.D., Bahr, A.M., 2000. Computed tomographic findings of dogs with cubital joint lameness. Veterinary Radiology & Ultrasound 41, 125-130.

Samoy, Y., Van Ryssen, B., Gielen, I., Walschot, N., van Bree, H., 2006. Review of the literature: elbow incongruity in the dog. Veterinary and Comparative Orthopaedics and Traumatology 19, 1-8.

Schulz K., 2003. What's new in elbow arthroscopy. Proceedings of the 13th Annual American College of Veterinary Surgeons Symposium. Washington DC, 329-331.

Smith, T.J., Fitzpatrick, N., Evans, R.B., Pead, M.J., 2009. Measurement of ulnar subtrochlear sclerosis using a percentage scale in labrador retrievers with minimal radiographic signs of periarticular osteophytosis. Veterinary Surgery 38, 199-208.

Tellhelm, B., 2011. Grading primary ED-lesions and elbow osteoarthrosis according to the IEWG protocol. Proceedings of the 26th Annual Meeting of International Elbow Working Group. Amsterdam, 14-15.

Van Ryssen B., van Bree H., 1997. Arthroscopic findings in 100 dogs with elbow lameness. The Veterinary Record 140, 360-362.

Van Ryssen B., van Bree H., Simoens P., 1993. Elbow arthroscopy in clinically normal dogs. American Journal of Veterinary Research 54, 191-198.

Voorhout, G., Hazewinkel, H.A.W., 1987. Radiographic evaluation of the canine elbow joint with special reference to the medial humeral condyle and the medial coronoid process. Veterinary Radiology 28, 158-165.

Wagner, K., Griffon, D.J., Thomas, M.W., Schaeffer, D.J., Schulz, K., Samii, V.F., Necas, A., 2007. Radiographic, computed tomographic, and arthroscopic evaluation of experimental radio-ulnar incongruence in the dog. Veterinary Surgery 36, 691-698.

Wosar, M.A., Lewis, D.D., Neuwirth, L., Parker, R.B., Spencer, C.P., Kubilis, P.S., Stubbs, W.P., Murphy, S.T., Shiroma, J.T., Stallings, J.T., Bertrand, S.G., 1999. Radiographic evaluation of elbow joints before and after surgery in dogs with possible fragmented medial coronoid process. Journal of the American Veterinary Medical Association 214, 52-58.

Chapter 4

The early development of medial coronoid disease in growing Labrador retrievers: Radiographic, computed tomographic, necropsy and micro-computed tomographic findings

S.F. Lau[1], C.F. Wolschrijn[2], H.A.W. Hazewinkel[3], M. Siebelt[4], G. Voorhout[1]

[1] Division of Diagnostic Imaging, Faculty of Veterinary Medicine, Utrecht University, Yalelaan 108, 3584CM, Utrecht, The Netherlands

[2] Department of Pathobiology, Division of Anatomy and Physiology, Faculty of Veterinary Medicine, Utrecht University, Yalelaan 1, 3584CL, Utrecht, The Netherlands

[3] Department of Clinical Sciences of Companion Animals, Faculty of Veterinary Medicine, Utrecht University, Yalelaan 108, 3584CM, Utrecht, The Netherlands

[4] Department of Orthopedic Surgery, Erasmus Medical Center, Rotterdam, The Netherlands

Adapted from The Veterinary Journal, 2013

http://dx.doi.org/10.1016/j.tvjl.2013.04.002

Abstract

Objective:

To use radiography, computed tomography, necropsy examination, and micro-computed tomography to investigate the earliest signs of medial coronoid disease (MCD) in Labrador retrievers in the first six months of their life.

Methods:

Radiography and computed tomography were used to monitor the development of MCD of 14 Labrador retrievers, from 6 or 7 weeks of age until euthanasia. The definitive diagnosis of MCD was based on necropsy and micro-computed tomography findings.

Results:

The prevalence of MCD was 50%. Radiographic findings did not provide evidence of MCD, ulnar subtrochlear sclerosis, or blunting of the cranial edge of the medial coronoid process (MCP). Computed tomography proved to be more sensitive (30.8%) than radiography (0%) in detecting early MCD, with the earliest signs detectable at 14 weeks of age. Combination of the necropsy and micro-computed tomography findings of the MCP showed that MCD was manifested as a lesion of only the subchondral bone in the dogs younger than 18 weeks of age. In all dogs (affected and unaffected), there was close contact between the base of MCP and the proximal radial head in the congruent joints.

Conclusion:

MCD can be detected by means of computed tomography in dogs as young as 14 weeks old, and that the lesion probably originates at the base of the MCP. Radiographically, subtrochlear sclerosis might develop in an advanced stage of MCD and should be regarded as a secondary change.

Introduction

The term medial coronoid disease (MCD) describes pathological changes to both the cartilage and the subchondral bone of the medial coronoid process (MCP; Moores et al., 2008; Fitzpatrick et al., 2009). MCD is one of the most common heritable diseases in dogs (Boulay, 1998; Janutta et al., 2006) and has been reported for a variety of breeds (Ubbink et al., 1999; Haudiquet et al., 2002; Groth et al., 2009). Clinical signs and diagnosis of MCD has been reported as early as 3 months of age (Fitzpatrick et al., 2009).

Radiography is usually used to diagnose MCD with a sensitivity of 10–62% (Carpenter et al., 1993; Wosar et al., 1999). The radiographic diagnosis of MCD is mainly based on the presence of secondary changes associated with degenerative joint disease. Primary lesions, such as fragmented MCP (FMCP), contact lesions of the humeral trochlea, and radioulnar joint incongruity (RUI), are occasionally seen (Keller et al., 1997; Hornof et al., 2000). It is often difficult to make a definitive radiographic diagnosis because of the superimposition of the radial head over the MCP and the tight fit between the ulnar trochlear notch and the humeral condyle. Computed tomography (CT) is a better diagnostic technique as images are not superimposed and can be evaluated in different reconstructed views (Reichle et al., 2000; Holsworth et al., 2005; Kramer et al., 2006; Samoy et al., 2006; Wagner et al., 2007). CT is superior to plain film radiography, xeroradiography, linear tomography, and arthrography in detecting MCD, having the highest accuracy (86.7%), sensitivity (88.2%), and negative predictive value (84.6%; Carpenter et al., 1993). Like radiography, CT is unable to assess cartilage integrity, and because animals are not in weight-bearing positions during CT investigations (De Rycke et al., 2002; Mason et al., 2002), physiological incongruities due to ground reaction forces and muscular activity might be missed (Preston et al., 2000; House et al., 2009).

To our knowledge, there are no longitudinal studies of the elbow joints in Labrador retrievers and precise descriptions of early diagnostic findings in MCD are sparse. The purpose of this longitudinal study was to use both radiography and CT to investigate the earliest signs of MCD in Labrador retrievers in the first six months of their life. Dogs were euthanized when signs of MCD were detected or as age- and weight-matched negative controls of the same litter. The definitive diagnosis was based on necropsy and micro-computed tomography (microCT) findings.

Materials and methods

The study was approved by the Ethics Committee of Utrecht University, as required by Dutch law. The dogs used in the study, 14 growing Labrador retrievers (seven aged 6 weeks and seven aged 7 weeks) originating from two litters from a MCD-affected dam and two MCD-affected sires, were housed two to three per pen and fed on commercially available and nutritionally balanced diets. Radiographic and CT investigations of the dogs were performed every 14 days until lesions indicative of MCD were detected, at which stage the dogs were euthanized. When one of the dogs was diagnosed "positive" or "suspected" with MCD, an age- and weight-matched dog (diagnosed negative for MCD based on CT findings) within the same litter was euthanized as control. In the first litter, there were four dogs euthanized at the end of the study (Table 1), despite the absence of the indication of MCD on radiography and CT, in order to be confirmed as true negative by using microCT. In the second litter, due to the unexpected high number of MCD positive animals, two dogs euthanized at 16 and 17 weeks of age had no negative age-matched control. The closest age of the negative control which they can be compared with, were 15 and 18 weeks of age (Table 1). In addition, each dog was physically examined twice (at 14 and 23 weeks of age for the first litter and 10 and 14 weeks of age for the second litter) according to method described previously (Hazewinkel et al., 2009), and the dogs' daily activity was closely monitored.

Radiographic technique and evaluation

Radiographs of the elbow joints were made with a digital radiography system (Philips digital Rad TH, Philips) using 50 kVp and 8 mA. Between 6 and 11 weeks of age, only mediolateral (ML) and craniocaudal (CrCd) views of the elbow joints were made. From 12 weeks onward, craniolateral-caudomedial oblique (CrL-CdMO) and extended supinated ML views were included, as described previously (Voorhout and Hazewinkel, 1987). All radiographs were evaluated systematically to detect early signs of MCD based on the criteria used in the International Elbow Working Group (IEWG) Elbow Screening Scheme (Tellhelm, 2011).

Dog	Age (week)	Sex	Weight (kg)	Limb	CT	Necropsy (Cartilage)	MicroCT (Subchondral bone)
1	15	F	14.8	L	Negative	No fissure	Normal
				R	Negative	No fissure	Normal
2	15	F	16.2	L	Suspect	No fissure	Fissure
				R	Negative	No fissure	Normal
3	16	M	16.6	L	Suspect	No fissure	Fissure
				R	Suspect	No fissure	Fragment
4	17	F	20.5	L	Suspect	No fissure	Fissure
				R	Suspect	No fissure	Fissure
5	18	M	19.2	L	Negative	No fissure	Normal
				R	Negative	No fissure	Normal
6	18	M	19.1	L	Positive	Fissure	Fragment
				R	Positive	Inc. fissure	Fragment
7	19	M	21.5	L	Positive	No fissure	Fissure
				R	Positive	Inc. fissure	Fragment
8	19	M	22.8	L	Negative	Fissure	Fragment
				R	Negative	Inc. fissure	Fragment
9	25	M	28.6	L	Suspect	Fissure	Fragment
				R	Suspect	Fissure	Fragment
10	25	M	28.4	L	Negative	No fissure	Normal
				R	Negative	No fissure	Normal
11	26	M	28.4	L	Negative	No fissure	Normal
				R	Negative	No fissure	Normal
12	26	F	29.4	L	Negative	No fissure	Normal
				R	Negative	No fissure	Normal
13	27	F	24.4	L	Negative	No fissure	Normal
				R	Negative	No fissure	Normal
14	27	M	33.6	L	Negative	No fissure	Normal
				R	Negative	No fissure	Normal

Table 1. *Summary of the results of the dogs from the first and second litters. Dog 1 to 6 were from the second litter and 7 to 14 were from the first litter. F, Female; M, Male; L, Left; R, Right; Inc., incomplete.*

Computed tomographic technique and evaluation

For CT, the dogs were anesthetized and positioned in dorsal recumbency on the CT scanning table with the elbow joints extended about 135°. The antebrachia were positioned parallel to each other and as symmetrically as possible at the same level using a custom-made positioning device. Transverse views, perpendicular to the antebrachia, were made with a third- generation single-slice helical CT scanner (Philips Secura, Philips) using 120 kV and 120 mA with an exposure time of 1000 ms. The full length of the antebrachium was scanned from proximal to the olecranon to distal to the radiocarpal joint in 1-mm thick slices in dogs up to 12 weeks of age, and thereafter the full length of the antebrachium was scanned from proximal to the olecranon to distal to the radiocarpal joint in 2-mm thick slices. In addition, 1-mm thick slices of the elbow joints were made with

the joints in neutral, pronated, and supinated position. In order to position the elbows, both carpal joints were secured in a positioning device (Fig. 1a) according to the method described (House et al., 2009). With the animal in dorsal recumbency, the carpal joint was inline with the antebrachium (neutral position) and the palmar aspect of the carpal joint was considered as zero starting position (Newton, 1985). Pronation was measured approximately 65° away from the zero starting position at the heads of the metacarpal bones whereas supination was measured approximately 45° away from the zero starting position (Fig. 1b, c). Maximal pronation and supination were achieved until the elbow joint could no longer be maintained at 135° or the carpal joint could no longer be remained within the positioning device. The resulting CT images were evaluated for the presence of primary lesions such as FMCP, evidence of RUI and secondary degenerative changes, namely, periarticular osteophytosis and subtrochlear notch sclerosis. FMCP was characterized as a visibly mineralized bone structure that was totally separated from the adjacent bone in one or more CT images.

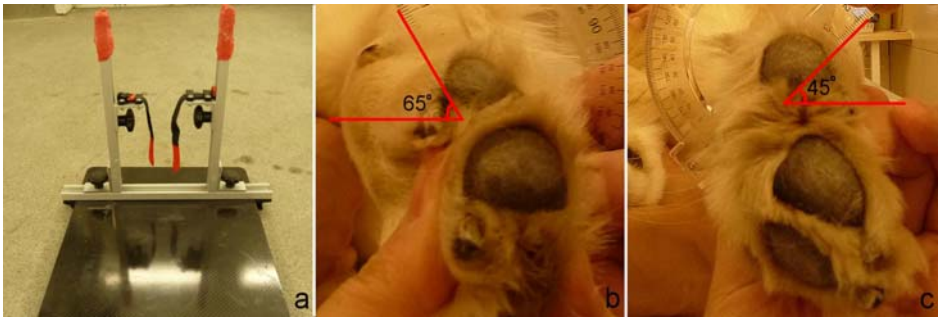

Fig. 1. *The right forelimb of a dog positioned in dorsal recumbency; (a) Positioning device, (b) Pronation was measured approximately 65° away from the zero starting position at the heads of the metacarpal bones and (c) supination was measured approximately 45° away from the zero starting position*

Necropsy examination

Dogs were euthanized with an IV overdose of barbiturate when lesions were observed on radiographs or CT images, or as age- matched negative controls. The forelimb was disarticulated at the shoulder joint, placed in 135° extension, and soaked until further processing in 4% buffered formaldehyde solution (Gebufferde Formaldehyde, Klinipath BV). Necropsy examination of these elbow joints was performed after separation of the humerus from the radioulnar joint, and separation of the radius from the ulna. Joint congruity was carefully assessed, as defined by smooth transition from the articular surface of the ulnar trochlear notch onto the articular surface of radius, and the gross appearance of the articular cartilage surface overlying the MCP.

Micro-computed tomographic technique and evaluation

After necropsy examination, the proximal one third of the ulna was cut and scanned in an in-vivo microCT system (Skyscan 1076, Skyscan), starting from 2 cm proximal to the MCP until approximately 2 cm distal to MCP. During scanning, the bones were secured in a cylindrical plastic holder to prevent movement. Scanning parameters were 60 kV and 170 µA with an exposure time of 948 ms and a pixel size of 36 µm. Skyscan software (CTAnalyser CTVolume, Skyscan) was used to reconstruct 3-D images. As the gold standard for definitive diagnosis, the results of microCT were used in combination with necropsy findings.

Statistical analysis

A calculation of sensitivity, specificity, positive predictive value and negative predictive value for radiographic and computed tomographic technique was performed as described previously (Carpenter et al., 1993).

Results

Fourteen Labrador retrievers, nine males and five females, were investigated (Table 2). Dogs from the first litter were euthanized at 19–27 weeks of age and those from the second litter at 15–18 weeks of age. At the time of euthanasia, the dogs weighed 23.1 ± 5.8 kg (mean±SD). None of the dogs showed abnormalities or lameness on physical examination or in their daily activities. On the basis of the combined results of necropsy and microCT, seven of the 14 dogs were diagnosed with MCD (Table 2). Bilateral elbows were affected in six dogs (five male and one female), and one elbow was affected in one dog (female).

Gender	**Dogs with MCD (*n* = 7)**		**Dogs with normal MCP (*n* = 7)**	
	First litter	Second litter	First litter	Second litter
Male (*n* = 9)	3	2	3	1
Female (*n* = 5)	0	2*	2	1

Table 2. *Number of dogs diagnosed with and without medial coronoid disease (MCD) in the first and second litters. MCD, medial coronoid disease; MCP, medial coronoid process; n, number of dogs; *, one of the female dogs was affected unilaterally.*

Radiographic findings

Radiographically, none of the elbow joints showed signs of MCD: there was no evidence of osteophytosis, subtrochlear sclerosis, blurring of the cranial edge of the MCP, or primary lesions indicative of MCD (Fig. 2).

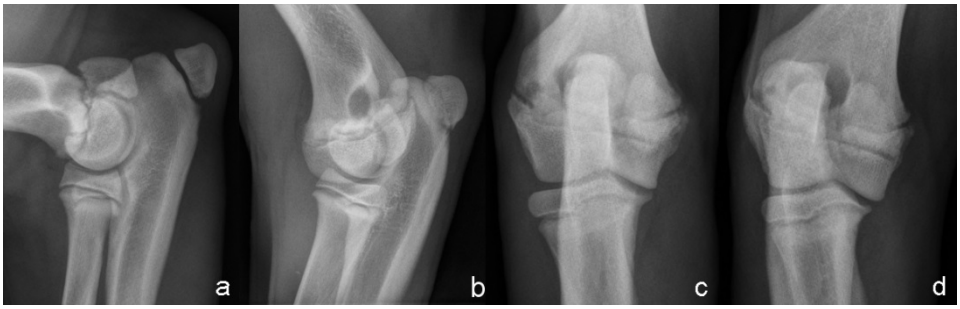

Fig. 2. *Radiographic images from the right elbow joint of a 14-week-old dog; (a) Mediolateral (ML) view showed no evidence of ulnar subtrochlear sclerosis and (b) Extended supinated ML view showed well-defined cranial edge of medial coronoid process. (c) and (d) showed normal findings on craniocaudal and craniolateral-caudomedial oblique views. This dog had a suspicious lesion on computer tomographic investigation performed at 14 weeks of age and was diagnosed with medial coronoid disease on the basis of microCT findings.*

Computed tomographic findings

On CT, no abnormalities were found in 17 out of 28 elbow joints. The findings in seven elbow joints were suspected of MCD, and fragmentation in the MCP was found in the remaining four elbow joints. The earliest CT signs of MCD were detected at 14 weeks with a mineralized bone fragment detected at the base of the MCP subchondral bone (similar as shown in Fig. 3b and d), which did not extend to the apex of the MCP (similar as shown in Fig. 3c). This finding was seen on CT in all MCD-affected dogs from the second litter younger than 19 weeks. In the first litter, a dog was euthanized at 19 weeks of age after a non-displaced fragment was detected at the apex of the MCP subchondral bone on CT (Fig. 3e); however, reassessment of earlier CT images showed that lesions similar to those seen at 14 weeks of age were present at an earlier age but had not been detected. One of the dogs that served as age-matched negative control for a 19 weeks of age littermate appeared to be MCD positive on microCT finding. On re-evaluation, a fragment at the base of the MCP subchondral bone was found on CT images taken at 15 weeks.

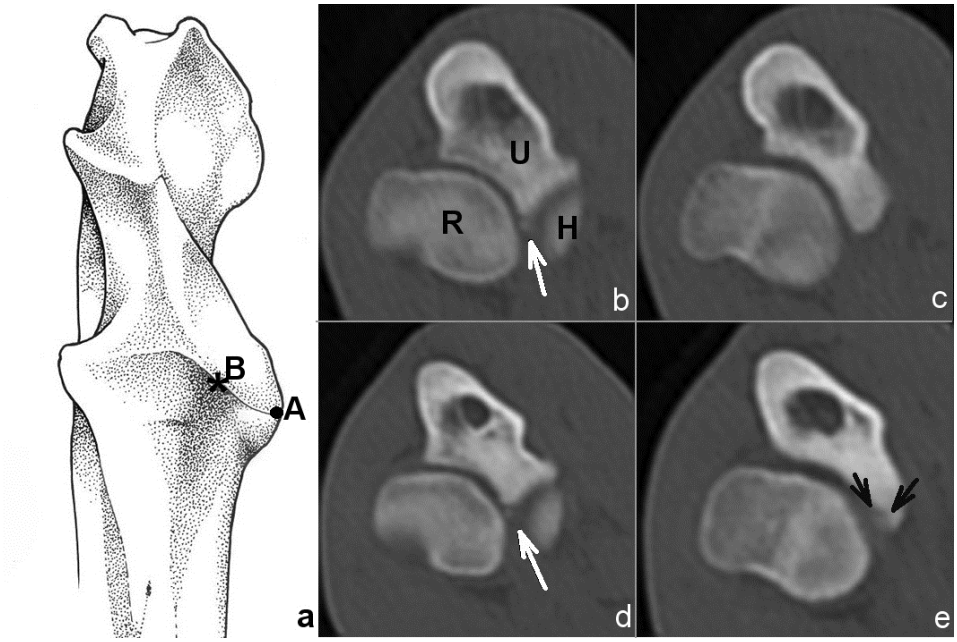

Fig. 3. *(a) Proximal ulna of right elbow shows the base (B at the *) of medial coronoid process (MCP) and apex (A at the ●) of MCP. Transverse slice from the right elbow joint of a dog at 18 weeks of age (b) taken at the base of the MCP showed a fragment (white arrow). R, radius; U, ulna; H, humeral condyle. (c) Taken at the apex of MCP showed no indication of medial coronoid disease. Transverse slice from the right elbow joint of a dog at 19 weeks of age (d) taken at the base of MCP showed a fragment (white arrow) and (e) taken at the apex of MCP showed a non-displaced fragment (black arrows).*

Necropsy findings

At necropsy (Table 3), of the 13 diseased MCPs, six did not have fissure lines on the articular cartilage (Fig. 4a), four had complete fissure lines at articular cartilage (Fig. 4c), and three had incomplete fissure lines across part of the apex of MCPs (Fig. 4b). Dogs younger than 19 weeks diagnosed with MCD tended to have incomplete fissure lines on the articular cartilage surface, whereas older animals had complete fissure lines crossing the articular cartilage. Up to 17 weeks of age, MCD consisted solely of lesions of the subchondral bone layer. On the basis of microCT findings, none of the normal MCPs showed abnormalities of the articular cartilage surface (Table 3), and nor were other lesions, such as erosion, chondromalacia, and osteophytosis detected. Necropsy revealed that the base of the MCP was in close contact with the proximal radial head in all the congruent joints (with or without MCD; Fig. 5a). It also revealed that one of the radioulnar joints (from a 15-week-old dog) clearly showed stepping of about 1.5 mm, with a steeper downward slope of the

MCP against the proximal radius (Fig. 5b), resulting in a loss of contact between the base of MCP and the proximal radial head. This particular joint was diagnosed normal.

Necropsy examination		**MCD**		**Normal MCP**	
		First litter (*n* = 6)	Second litter (*n* = 7)	First litter (*n* = 10)	Second litter (*n* = 5)
Articular cartilage	Normal	1	5	10	5
	Incomplete fissure	2	1	0	0
	Complete fissure	3	1	0	0
Joint alignment	Congruent	6	7	10	4
	Incongruity	0	0	0	1

Table 3. *Summary of the results from necropsy examination of elbow joints from the first and second litters. MCD, medial coronoid disease; MCP, medial coronoid process; n, number of elbow joints.*

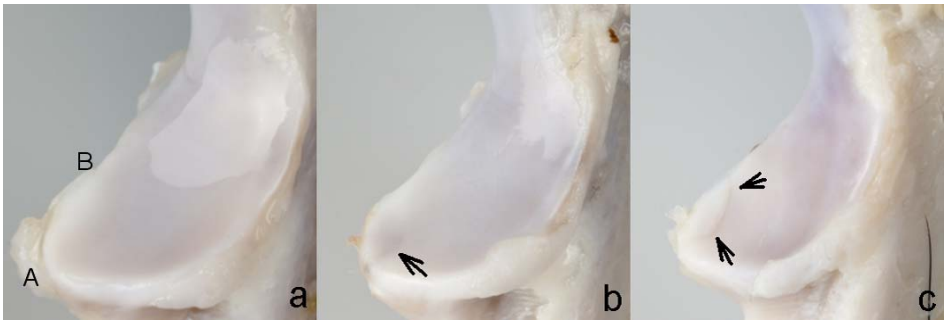

Fig. 4. *Right medial coronoid processes (MCPs) of different ages with medial cornoid disease, based on microCT 3-D reconstructed images. (a) Seventeen weeks of age; no fissure of the articular cartilage surface. A, apex of MCP; B, base of MCP. (b) Eighteen weeks of age; incomplete fissure of the articular surface (arrow) at the apex of MCP. (c) Twenty five weeks of age; complete fissure (arrows) across from the base to the apex of the MCP.*

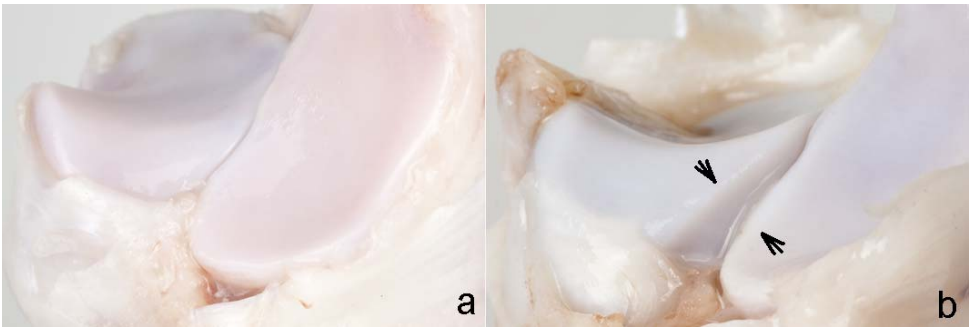

Fig. 5. *Right radioulnar joints from dogs with normal medial coronoid process (MCP) based on microCT reconstructed images. (a) Fifteen weeks of age; right radioulnar joint congruence with close contact between the base of the MCP with proximal radial head. (b) Fifteen weeks of age; right radioulnar joint incongrunce with a step defect about 1.5mm (arrows) with steeper slope of ulnar articular cartilage surface downward against the proximal radial head. There was no contact between the base of the MCP and the proximal radial head.*

Micro-computed tomographic findings

In total, 13 of the 28 MCPs showed either fragmentation or fissure of the subchondral bone and were considered to be affected by MCD (Table 4). In five MCPs, incomplete fissures in the subchondral bone were observed; four of these MCPs came from dogs younger than 19 weeks old. The incomplete fissure lines extended in the direction of base-to-apex of the subchondral bones (Fig. 6b). Five of eight diseased MCPs with complete fragmentation came from dogs older than 19 weeks. In these MCPs, fragmentation was detected either crossing the tip from base to apex of the lateral aspect of the MCP (Fig. 6c and d) or crossing from the base of the lateral aspect of MCP toward the apex of the medial aspect of MCP.

MicroCT		**MCD positive**		**Normal MCP**	
		First litter (*n* = 6)	Second litter (*n* = 7)	First litter (*n* = 10)	Second litter (*n* = 5)
Subchondral bone	Normal	0	0	10	5
	Incomplete fissure	1	4	0	0
	Fragmentation	5	3	0	0

Table 4. *Summary of the results of micro-computed tomography of dogs from the first and second litters. MCD, medial coronoid disease; MCP, medial coronoid process; n, number of MCPs.*

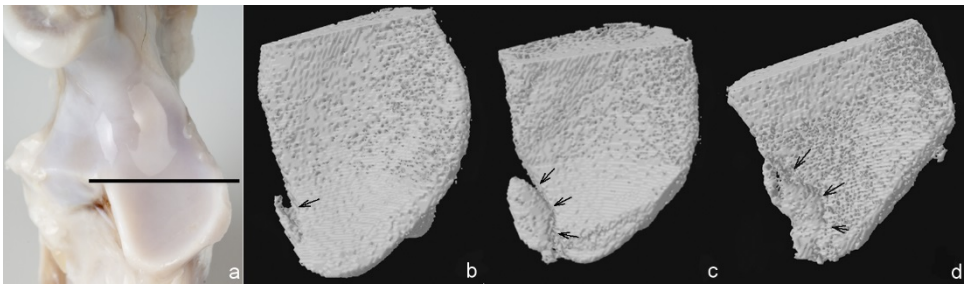

Fig. 6. *Three-dimensional reconstructed microCT images of medial coronoid processes (MCPs). (a) Whole MCP isolated from the proximal ulna (line). (b) Seventeen weeks of age; fissure line at the subchondral bone extending in the direction of base-to-apex of the MCP (arrow). (c) Eighteen weeks of age; fragmentation across the base to the apex of the MCP (arrows). (d) Twenty five weeks of age; fragmentation across the base to the apex of the MCP (arrows).*

Radiographic versus computed tomographic evidence of MCD

None of the radiographs showed evidence of MCD, whereas CT identified four of the 13 cases of MCD. Both radiography and CT failed to demonstrate the joint incongruity in the right elbow of a 15-week-old dog. CT had the higher sensitivity (30.8%) and negative predictive value (62.5%) in comparison with radiography with sensitivity of 0% and negative predictive value of 53.6%. Both techniques had specificity of a 100%. A positive predictive value for CT was 100%, but undefined for radiography, due to the fact that radiography failed to detect any MCD in our study.

Discussion

This longitudinal study involved growing Labrador retrievers, a breed with a high prevalence of MCD (Ubbink et al., 2000; Lavrijsen et al., 2012). In an attempt to increase the frequency of MCD (Keller et al., 2011), pups were bred from a dam and sires affected by MCD. We studied growing dogs in an attempt to identify lesions at an early age, in order to learn more about the etiopathogenesis of MCD, knowledge that in turn might help optimize treatment outcomes. The MCP was abnormal in 50% of the dogs, with abnormalities occurring more often in male dogs (five of nine males) than in female dogs (two of five females). Despite the relatively high prevalence of MCD, none of the dogs showed abnormalities in daily activities or on physical examination. This is probably because articular cartilage was not severely eroded and secondary degenerative joint changes had not developed by the time the dogs were euthanized. We were thus in a position to study lesions that developed early in the course of MCD.

We included the CrL-CdMO and extended supinated ML radiographic views for

dogs older than 12 weeks because the increasing complexity of the joint with age makes extra views potentially useful to optimize interpretation. The CrL-CdMO view is an excellent projection for detecting contact lesions at the humeral trochlea (Chanoit et al., 2010), and the extended supinated ML view is considered the best projection for showing the outline of the cranial edge of the MCP (Miyabayashi et al., 1995). However, we did not detect abnormalities with these views. We did not observe signs of subtrochlear sclerosis on either radiographs or CT images. It is much debated whether subtrochlear sclerosis reflects primary changes that contribute to MCD or secondary changes due to degenerative joint disease. Categorized as a primary change, subtrochlear sclerosis is proposed to be an indicator of the potential cause of MCD, reflecting an imbalance in the rate of bone apposition and resorption, resulting in stiffness in the subchondral bone layer, which predisposes the overlying articular cartilage layer to injury as more forces are transmitted during movement (Dequeker et al., 1995). However, our findings suggest that subtrochlear sclerosis develops in an advanced stage of MCD and should be regarded as a secondary change. We did not detect any blurring or blunting at the cranial edge of the MCP in extended supinated ML views, which is in contrast to the findings from clinical canine patients which suggested that signs such as sclerosis and shape changes occur prior to fissuring or fragmentation (Reichle et al., 2000).

In our study, four of the 13 diseased MCPs were accurately diagnosed on the basis of CT findings; the other MCPs were either suspected (n = 7) of being affected by MCD or were undiagnosed (n = 2). MCD was suspected due to the fact that there was only a small fragment of bone detected at the base of the MCP instead of a fragment that extended towards the apex of the MCP and we took into consideration the partial volume effect of CT during interpretation. However, MCD was confirmed on microCT. The earliest MCD was detected by CT at 14 weeks of age, with abnormalities most likely starting at the base of the coronoid located at the lateral aspect of the MCP. Similar findings were described as radial incisure fragmentation in a microCT study in clinical patients (Fitzpatrick et al., 2011). There was a learning curve in the recognition of early lesions on CT images in our study, such that we managed to detect lesions earlier in the second litter. In the first litter, lesions at 14 or 15 weeks of age were only detected at retrospective review of CT images.

Combination of the necropsy and microCT findings of the MCP showed that MCD was manifested as a lesion of only the subchondral bone in the dogs younger than 18 weeks of age. This might indicate that MCD starts in the deeper layer of underlying articular cartilage or even in the subchondral bone as suggested in a previous study (Danielson et al., 2006) rather than in the superficial articular cartilage layer. Gross anatomy also demonstrated close contact between the base of the MCP and the proximal radial head.

Compressive forces during the rotation of the MCP against the proximal radial head might generate internal shear stress, thereby favoring the development of MCD. This can happen even in joints of apparently normal congruity (Fitzpatrick and Yeadon, 2009; Burton et al., 2010). One of the dogs had unilateral RUI, which was not visible on radiographs or CT. In spite of this particular incongruence in a right elbow joint, the MCP was normal, whereas the left elbow of this same patient which was ostensibly congruent, was diagnosed with MCD. It is possible that a steeper slope of the MCP relative to the proximal radius head diverted the weight-bearing load from the humeral condyle away from the MCP; as well as the shear stress from the proximal radial head. It is also possible that MCD within this right elbow would have become apparent at a later date. The appearance of RUI in this dog differed from that described in earlier reports, which stated that RUI is more likely to be present at the apex of the MCP rather than at the base of MCP (Gemmill et al., 2005). MicroCT enabled visualization of the subchondral bone and allowed us to reconstruct the whole MCP non-destructively. This technique avoids the problems encountered in histological studies, where specimens are easily detached from slides, and trabecular bone details may be altered or lost due to slicing. We could detect bone abnormalities in dogs younger than 19 weeks of age, incomplete fissure lines at the base of MCP, and these findings supported our CT findings.

From our study, CT appears to be more sensitive than plain radiography in detecting the early lesions. Radiographic signs relying on secondary lesions should not be used as the sole criterion for diagnosing early-stage MCD, because this might lead to false negative results, especially in young dogs. Unfortunately, microCT is currently not available for clinical use because of technical limitations. It has been used extensively for studying bone microarchitecture (Laib et al., 2000; Patel et al., 2003; Wolschrijn and Weijs, 2004; Wolschrijn et al., 2005), and we used it as the gold standard to define the structure of subchondral bone. Because only superficial evaluation of the articular cartilage surface was possible at necropsy and microCT enabled visual inspection of the subchondral bone, we used both techniques together to provide a definitive diagnosis of MCD. In the absence of signs of secondary degenerative joint changes, we are confident that these findings do represent the development of MCD.

References

Boulay, J.P., 1998. Fragmented medial coronoid process of the ulna in the dog. Veterinary Clinics of North America: Small Animal Practice 28, 51-74.

Burton, N.J., Perry, M.J., Fitzpatrick, N., Owen, M.R., 2010. Comparison of bone mineral density in medial coronoid processes of dogs with and without medial coronoid process fragmentation. American Journal of Veterinary Research 71, 41-46.

Carpenter, L.G., Schwarz, P.D., Lowry, J.E., Park, R.D., Steyn, P.F., 1993. Comparison of radiologic imaging techniques for diagnosis of fragmented medial coronoid process of the cubital joint in dogs. Journal of the American Veterinary Medical Association 203, 78-83.

Chanoit, G., Singhani, N.N., Marcellin-Little, D.J., Osborne, J.A., 2010. Comparison of five radiographic views for assessment of the medial aspect of the humeral condyle in dogs with osteochondritis dissecans. American Journal of Veterinary Research 71, 780-783.

Danielson, K.C., Fitzpatrick, N., Muir, P., Manley, P.A., 2006. Histomorphometry of fragmented medial coronoid process in dogs: a comparison of affected and normal coronoid processes. Veterinary Surgery 35, 501-509.

De Rycke, L.M., Gielen, I.M., van Bree, H., Simoens, P.J., 2002. Computed tomography of the elbow joint in clinically normal dogs. American Journal of Veterinary Research 63, 1400-1407.

Dequeker, J., Mokassa, L., Aerssens, J., 1995. Bone density and osteoarthritis. The Journal of Rheumatology.Supplement 43, 98-100.

Fitzpatrick, N., Garcia-Nolen, T., Daryani, A., Watari, S., Hayashi, K., 2011. Structural analysis of canine medial coronoid disease by microCT: radial incisure versus tip fragmentation. In: Scientific Presentation Abstracts of American College of Veterinary Surgeons Veterinary Symposium, Chicago, Illinois, E26.

Fitzpatrick, N., Smith, T.J., Evans, R.B., Yeadon, R., 2009. Radiographic and arthroscopic findings in the elbow joints of 263 dogs with medial coronoid disease. Veterinary Surgery 38, 213-223.

Fitzpatrick, N., Yeadon, R., 2009. Working algorithm for treatment decision making for developmental disease of the medial compartment of the elbow in dogs. Veterinary Surgery 38, 285-300.

Gemmill, T.J., Mellor, D.J., Clements, D.N., Clarke, S.P., Farrell, M., Bennett, D., Carmichael, S., 2005. Evaluation of elbow incongruency using reconstructed CT in dogs suffering fragmented coronoid process. Journal of Small Animal Practice 46, 327-333.

Groth, A.M., Benigni, L., Moores, A.P., Lamb, C.R., 2009. Spectrum of computed tomographic findings in 58 canine elbows with fragmentation of the medial coronoid process. Journal of Small Animal Practice 50, 15-22.

Haudiquet, P.R., Marcellin-Little, D.J., Stebbins, M.E., 2002. Use of the distomedial-proximolateral oblique radiographic view of the elbow joint for examination of the medial coronoid process in dogs. American Journal of Veterinary Research 63, 1000-1005.

Hazewinkel, H.A.W., Meij, B.P., Theyse, L.F.H., van Rijssen, B., 2009. Locomotor system. In: Medical History and Physical Examination in Companion Animals, Second Ed. Elsevier Limited, Houten, NL, pp.136-148.

Holsworth, I.G., Wisner, E.R., Scherrer, W.E., Filipowitz, D., Kass, P.H., Pooya, H., Larson, R.F., Schulz, K.S., 2005. Accuracy of computerized tomographic evaluation of canine radio-ulnar incongruence in vitro. Veterinary Surgery 34, 108-113.

Hornof, W.J., Wind, A.P., Wallack, S.T., Schulz, K.S., 2000. Canine elbow dysplasia. The early radiographic detection of fragmentation of the coronoid process. Veterinary Clinics of North America: Small Animal Practice 30, 257-266.

House, M.R., Marino, D.J., Lesser, M.L., 2009. Effect of limb position on elbow congruity with CT evaluation. Veterinary Surgery 38, 154-160.

Janutta, V., Hamann, H., Klein, S., Tellhelm, B., Distl, O., 2006. Genetic analysis of three different classification protocols for the evaluation of elbow dysplasia in German shepherd dogs. Journal of Small Animal Practice 47, 75-82.

Keller, G.G., Dziuk, E., Bell, J.S., 2011. How the Orthopedic Foundation for Animals (OFA) is tackling inherited disorders in the USA: Using hip and elbow dysplasia as examples. The Veterinary Journal 189, 197-202.

Keller, G.G., Kreeger, J.M., Mann, F.A., Lattimer, J.C., 1997. Correlation of radiographic, necropsy and histologic findings in 8 dogs with elbow dysplasia. Veterinary Radiology & Ultrasound 38, 272-276.

Kramer, A., Holsworth, I.G., Wisner, E.R., Kass, P.H., Schulz, K.S., 2006. Computed tomographic evaluation of canine radioulnar incongruence in vivo. Veterinary Surgery 35, 24-29.

Laib, A., Barou, O., Vico, L., Lafage-Proust, M., Alexandre, C., Rügsegger, P., 2000. 3D micro-computed tomography of trabecular and cortical bone architecture with application to a rat model of immobilisation osteoporosis. Medical and Biological Engineering and Computing 38, 326-332.

Lavrijsen, I.C., Heuven, H.C., Voorhout, G., Meij, B.P., Theyse, L.F., Leegwater, P.A., Hazewinkel, H.A., 2012. Phenotypic and genetic evaluation of elbow dysplasia in Dutch Labrador retrievers, Golden retrievers, and Bernese Mountain Dogs. The Veterinary journal 193, 486-492.

Mason, D.R., Schulz, K.S., Samii, V.F., Fujita, Y., Hornof, W.J., Herrgesell, E.J., Long, C.D., Morgan, J.P., Kass, P.H., 2002. Sensitivity of radiographic evaluation of radio-ulnar incongruence in the dog in vitro. Veterinary Surgery 31, 125-132.

Miyabayashi, T., Takiguchi, M., Schrader, S.C., Biller, D.S., 1995. Radiographic anatomy of the medial coronoid process of dogs. Journal of the American Animal Hospital Association 31, 125-132.

Moores, A.P., Benigni, L., Lamb, C.R., 2008. Computed tomography versus arthroscopy for detection of canine elbow dysplasia lesions. Veterinary Surgery 37, 390-398.

Newton, C.D., 1985. Appendix B-Normal joint range of motion in the dog and cat. In: Textbook of Small Animal Orthopaedics. JB Lippincott, Philadelphia, pp. 1101-1106.

Patel, V., Issever, A.S., Burghardt, A., Laib, A., Ries, M., Majumdar, S., 2003. MicroCT evaluation of normal and osteoarthritic bone structure in human knee specimens. Journal of Orthopaedic Research 21, 6-13.

Preston, C.A., Schulz, K.S., Kass, P.H., 2000. In vitro determination of contact areas in the normal elbow joint of dogs. American Journal of Veterinary Research 61, 1315-1321.

Reichle, J.K., Park, R.D., Bahr, A.M., 2000. Computed tomographic findings of dogs with cubital joint lameness. Veterinary Radiology & Ultrasound 41, 125-130.

Samoy, Y., Van Ryssen, B., Gielen, I., Walschot, N., van Bree, H., 2006. Review of the literature: elbow incongruity in the dog. Veterinary and Comparative Orthopaedics and Traumatology 19, 1-8.

Tellhelm, B., 2011. Grading primary ED-lesions and elbow osteoarthrosis according to the IEWG protocol. Proceedings of the 26th Annual Meeting of International Elbow Working Group. Amsterdam, Holland. , 14-15.

Ubbink, G.J., Hazewinkel, H.A., van de Broek, J., Rothuizen, J., 1999. Familial clustering and risk analysis for fragmented coronoid process and elbow joint incongruity in Bernese Mountain Dogs in The Netherlands. American Journal of Veterinary Research 60, 1082-1087.

Ubbink, G.J., van de Broek, J., Hazewinkel, H.A., Wolvekamp, W.T., Rothuizen, J., 2000. Prediction of the genetic risk for fragmented coronoid process in Labrador retrievers. Veterinary Record 147, 149-152.

Voorhout, G., Hazewinkel, H.A.W., 1987. Radiographic evaluation of the canine elbow joint with special reference to the medial humeral condyle and the medial coronoid process. Veterinary Radiology 28, 158-165.

Wagner, K., Griffon, D.J., Thomas, M.W., Schaeffer, D.J., Schulz, K., Samii, V.F., Necas, A., 2007. Radiographic, computed tomographic, and arthroscopic evaluation of experimental radio-ulnar incongruence in the dog. Veterinary Surgery 36, 691-698.

Wolschrijn, C.F., Gruys, E., Weijs, W.A., 2005. Microcomputed tomography and histology of a fragmented medial coronoid process in a 20-week-old golden retriever. Veterinary Record 157, 383-386.

Wolschrijn, C.F., Weijs, W.A., 2004. Development of the trabecular structure within the ulnar medial coronoid process of young dogs. The Anatomical Record.Part A, Discoveries in molecular, cellular, and evolutionary biology 278, 514-519.

Wosar, M.A., Lewis, D.D., Neuwirth, L., Parker, R.B., Spencer, C.P., Kubilis, P.S., Stubbs, W.P., Murphy, S.T., Shiroma, J.T., Stallings, J.T., Bertrand, S.G., 1999. Radiographic evaluation of elbow joints before and after surgery in dogs with possible fragmented medial coronoid process. Journal of the American Veterinary Medical Association 214, 52-58.

Chapter 5

Effects of dietary cartilage and incipient medial coronoid disease on a collagenase generated osteoarthritis biomarker (C2C) in dogs

S.F. Lau[1]; R.J. Corbee[2]; M.A. Tryfonidou[2]; H.A.W. Hazewinkel[2]

[1] Division of Diagnostic Imaging, Faculty of Veterinary Medicine, Utrecht University, Yalelaan 108, 3584CM, Utrecht, The Netherlands

[2] Department of Clinical Sciences of Companion Animals, Faculty of Veterinary Medicine, Utrecht University, Yalelaan 108, 3584CM, Utrecht, The Netherlands

Submitted to Veterinary Surgery

Abstract

Objective:

To investigate the possible influence of dietary cartilage on the C2C concentration of plasma and urine and the potential clinically applicable plasma and synovial C2C biomarker in detecting the incipient MCD before severe OA.

Methods:

The effect of dietary cartilage supplementation on plasma and urine C2C concentration was investigated with serial plasma and urine samples obtained from seven healthy Beagles (3 to 11 years of age). Plasma and synovial fluid from 13 Labrador retrievers (15 to 27 weeks of age), including 26 elbow joints (12 MCD positive, 14 MCD negative) were collected.

Results:

Both plasma and urine C2C concentration in healthy Beagles were not affected by the cartilage content of the food ($P>0.05$). In Labrador retrievers, concentration of plasma and synovial C2C revealed no significant differences ($P>0.05$) between dogs with MCD or without MCD.

Conclusion:

Both the extruded and raw cartilage content given to dogs does not affect the results of the C2C biomarker in plasma and urine. The plasma and synovial C2C concentration is not useful as a biomarker to detect early stage of the MCD without signs of OA.

Introduction

Medial coronoid disease (MCD) encompasses the entire lesions at both the articular cartilage and subchondral bone of the medial coronoid process (MCP; Moores et al., 2008; Fitzpatrick et al., 2009) and it frequently affects young, large breed dogs, including Labrador retrievers (Boulay, 1998; Ubbink et al., 2000; Janutta and Distl, 2008; Lavrijsen et al., 2012). This developmental disease has been reported to causes lameness as early as 3 months of age (Fitzpatrick et al., 2009) and subsequent, development of osteoarthritis (OA) of the affected elbow joint (Draffan et al., 2009).

The diagnosis of MCD is most of the time corroborated by radiographical investigation, with special attention for secondary degenerative changes such as ulnar subtrochlear sclerosis and periarticular osteophytosis (Wosar et al., 1999; Fitzpatrick et al., 2009; Goldhammer et al., 2009; Lavrijsen et al., 2012). Other diagnostic tools such as computed tomography (Reichle et al., 2000; Holsworth et al., 2005; Kramer et al., 2006; Samoy et al., 2006; Wagner et al., 2007), exploratory arthrotomy or arthroscopy (Van Ryssen et al., 1993; Hazewinkel et al., 1998), bone scintigraphy (van Bruggen et al., 2010; Peremans et al., 2011), ultrasonography (Kramer et al., 1997; Knox IV et al., 2003; Seyrek-Intas et al., 2009), and magnetic resonance imaging (Snaps et al., 1998; Snaps et al., 1999) have been used, but with restricted availability. There is a need for a sensitive, minimally invasive, widely available, and not too expensive technique to confirm the diagnosis of incipient MCD, in order to exclude the MCD-affected dogs from the breeding stock and to start early treatment.

Recently, by using contrast enhanced micro-computed tomography (microCT), we demonstrated changes in mean microCT attenuation of the articular cartilage of the MCP diagnosed with incipient MCD in growing Labrador retrievers. These results indicated that the articular cartilage glycosaminoglycans (GAGs) content, which was reflected through the mean microCT attenuation, started to deplete in the early stage of this disease, before the development of clinical signs of OA. In similarity with GAGs, type II collagen is one of the main components of cartilage matrix (Kuettner et al., 1991). Although collagenase cleavage of type II collagen and evidence of GAGs loss might not occur contemporarily, both are used to monitor joint cartilage degeneration (Goranov, 2008; Huebner et al., 2010). Degradation of type II collagen triple helix occurs by collagenases. Cleavage of type II collagen triple helix at a single site (Gly_{775}-Leu/Ile_{776}) divides type II collagen into three quarter and one quarter fragments (Billinghurst et al., 1997). This collagenase-generated cleavage neoepitope, namely Col2-3/4$C_{long\ mono}$, or C2C, is detectable by using immunoassays (Garvican et al., 2010).

C2C has been reported to be elevated in various animal models of OA, including

dogs and rabbits (Matyas et al., 2004; Lindhorst et al., 2005; Lopez et al., 2006; Prink et al., 2010), and is in use as a cartilage degradation biomarker for equine joint disease (de Grauw et al., 2009; Trumble et al., 2009), or for the monitoring of cartilage metabolism during osteochondrosis in fowls (Donabédian et al., 2008). In the canine elbow joint, C2C has been reported to have potential as a reliable biomarker in diagnosing MCD in clinically lame dogs and objectively, reflect the degree of articular cartilage damage (Prink et al., 2010). Hence, C2C test could be a valuable add to the diagnostic procedure. However, dietary factors may interfere with biomarkers of cartilage degradation since the dietary cartilage intake, as part of the meat and bone meal, can be up to 50% in dog food (de-Oliveira et al., 2012). For example, hydroxyproline originating from bone meal, has been evidenced excreting in the urine in dose response way (Dijcker et al, 2012). Therefore, in the present study, we investigated the possible influence of dietary cartilage on the C2C concentration of plasma and urine and the potential clinically applicable plasma and synovial C2C biomarker in detecting the incipient MCD before severe OA.

Methods and material

Both studies were approved by the Ethics Committee at Utrecht University as required by Dutch law.

Study I: Evaluation of C2C in the plasma and urine from dogs with extra dietary cartilage

Seven healthy mature male Beagle dogs (3 to 11 years of age) were given a standardized diet (diet 1) before starting on a cartilage-free diet (diet 2) for a 4-week period (Table 1 and 2). Blood (4 ml) was collected by jugular venipuncture in heparinized tubes, and urine was collected by catheterization before and after feeding the diet 2. Thereafter, dogs were fed on diet 2 supplemented with 10g of raw articular cartilage fragments obtained from horse distal femurs (diet 3). Blood was collected immediately and hourly after the feeding (in 1 ml aliquots) during a 24 hours period and urine was collected immediately, one hour after the feeding, and followed by every 3 hours during a 24 hours period.

	Diet types/composition
Diet 1	Hill's Science Plan Canine Advanced Fitness Lamb & Rice (Hill's Pet Nutrition BV., Breda, The Netherlands)
Diet 2	Home-made diet (Horse meat, white rice, green beans, corn oil, and salmon oil)
Diet 3	Home-made diet (Diet 2 with additional 10g of raw cartilage obtained from horse distal femur)

Table 1. *Types of diets received by Beagles in study II.*

	Nutrition information	
	Diet 1	Diet 2
Protein (g)	5.8	5.4
Fat (g)	4	2.8
NFE* (g)	13.1	12.7
Fiber (g)	0.5	n/a
Ash (g)	1.2	n/a
Moisture (g)	2.1	43.7
Calcium (mg)	196	7.7
Phosphorus (mg)	171	56.4
Sodium (mg)	61	8.5
Potassium (mg)	172	77.9
Magnesium (mg)	28	9.8
Omega-3 (mg)	128	n/a
Omega-6 (mg)	854	n/a
Vitamin A (IU)	253	17
Vitamin D (IU)	11	0
Vitamin E (mg)	16	0.2
Vitamin C (mg)	1.9	n/a
kcal/100g	375	154
kcal/100g DM†	407	468

Table 2. *Diet specification indicating the energy and nutrient intake in dogs receiving diet 1, and 2. *Nitrogen-free extract; †Dry matter*

Study II: Evaluation of C2C in the plasma and synovial fluid from dogs with and without incipient medial coronoid disease

Thirteen young Labrador retrievers (15 to 27 weeks of age) originating from two litters from MCD affected dam and sires were euthanized and used for necropsy examination and microCT studies (Lau et al., 2013a; Lau et al., 2013b). Based on the combination of the gross pathological examination and microCT reconstructed images, ulnas were defined as positive for MCD when there was evidence of fissure or fragmentation in the articular cartilage and/or subchondral bone of the MCP. Ulnas were grouped by MCP status (MCD negative and MCD positive groups) and body weight on the day of euthanasia (<20 kg, 21–25 kg, and >25 kg). Blood was collected by jugular venipuncture in heparinized tubes before euthanasia (4 ml) and synovial fluid was collected from each elbow joint (0.3-0.8 ml) with arthrocentesis by using 3 ml syringe and 20G needle, immediately after the dog was euthanized.

Analysis by using enzyme-linked immunosorbent assay

Blood samples were centrifuged and plasma was stored in a sterile tube at -80 °C until analysis. Urine and synovial fluid was stored at -80 °C without pre-storage centrifugation performed. A commercially available ELISA kit was used for measuring the neoepitope created by the cleavage of type II collagen by collagenases (ELISA, IBEX Pharmaceuticals Inc.). The used C2C antibody is claimed to have broad cross-reactivity and recognizes multispecies C2C, including dogs (Hayashi et al., 2009; Prink et al., 2010). All the plasma, urine, and synovial fluid samples were analyzed in one batch, according to the protocols described previously (Hayashi et al., 2009; Prink et al., 2010). All standards and samples were run in duplicate and data was reported as C2C concentration, expressed in ng/ml. The concentration of C2C in urine were corrected for urinary creatinine excretion. The intra-assay coefficient of variation (CV) was calculated.

Statistical analysis

Statistical analyses were performed using SPSS (SPSS Version 16.0, SPSS Inc.). In both studies, linear mixed models, containing both fixed and random effects, were used to analyze the plasma, urine, and synovial fluid C2C concentration as dependent outcome. A random intercept for each dog was added to each model to take the correlation of the observations within a dog into account. Model selection was based on the Akaike Information Criterion (AIC). Conditions for the use of mixed models, such as normal distribution of the data, were assessed by analyzing the residuals (PP- and QQ plots) of the acquired models and no violations of these conditions were observed. *P*-values were calculated to analyze differences of interest in fixed effects, namely, different diets and time points in study I and litter, MCP status, and bodyweight in study II. The differences were considered statistically significant at $P<0.05$. The linear correlation coefficient was calculated by using the Pearson correlation coefficient between the synovial C2C concentration between left and right limb, and between the plasma and synovial C2C concentration (with left and right limb separately).

Results

The intra-assay coefficient of variation in our study was 11%. In study I, the average C2C concentration in plasma was 46.0 ± 18.4 ng/ml before the diet 2, 56.5 ± 15.1 ng/ml after the diet 2, and 55.7 ± 13.0 ng/ml after the diet 3. C2C concentration in the urine normalized to urine creatinine concentration was 2.4 ± 0.3 ng/ml before the diet 2, 2.5 ± 0.4 ng/ml after the diet 2, and 2.4 ± 0.4 ng/ml after diet 3. Statistically, there was no significant difference between different diets ($P>0.05$).

In study II, based on the gross pathological examination and microCT reconstructed images, 12 elbows in six dogs were diagnosed as MCD positive, as early as 16 weeks of age. None of the dogs showed evidence of periarticular osteophytosis at gross pathological examination (Lau et al., 2013a). Cartilage fissure was absent in the MCD-positive dogs younger than 18 weeks of age. Synovial fluid obtained from 26 elbows from 13 Labrador retrievers appeared colorless with high viscosity. In the MCD positive group, the mean ± SD for the plasma and synovial C2C concentration was 122.3 ± 67.8 ng/ml and 63.1 ± 27.0 ng/ml respectively, which did not differ significantly from the plasma and synovial C2C concentration in the MCD negative group, which was 162.3 ± 41.3 ng/ml and 74.9 ± 28.3 ng/ml (P>0.05), respectively. There was no significant effect of MCP status and body weight on plasma and synovial C2C concentration (P>0.05). The synovial C2C obtained from left and right was weakly correlated and not significant (r=0.05, P>0.05). The correlation of the plasma C2C with synovial C2C obtained from left (r=-0.34) or right limb (r=0.35) were not significant (P>0.05).

Discussion

Type II collagen is one of the major constitutes of the articular cartilage, and therefore epitopes generated by degradation of collagen can be an ideal biomarker to detect OA. Recent studies support that this biomarker can be a specific marker for early OA with concurrent radiographic changes (Matyas et al., 2004). However, taking into account that dog food contains vast amounts of collagen, it is surprising that thus far there are no reports on the possible effect of the dietary cartilage intake on the plasma and urine C2C concentration.

Study I: Evaluation of C2C in the plasma and urine from dogs with extra dietary cartilage

Dietary cartilage intake of dogs does not affect the C2C biomarker concentration in plasma and urine. This unlike hydroxyproline originating from bone meal, which is very well absorbed and in a dose-response way, excreted in cats in the urine (Dijcker et al., 2012). Increase in urinary hydroxyproline excretion has been evidenced in bone metabolic studies, reflecting bone resorption (Maeda et al., 1997), where dietary bone meal in dog food can influence the outcome of the bone metabolic studies (Hazewinkel, personal communication). Nevertheless, dietary cartilage neither extruded nor raw did not result in an increase of the C2C concentration in plasma and urine. The absence of a dietary effect may be due to the fact that cartilage is not well absorbed, or that the cartilage degradation products in the gastrointestinal tract are different from the degradation products inside the joint, during ongoing OA.

Study II: Evaluation of C2C in the plasma and synovial fluid from dogs with and without incipient medial coronoid disease

In 13 Labrador retrievers purposely bred from the MCD positive dam and sires, 46% of the dogs were diagnosed with MCD based on presence of a fissure or fragmentation in the subchondral bone of the MCP as revealed from microCT investigation (Lau et al., 2013a). Based on the earlier performed contrast enhanced microCT, we demonstrated a significant depletion of GAGs from articular cartilage in an early stage of MCD (Lau et al. 2013b). It is reasonable to expect (Prink et al., 2010) that the major component of the cartilage matrix, i.e. type II collagen is also affected.

We investigated the very early stage of the MCD without concurrent OA, and showed that both the plasma and synovial C2C biomarker was not significantly different between affected and unaffected growing Labrador retrievers. This finding is in contrast with a previous report revealing synovial C2C concentration as a reliable parameter in detecting cartilage degradation in elbow joints of dogs radiographically diagnosed with MCD with secondary OA. There was even a moderate correlation of the degree of cartilage damage with the synovial C2C concentration (Prink et al., 2010). The most likely explanation for the difference of our findings with that study is that the C2C biomarker is not sensitive enough for the early stage of MCD without prominent OA. Notably, the plasma C2C concentration was higher in growing healthy Labrador retrievers (162.3 ± 41.3 ng/ml) in comparison to the adult healthy Beagles in study I, (46.0 ± 18.4 ng/ml). It was also higher than the plasma C2C concentration of a Labrador retriever with known OA, which was 79.8 ± 3.4 ng/ml (unpublished data). This can well be explained by the fact that the Labrador retrievers in our study were at active growth phase with high skeletal remodeling (Donabédian et al., 2008). Synovial C2C concentration in dogs with incipient MCD from our study was 63.1 ± 27.0 ng/ml, being lower in comparison to the reported synovial C2C concentration in MCD dogs with signs of OA, 112.3 ± 24.8 ng/ml; but similar to the synovial C2C concentrations (76.1 ± 16.9 ng/ml) in the control dogs (i.e. OA negative) in the study of Prink *et al.* (2010). The lack of correlation between the plasma and the left or right limb C2C concentration supports the notion that in growing animals other cartilaginous tissues, such as the spine and respiratory system, contribute to the C2C plasma concentration, next to the focal OA lesions.

In conclusion, both the extruded and raw cartilage given to dogs does not affect the concentration of the C2C biomarker in plasma and urine. Both the plasma and synovial C2C biomarker are not useful in detecting early stage of the MCD without concurrent signs of OA. Further investigation with other markers of cartilage degradation focusing on aggrecan and proteoglycans, should be studied as a new approach to detect incipient MCD.

Reference

Billinghurst, R.C., Dahlberg, L., Ionescu, M., Reiner, A., Bourne, R., Rorabeck, C., Mitchell, P., Hambor, J., Diekmann, O., Tschesche, H., Chen, J., Van Wart, H., Poole, A.R., 1997. Enhanced cleavage of type II collagen by collagenases in osteoarthritic articular cartilage. The Journal of Clinical Investigation 99, 1534-1545.

Boulay, J.P., 1998. Fragmented medial coronoid process of the ulna in the dog. Veterinary Clinics of North America: Small Animal Practice 28, 51-74.

de Grauw, J.C., Lest, C., Brama, P., Rambags, B., Weeren, P.R., 2009. In vivo effects of meloxicam on inflammatory mediators, MMP activity and cartilage biomarkers in equine joints with acute synovitis. Equine Veterinary Journal 41, 693-699.

de-Oliveira, L., de Carvalho Picinato, M., Kawauchi, I., Sakomura, N., Carciofi, A., 2012. Digestibility for dogs and cats of meat and bone meal processed at two different temperature and pressure levels. Journal of Animal Physiology and Animal Nutrition 96, 1136-1146.

Dijcker, J., Hagen-Plantinga, E., Everts, H., Bosch, G., Kema, I., Hendriks, W., 2012. Dietary and animal-related factors associated with the rate of urinary oxalate and calcium excretion in dogs and cats. Veterinary Record 171, 46-46.

Draffan, D., Carrera, I., Carmichael, S., Heller, J., Hammond, G., 2009. Radiographic analysis of trochlear notch sclerosis in the diagnosis of osteoarthritis secondary to medial coronoid disease. Veterinary and Comparative Orthopaedics and Traumatology 22, 7-15.

Donabédian, M., Weeren, P.R., Perona, G., Fleurance, G., Robert, C., Léger, S., Bergero, D., Lepage, O., Martin-Rosset, W., 2008. Early changes in biomarkers of skeletal metabolism and their association to the occurrence of osteochondrosis (OC) in the horse. Equine Veterinary Journal 40, 253-259.

Fitzpatrick, N., Smith, T.J., Evans, R.B., Yeadon, R., 2009. Radiographic and arthroscopic findings in the elbow joints of 263 dogs with medial coronoid disease. Veterinary Surgery 38, 213-223.

Garvican, E.R., Vaughan-Thomas, A., Innes, J.F., Clegg, P.D., 2010. Biomarkers of cartilage turnover. Part 1: Markers of collagen degradation and synthesis. The Veterinary Journal 185, 36-42.

Goldhammer, M.A., Smith, S.H., Fitzpatrick, N., Clements, D.N., 2009. A comparison of radiographic, arthroscopic and histological measures of articular pathology in the canine elbow joint. The Veterinary Journal 186, 96-103.

Goranov, N.V., 2008. Serum markers of lipid peroxidation, antioxidant enzymatic defence, and collagen degradation in an experiment (Pond-Nuki) canine model of osteoarthritis. Veterinary Clinical Pathology 36, 192-195.

Hayashi, K., Kim, S.U.N.Y., Lansdowne, J.L., Kapatkin, A., Dejardin, L.M., 2009. Evaluation of a collagenase generated osteoarthritis biomarker in naturally occurring canine cruciate disease. Veterinary Surgery 38, 117-121.

Hazewinkel, H.A.W., Meij, B. P., Theyse, L.F.H., 1998. Surgical treatment of elbow dysplasia. Veterinary Quartery. Supplement 1, 29-31.

Holsworth, I.G., Wisner, E.R., Scherrer, W.E., Filipowitz, D., Kass, P.H., Pooya, H., Larson, R.F., Schulz, K.S., 2005. Accuracy of computerized tomographic evaluation of canine radio-ulnar incongruence in vitro. Veterinary Surgery 34, 108-113.

Huebner, J.L., Williams, J.M., Deberg, M., Henrotin, Y., Kraus, V.B., 2010. Collagen fibril disruption occurs early in primary guinea pig knee osteoarthritis. Osteoarthritis Research Society 18, 397-405.

Janutta, V., Distl, O., 2008. Review on canine elbow dysplasia: pathogenesis, diagnosis, prevalence and genetic aspects. Deutsche Tierarztliche Wochenschrift 115, 172-181.

Knox IV, V.W., Sehgal, C.M., Wood, A.K.W., 2003. Correlation of ultrasonographic observations with anatomic features and radiography of the elbow joint in dogs. American Journal of Veterinary Research 64, 721-726.

Kramer, M., Gerwing, M., Hach, V., Schimke, E., 1997. Sonography of the musculoskeletal system in dogs and cats. Veterinary Radiology & Ultrasound 38, 139-149.

Kramer, A., Holsworth, I.G., Wisner, E.R., Kass, P.H., Schulz, K.S., 2006. Computed tomographic evaluation of canine radioulnar incongruence in vivo. Veterinary Surgery 35, 24-29.

Kuettner, K.E., Aydelotte, M.B., Thonar, E.J., 1991. Articular cartilage matrix and structure: a minireview. The Journal of Rheumatology. Supplement 27, 46-48.

Lau, S.F., Wolschrijn, C.F., Hazewinkel, H.A.W., Siebelt, M., Voorhout, G., 2013a. The early development of medial coronoid disease (MCD) in growing Labrador retrievers: Radiographic, computed tomographic, necropsy and micro-computed tomographic findings. The Veterinary Journal (doi: 10.1016/j.tvjl.2013.04.002).

Lau, S.F., Wolschrijn, C.F., Siebelt, M., Vernooij, J.C.M., Voorhout, G., Hazewinkel H.A.W., 2013b. Assessment of articular cartilage and subchondral bone using EPIC-microCT in Labrador retrievers with incipient medial coronoid disease. The Veterinary Journal (doi: 10.1016/j.tvjl.2013.05.038).

Lavrijsen, I.C., Heuven, H.C., Voorhout, G., Meij, B.P., Theyse, L.F., Leegwater, P.A., Hazewinkel, H.A., 2012. Phenotypic and genetic evaluation of elbow dysplasia in Dutch Labrador Retrievers, Golden retrievers, and Bernese Mountain Dogs. The Veterinary Journal 193, 486-492.

Lindhorst, E., Wachsmuth, L., Kimmig, N., Raiss, R., Aigner, T., Atley, L., Eyre, D., 2005. Increase in degraded collagen type II in synovial fluid early in the rabbit meniscectomy model of osteoarthritis. Osteoarthritis and Cartilage 13, 139-145.

Lopez, M.J., Robinson, S.O., Quinn, M.M., Hosgood, G., Markel, M.D., 2006. In vivo evaluation of intra-articular protection in a novel model of canine cranial cruciate ligament mid-substance elongation injury. Veterinary Surgery 35, 711-720.

Maeda, H., Koizumi, M., Yoshimura, K., Yamauchi, T., Kawai, T., Ogata, E., 1997. Correlation between bone metabolic markers and bone scan in prostatic cancer. The Journal of Urology 157, 539-543.

Matyas, J.R., Atley, L., Ionescu, M., Eyre, D.R., Poole, A.R., 2004. Analysis of cartilage biomarkers in the early phases of canine experimental osteoarthritis. Arthritis & Rheumatism 50, 543-552.

Moores, A.P., Benigni, L., Lamb, C.R., 2008. Computed tomography versus arthroscopy for detection of canine elbow dysplasia lesions. Veterinary Surgery 37, 390-398.

Peremans, K., Vermeire, S., Dobbeleir, A., Gielen, I., Samoy, Y., Piron, K., Vandermeulen, E., Slegers, G., van Bree, H., De Spiegeleer, B., Dik, K., 2011. Recognition of anatomical predilection sites in canine elbow pathology on bone scans using micro-single photon emission tomography. The Veterinary Journal 188, 64-72.

Prink, A., Hayashi, K., KIM, S.U.N.Y., Kim, J., Kapatkin, A., 2010. Evaluation of a collagenase generated osteoarthritis biomarker in the synovial fluid from elbow joints of dogs with medial coronoid disease and unaffected dogs. Veterinary Surgery 39, 65-70.

Reichle, J.K., Park, R.D., Bahr, A.M., 2000. Computed tomographic findings of dogs with cubital joint lameness. Veterinary Radiology & Ultrasound 41, 125-130.

Samoy, Y., Van Ryssen, B., Gielen, I., Walschot, N., van Bree, H., 2006. Review of the literature: elbow incongruity in the dog. Veterinary and Comparative Orthopaedics and Traumatology 19, 1-8.

Seyrek-Intas, D., Michele, U., Tacke, S., Kramer, M., Gerwing, M., 2009. Accuracy of ultrasonography in detecting fragmentation of the medial coronoid process in dogs. Journal of the American Veterinary Medical Association 234, 480-485.

Snaps, F.R., Park, R.D., Saunders, J.H., Balligand, M.H., Dondelinger, R.F., 1999. Magnetic resonance arthrography of the cubital joint in dogs affected with fragmented medial coronoid processes. American Journal of Veterinary Research 60, 190-193.

Snaps, F.R., Saunders, J.H., Park, R.D., Daenen, B., Balligand, M.H., Dondelinger, R.F., 1998. Comparison of spin echo, gradient echo and fat saturation magnetic resonance imaging sequences for imaging the canine elbow. Veterinary Radiology & Ultrasound 39, 518-523.

Trumble, T., Scarbrough, A., Brown, M., 2009. Osteochondral injury increases type II collagen degradation products (C2C) in synovial fluid of Thoroughbred racehorses. Osteoarthritis and Cartilage 17, 371-374.

Ubbink, G.J., van de Broek, J., Hazewinkel, H.A., Wolvekamp, W.T., Rothuizen, J., 2000. Prediction of the genetic risk for fragmented coronoid process in Labrador retrievers. Veterinary Record 147, 149-152.

van Bruggen, L.W., Hazewinkel, H.A., Wolschrijn, C.F., Voorhout, G., Pollak, Y.W., Barthez, P.Y., 2010. Bone scintigraphy for the diagnosis of an abnormal medial coronoid process in dogs. Veterinary Radiology & Ultrasound 51, 344-348.

Van Ryssen, B., van Bree, H., Simoens, P., 1993. Elbow arthroscopy in clinically normal dogs. American Journal of Veterinary Research 54, 191-198.

Wagner, K., Griffon, D.J., Thomas, M.W., Schaeffer, D.J., Schulz, K., Samii, V.F., Necas, A., 2007. Radiographic, computed tomographic, and arthroscopic evaluation of experimental radio-ulnar incongruence in the dog. Veterinary Surgery 36, 691-698.

Wosar, M.A., Lewis, D.D., Neuwirth, L., Parker, R.B., Spencer, C.P., Kubilis, P.S., Stubbs, W.P., Murphy, S.T., Shiroma, J.T., Stallings, J.T., Bertrand, S.G., 1999. Radiographic evaluation of elbow joints before and after surgery in dogs with possible fragmented medial coronoid process. Journal of the American Veterinary Medical Association 214, 52-58.

Chapter 6

Assessment of articular cartilage and subchondral bone using EPIC-microCT in Labrador retrievers with incipient medial coronoid disease

S.F. Lau[1], C.F. Wolschrijn[2], M. Siebelt[3], J.C.M. Vernooij[4], G. Voorhout[1], H.A.W. Hazewinkel[5]

[1] Division of Diagnostic Imaging, Faculty of Veterinary Medicine, Utrecht University, Yalelaan 108, 3584CM, Utrecht, The Netherlands

[2] Department of Pathobiology, Division of Anatomy and Physiology, Faculty of Veterinary Medicine, Utrecht University, Yalelaan 1, 3584CL, Utrecht, The Netherlands

[3] Department of Orthopedic Surgery, Erasmus Medical Center, Rotterdam, The Netherlands

[4] Department of Farm Animal Health, Faculty of Veterinary Medicine, Utrecht University, Yalelaan 7, 3584CL, Utrecht, The Netherlands

[5] Department of Clinical Sciences of Companion Animals, Faculty of Veterinary Medicine, Utrecht University, Yalelaan 108, 3584CM, Utrecht, The Netherlands

Adapted from The Veterinary Journal, 2013

http://dx.doi.org/10.1016/j.tvjl.2013.05.038

Abstract

Objective:

To investigate changes to both articular cartilage and subchondral bone of the medial coronoid process (MCP) of growing Labrador retrievers in an early stage of the disease and of different weight.

Methods:

Equilibrium partitioning of an ionic contrast agent with micro-computed tomography (microCT) was used to investigate changes to both articular cartilage and subchondral bone of the medial coronoid process (MCP) of 14 purpose-bred growing Labrador retrievers with and without medial coronoid disease (MCD) and of different weight.

Results:

Of 14 purpose-bred Labrador retrievers (15 to 27 weeks), six were diagnosed with bilateral MCD and one was diagnosed with unilateral MCD on the basis of microCT studies. The mean x-ray attenuation of articular cartilage was significantly higher in dogs with MCD than in dogs without MCD (P<0.01). In all dogs, the mean x-ray attenuation of articular cartilage was significantly higher at the lateral aspect of the MCP (P<0.001) than at the proximal aspect of the MCP, indicating a decreased content of glycosaminoglycan (GAG). Changes in parameters of subchondral bone micro-architecture, namely, the ratio of bone volume over tissue volume (BV/TV), bone surface density (BS/TV), bone surface to volume ratio (BS/BV), trabecular thickness (Tb.Th; mm), size of marrow cavities described by trabecular spacing (Tb.Sp; mm), and structural model index (SMI), differed significantly by litter effect (P<0.05) due to the difference in age and weight, but not by the presence/absence of MCD (P>0.05), indicating that subchondral bone density is not affected in early MCD. Our study showed that the cartilage matrix and not subchondral bone density is affected in the early stages of MCD.

Conclusion:

We demonstrated that MCP lesions can occur in Labrador retrievers as young as 15 weeks and that there is a significant depletion of GAG from articular cartilage in an early stage of MCD, before clinical signs are manifested.

Introduction

Medial coronoid disease (MCD) is a common developmental orthopaedic disease in young, large-breed dogs (Kirberger and Fourie, 1998; Janutta et al., 2006; Moores et al., 2008; Fitzpatrick et al., 2009; Temwichitr et al., 2010). The etiopathogenesis of this heritable disease has yet to be elucidated, although several hypotheses have been proposed, such as those involving osteochondrosis (Tirgari, 1980; Grøndalen and Grøndalen, 1981; Olsson, 1987), subchondral bone osteosclerosis (Temwichitr et al., 2010), micro-damage in subchondral bone (Danielson et al., 2006), underdevelopment of the trochlear notch of the ulna (Wind and Packard, 1986), joint incongruity (Preston et al., 2001), or differences in the distribution of shear stresses and forces within the joint alignments (Wolschrijn and Weijs, 2004; Hulse et al., 2010). Although both the articular cartilage and the subchondral bone of the medial coronoid process (MCP) are affected, it remains unclear whether the disease originates in the articular cartilage or in the subchondral bone. The disease is typically detected in an advanced stage because clinical signs are usually caused by secondary joint degeneration and because of limitations of diagnostic techniques. For these reasons, many of the reported findings are for advanced stages of MCD complicated by, e.g., periarticular osteophytosis (Fitzpatrick et al., 2009; Lavrijsen et al., 2012).

Micro-computed tomography (microCT) has been used in bone research because it enables bone tissue to be assessed quantitatively at a micron-level resolution and non-destructively in three dimensions (3-D) (Wolschrijn and Weijs, 2004; van Ruijven et al., 2005; Botter et al., 2006; Sniekers et al., 2008; Zhao et al., 2010). Cartilage quality can be assessed by equilibrium partitioning of an ionic contrast agent with microCT (EPIC-microCT), a technique that makes it possible to assess the morphology and biochemical composition of articular cartilage with great precision and accuracy (Palmer et al., 2006; Piscaer et al., 2008a; Xie et al., 2009; Benders et al., 2010; Xie et al., 2010). With this technique, negatively charged contrast molecules diffuse into the cartilage at sites where glycosaminoglycan (GAG) depletion has occurred. After yielding an equilibrium distribution of the ionic contrast agent, which is inversely related to the density of the negatively charged GAG, microCT is performed to detect the attenuation of the x-ray radiation (Palmer et al., 2006).

The aim of the present study was to quantitatively assess the changes occurring in articular cartilage and subchondral bone in early stages of MCD in growing Labrador retrievers, in order to provide additional information in investigating the etiopathogenesis of MCD.

Materials and methods

Specimen collection

The study was approved by the Ethics Committee of Utrecht University, as required by Dutch law. Twenty-eight elbows were collected from 14 purpose-bred growing Labrador retrievers (nine males and five females) aged 15-27 weeks and weighing 23.1 ± 5.8 kg (mean ± SD) that had been euthanized with an overdose of intravenously administered barbiturate. The dogs originated from two litters from a MCD-affected dam and two MCD-affected sires. The dogs had been used in another study, in which the dogs had been examined using radiography and computed tomography (CT) fortnightly from the age of 6 (*n*=7 dogs) or 7 weeks (*n*=7 dogs) until euthanasia (15 to 27 weeks). The dogs were fed on commercial puppy/young dog food and were weighed weekly and before euthanasia. Euthanasia was performed on dogs when MCD was suspected on the basis of radiographic or CT findings, or on dogs that served as an age- and weight-matched negative control. The dogs were regularly examined by a board certified veterinary surgeon (H.A.W.H.) as described previously (Hazewinkel et al., 2009). At the time of euthanasia, none of the dogs had clinical signs of MCD on physical examination or a changed level of daily activity. Immediately after euthanasia, both forelimbs were harvested and soaked as such in 4% buffered formaldehyde solution (Gebufferde Formaldehyde, Klinipath) until the EPIC-microCT study was performed.

Data analysis

The definitive diagnosis of MCD was obtained by interpretation of 3-D reconstructed images of the subchondral bone of the MCP, using SkyScan software (CTVolume, SkyScan) which enables the demonstration of an overall MCP subchondral bone structure. Ulnas were defined as being positive for MCD when there was evidence of fissure (Fig. 1b) or fragmentation (Fig. 1c and d) of the subchondral bone; the normal MCP is free from such changes (Fig. 1e-g). Ulnas were grouped by MCP status (MCD-negative and MCD-positive groups) and bodyweight (<20 kg, 21–25 kg, and >25 kg, based on the bodyweight on the day of euthanasia).

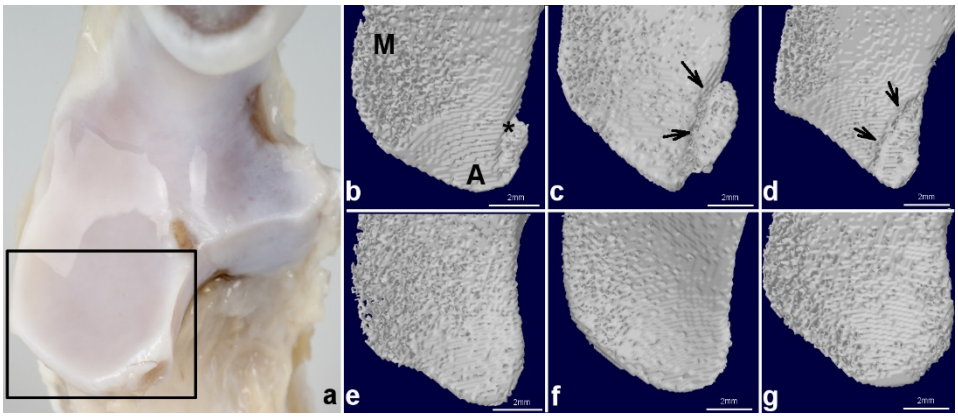

Fig. 1. *(a) Left ulna obtained from a Labrador retriever at 26 weeks of age, indicating the proximal view of the medial coronoid process (MCP) (in box). Proximal views of the 3-D reconstructed MCPs obtained from the left elbows of Labrador retrievers of different age. (b) 15 (c) 18, and (d) 25 weeks old, diagnosed medial coronoid disease (MCD) based on the fissure (*) or fragments (arrows) at the lateral aspect of the MCP. (e-g) Normal appearance of MCPs from the left elbows of the Labrador retrievers at 15, 18, and 26 weeks old. Some confluence of the trabecular structure can be seen at the caudomedial aspect of the MCP (M), the subchondral bone at the lateral aspect and apex of the MCP (A) is consolidated and rather smooth.*

Equilibrium partitioning of an ionic contrast agent via microCT

The proximal one third of the ulna was cut and immersed in the contrast agent, i.e. sodium and meglumine ioxaglate containing 320 mg iodine/ml (Hexabrix 320, Guerbet Nederland B.V.). Both the concentration of the contrast agent and the immersion time had been pre-determined during a trial in order to produce an optimal segmentation, using the method as described earlier (Xie et al., 2009). Immersion in 40% Hexabrix / 60% PBS solution for minimally 8 h was optimal for segmenting cartilage from the underlying subchondral bone. Ulnas were scanned in an in-vivo microCT system (SkyScan 1076, SkyScan; Fig. 2) at 60 kV and 170 µA with a 1.0-mm aluminium filter, resulting in 36-µm isotropic voxel size. The exposure time was 948 ms and x-ray projections were obtained with rotation steps of 0.5°. Scanning time for a bone length of 4 cm was approximately 90 min. During scanning, bones were wrapped in plastic foil, to prevent dehydration, and fixed in a cylindrical plastic holder, to prevent movement.

Fig. 2. *Micro-computed tomography system (SkyScan 1076, SkyScan)*

Quantitative assessment of the articular cartilage of the MCP

EPIC-microCT images were interpreted by using SkyScan software (CTAnalyser, SkyScan). The volume of interest (VOI), consisting of a stack of regions of interest (ROI), was selected from over 100 cross-sections of the MCP. Based on the sagittal view, approximately 60 slices proximal to the apex of the MCP and 40 slices distal to the apex of the MCP were selected as VOI. ROI at the different anatomical locations of the MCP were drawn, namely, the lateral aspect at the radial notch side, the proximal aspect at the humeral articular side, and the medial aspect of the MCP (Fig. 3). The distal end of the sagittal ridge of the trochlear notch was considered as the caudal limit of the MCP. Within the VOI, ROI were selected based on the articular side with a freehand drawing technique and semi-automatic contouring was applied every 4 to 5 slices in order to accurately segment articular cartilage from subchondral bone. Mean microCT attenuation (arbitrary units; Piscaer et al., 2008b) of full-thickness articular cartilage within the VOI was obtained by segmenting cartilage from bone tissue, using one fixed threshold for all scans that were selected visually. Morphological parameters of the segmented articular cartilage, namely, mean volume (mm^3), surface area (mm^2), and thickness (mm) at different anatomical locations, were calculated using CTAnalyser software (SkyScan, 2010).

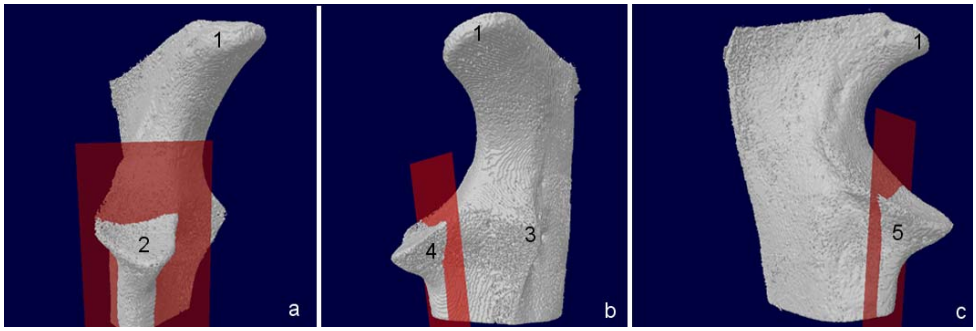

Fig. 3. *3-D reconstructed microCT images of the left ulna obtained from a 15-week-old dog, the medial coronoid process (MCP) is separated from the rest of the ulna by the red plate. (a) Cranial view with the subchondral bone of humeral articular side, proximal aspect of the MCP. (b) Craniolateral view of the ulna at radial notch side, lateral aspect of the MCP. (c) Medial view of the ulna, medial aspect of the MCP. 1, anconeal process; 2, proximal aspect of the MCP; 3, lateral coronoid process; 4, lateral aspect of the MCP; 5, medial aspect of the MCP.*

Quantitative assessment of the subchondral bone of the MCP

VOIs, consisting of stacks of ROI from over 100 cross-sections of the MCP, excluding cortical bone, were selected. Subchondral bone was segmented from articular cartilage by using one fixed threshold for all scans. Morphological parameters, namely, the ratio of bone volume over tissue volume (BV/TV), bone surface density (BS/TV), bone surface to volume ratio (BS/BV), trabecular thickness (Tb.Th; mm), size of marrow cavities described by trabecular spacing (Tb.Sp; mm), and structural model index (SMI), were calculated using CTAnalyser software. The SMI varies from 0 to 3, with 0 representing a plate structure and 3 representing a rod structure of trabecular bone. Values between 0 and 3 indicate a mixed structure of plates and rods (Hildebrand and Rüegsegger, 1997).

Statistical analysis

Statistical analyses were performed using SPSS (SPSS Version 16.0, SPSS Inc.). Linear mixed models, containing both fixed and random effects, were used to analyze the described parameters separately for the articular cartilage and subchondral bone. A random intercept for each dog was added to each model to take the correlation of the observations within a dog into account. Model selection was based on the Akaike Information Criterion (AIC). Conditions for the use of mixed models, such as normal distribution of the data, were assessed by analyzing the residuals (PP and QQ plots) of the acquired models and no violations of these conditions were observed. *P*-values were calculated for articular cartilage and subchondral bone parameters to analyze differences of interest in main effects, namely, litter, limb, MCP status, bodyweight/age, and

anatomical locations. Mean attenuation, volume, surface area, and thickness of the articular cartilage were analyzed as dependent variables for the articular cartilage. Meanwhile, different morphological parameters of the subchondral bone of the MCP i.e. BV/TV, BS/TV, BS/BV, Tb.Th, Tb.Sp, and SMI were analyzed as dependent variables for subchondral bone. The differences were considered statistically significant at $P<0.05$. Associations between age and bodyweight were assessed by using Pearson correlation coefficient, *r*. The strength of relationship was considered strong when $r>0.5$ (Choudhury, 2009). One of these main effects (bodyweight or age) was chosen as independent variable in our study as substitution to another one against the dependent variables when both main effects were strongly correlated.

Results

Age

The age of the animal was strongly correlated with the bodyweight (Pearson's correlation $r=0.93$, $P<0.01$). Similar patterns of correlation were obtained when bodyweight was chosen as independent variable in our study as substitution to age against the dependent variables.

Specimens collected

In the first litter, eight dogs aged 19-27 weeks and weighing 27.1 ± 3.8 kg (mean ± SD) were studied, and in the second litter, six dogs aged 15-18 weeks and weighing 17.7 ± 2.1 kg (mean ± SD) were studied. In total, 13 ulnas (six from the first litter, seven from the second litter) showed evidence of MCD on microCT-reconstructed images; the remaining 15 ulnas were regarded as normal. Ten ulnas were obtained from dogs weighing less than 20 kg, eight from dogs weighing 20-25 kg, and ten from dogs weighing more than 25 kg. Six dogs in the MCD group were affected bilaterally and one female dog was affected unilaterally. The youngest dog diagnosed with MCD on the basis of microCT findings was 15 weeks old. All the ulnas in the MCD group were free from periarticular osteophytosis based on the reconstructed images, indicating that the dogs had early disease.

Quantitative assessment of the articular cartilage of the MCP

Mean microCT attenuation of segmented articular cartilage

Mean microCT cartilage attenuation was significantly affected by anatomical locations ($P<0.001$) and MCP status ($P=0.008$). In all MCPs (n=28), the mean microCT cartilage attenuation at the lateral aspect (mean ± SD, 40.39 ± 3.61 arbitrary units) was significantly higher ($P<0.001$) than at the proximal aspect of the MCP (mean ± SD, 34.88 ± 4.55 arbitrary

units). In MCD-positive dogs, the mean microCT cartilage attenuation (mean ± SD, 38.72 ± 3.25 arbitrary units) was significantly higher (*P*=0.008) than in MCD-negative dogs (mean ± SD, 35.46 ± 5.80 arbitrary units), reflecting a greater diffusion of contrast molecules into the articular cartilage at the lateral aspect of the MCP than at other anatomical locations and greater diffusion in the MCD-positive group than in the MCD-negative group. There were no significant effects of litter, limb, and bodyweight on mean microCT cartilage attenuation (mean ± SD, shown in Table 1; Linear mixed model results, shown in Table 3 and 4). No interaction effect of MCP status and different anatomical locations was found on mean microCT cartilage attenuation.

Mean volume, surface area, and thickness of segmented articular cartilage

The mean volume, surface area, and thickness of segmented articular cartilage were significantly affected by different anatomical locations (*P*<0.001). All three morphological parameters were highest at the proximal aspect of the MCP. Mean surface area of segmented articular cartilage was also significantly affected by bodyweight (*P*=0.027) and mean thickness was significantly affected by litter (*P*=0.041). There were no significant effects of limb and MCP status on mean volume, surface area, and thickness (*P*=0.067-0.924) of segmented articular cartilage (mean ± SD, shown in Table 1; Linear mixed model results, shown in Table 3 and 4). No interaction effect of MCP status and different anatomical locations was found on mean volume, surface area, and thickness of segmented articular cartilage.

Quantitative assessment of the subchondral bone of the MCP

Limb, MCP status, and bodyweight did not significantly affect the parameters of subchondral bone micro-architecture (*P*=0.069-0.913); however, all the parameters, were significantly affected by litter effect (*P*=0.001-0.015): BV/TV, BS/TV, and Tb.Th were significantly higher in the first litter than in the second litter, whereas BS/BV, Tb.Sp, and SMI were significantly lower in the first litter than in the second litter (mean ± SD, shown in Table 2; Linear mixed model results, shown in Table 3 and 4).

Main effects	Articular cartilage, mean (SD)			
	MicroCT attenuation	Volume	Surface area	Thickness
Litter				
First litter (*n*=16)	36.44 (5.48)	6.64 (4.26)	46.08 (23.90)	0.247(0.045)
Second litter (*n*=12)	37.69 (4.34)	7.77 (5.28)	45.05 (20.35)	0.337(0.107)
Limb				
Left (*n*=14)	36.87 (5.52)	6.96 (4.72)	44.74 (22.11)	0.289 (0.088)
Right (*n*=14)	37.08 (4.56)	7.29 (4.78)	46.54 (22.78)	0.283 (0.092)
MCP status				
MCD-negative (*n*=15)	35.46 (5.80)	6.38 (4.17)	44.44 (23.48)	0.264 (0.082)
MCD-positive (*n*=13)	38.72 (3.25)	7.98 (5.22)	47.02 (21.13)	0.311 (0.092)
Bodyweight				
<20 kg (*n*=10)	37.45 (4.65)	7.37 (5.04)	43.61 (19.17)	0.331 (0.113)
21-25 kg (*n*=8)	35.37 (5.59)	7.81 (5.04)	47.97 (22.58)	0.269 (0.082)
>25 kg (*n*=10)	37.79 (4.80)	6.32 (4.15)	45.80 (25.42)	0.254 (0.039)
Anatomical locations				
Lateral (*n*=28)	40.39 (3.61)	4.06 (1.39)	29.23 (4.88)	0.283 (0.051)
Proximal (*n*=28)	34.88 (4.55)	13.02 (3.00)	74.71 (10.25)	0.329 (0.124)
Medial (*n*=28)	35.66 (5.08)	4.29 (1.85)	32.98 (9.04)	0.247 (0.055)

Table 1. *Mean microCT attenuation (arbitrary units), volume (mm^3), surface area (mm^2), and thickness (mm) of segmented articular cartilage of the medial coronoid processes (MCP) obtained from Labrador retrievers. MicroCT, micro-computed tomography; SD, standard deviation; MCD, medial coronoid disease; n, number of medial coronoid processes*

	Subchondral bone, mean(SD)					
Main effects	BV/TV	BS/TV	BS/BV	Tb.Th	Tb.Sp	SMI
Litter						
First litter	41.68	11.43	27.80	0.174	0.208	0.53
(*n*=16)	(10.61)	(1.61)	(5.67)	(0.016)	(0.030)	(1.09)
Second litter	26.51	9.13	34.58	0.151	0.258	1.59
(*n*=12)	(5.64)	(0.78)	(3.54)	(0.007)	(0.034)	(0.36)
Limb						
Left	32.71	10.48	30.33	0.167	0.236	1.13
(*n*=14)	(12.95)	(1.85)	(6.18)	(0.018)	(0.042)	(1.21)
Right	37.64	10.41	31.08	0.160	0.223	0.89
(*n*=14)	(9.87)	(1.69)	(5.78)	(0.016)	(0.039)	(0.75)
MCP status						
MCD negative	36.58	10.86	31.17	0.165	0.222	0.80
(*n*=15)	(12.87)	(1.92)	(7.01)	(0.021)	(0.041)	(1.21)
MCD-positive	33.56	9.97	30.17	0.163	0.238	1.20
(*n*=13)	(10.14)	(1.43)	(4.49)	(0.013)	(0.039)	(0.66)
Bodyweight						
<20 kg	26.22	9.20	35.17	0.150	0.256	1.60
(*n*=10)	(6.08)	(0.78)	(3.61)	(0.008)	(0.038)	(0.38)
21-25 kg	37.39	10.16	27.38	0.170	0.225	1.02
(*n*= 8)	(7.50)	(1.30)	(2.75)	(0.011)	(0.032)	(0.49)
>25 kg	42.36	11.91	28.90	0.173	0.207	0.34
(*n*=10)	(13.05)	(1.71)	(7.04)	(0.020)	(0.034)	(1.34)

Table 2. *Micro-architecture parameters of the medial coronoid process (MCP) subchondral bone obtained from Labrador retrievers. SD, standard deviation; MCD, medial coronoid disease; BV/TV, bone volume fraction; BS/TV, bone surface density; BS/BV, bone surface/volume ratio; Tb.Th, trabecular thickness (mm); Tb.Sp, trabecular spacing (mm); SMI, structural model index; n, number of medial coronoid processes.*

	Litter			Limb			MCP status			Bodyweight			Anatomical location		
Articular cartilage	F	df	*P*-value	F	df	*P*-value	F	df	*P*-value	F	df	*P*-value	F	df	*P*-value
Mean attenuation (arbitrary unit)	1.12	1,13	0.309	1.35	1,72	0.249	7.44	1,65	**0.008**	2.54	2,14	0.115	80.80	2,70	**<0.001**
Mean volume (mm^3)	1.63	1,13	0.225	1.69	1,72	0.198	2.04	1,25	0.166	1.08	2,14	0.366	360.5	2,69	**<0.001**
Mean surface area (mm^2)	4.55	1,12	0.054	3.46	1,70	0.067	0.01	1,14	0.924	4.96	2,12	**0.027**	498.8	2,68	**<0.001**
Mean thickness (mm)	5.05	1,14	**0.041**	0.25	1,72	0.618	1.164	1,46	0.286	0.468	2,15	0.635	34.07	2,70	**<0.001**
Subchondral bone	F	df	*P*	F	df	*P*	F	df	*P*	F	df	*P*	F	df	*P*
BV/TV	18.11	1,14	**0.001**	3.70	1,14	0.075	0.08	1,18	0.784	0.13	2,14	0.878			
BS/TV	15.15	1,14	**0.002**	0.04	1,14	0.838	0.02	1,20	0.879	1.74	2,14	0.212			
BS/BV	16.89	1,28	**<0.001**	0.07	1,28	0.789	2.00	1,28	0.168	0.67	2,28	0.521			
Tb.Th (mm)	23.84	1,28	**<0.001**	2.09	1,28	0.159	0.08	1,28	0.781	0.11	2,28	0.899			
Tb.Sp (mm)	11.85	1,14	**0.004**	3.88	1,14	0.069	0.02	1,23	0.889	0.12	2,14	0.892			
SMI	7.67	1,14	**0.015**	1.61	1,14	0.226	0.01	1,22	0.913	0.49	2,14	0.622			

Table 3. *Linear mixed model results for the assessment of articular cartilage and subchondral bone of medial coronoid processes obtained from Labrador retrievers. P-values for the mixed model explanatory factors 'Litter'(first litter, second litter), 'Limb' (left, right), 'MCP status' (MCD-negative, MCD-positive), 'bodyweight' (<20kg, 21-25kg, >25kg), and 'Anatomical locations' (lateral aspect, proximal aspect, medial aspect). P<0.05 was considered statistically significant. F, F-value; df, degree of freedom.*

Mean attenuation	Estimate	SE	t	*P*-value
Intercept	46.062	3.768	12.23	0.000
MCP status (MCD negative)	-3.107	1.140	-2.73	0.008
MCP status (MCD positive)[a]	0[a]	-	-	-
Anatomical location (Proximal)	-5.217	0.821	-6.36	0.000
Anatomical location (Medial)	-0.492	0.821	-0.60	0.551
Anatomical location (Lateral) [a]	-	-	-	-
Mean volume	**Estimate**	**SE**	**t**	***P*-value**
Intercept	4.711	0.687	6.85	0.000
Anatomical location (Proximal)	10.281	0.563	18.25	0.000
Anatomical location (Medial)	0.017	0.563	0.03	0.976
Anatomical location (Lateral) [a]	0[a]	-	-	-
Mean surface area	**Estimate**	**SE**	**t**	***P*-value**
Intercept	36.666	5.541	6.617	0.000
Bodyweight (<20 kg)	0.475	6.267	0.076	0.940
Bodyweight (21-25 kg)	-1.084	4.927	-0.220	0.827
Bodyweight (>25 kg) [a]	0[a]	-	-	-
Anatomical location (Proximal)	51.884	2.663	19.483	0.000
Anatomical location (Medial)	2.590	2.663	0.972	0.334
Anatomical location (Lateral) [a]	0[a]	-	-	-
Mean thickness	**Estimate**	**SE**	**t**	***P*-value**
Intercept	0.349	0.062	5.669	0.000
Litter (1st litter)	-0.125	0.056	-2.247	0.041
Litter (2nd litter) [a]	0[a]	-	-	-
Anatomical location (Proximal)	0.101	0.024	4.293	0.000
Anatomical location (Medial)	0.037	0.024	1.569	0.121
Anatomical location (Lateral) [a]	0[a]	-	-	-
BV/TV	**Estimate**	**SE**	**t**	***P*-value**
Intercept	28.976	2.986	9.705	0.000
Litter (1st litter)	15.175	3.566	4.256	0.001
Litter (2nd litter) [a]	0[a]	-	-	-
BS/TV	**Estimate**	**SE**	**t**	***P*-value**
Intercept	9.134	0.446	20.490	0.000
Litter (1st litter)	2.295	0.590	3.892	0.002
Litter (2nd litter) [a]	0[a]	-	-	-
BV/BV	**Estimate**	**SE**	**t**	***P*-value**
Intercept	33.541	1.505	22.291	0.000
Litter (1st litter)	-7.299	1.776	-4.110	0.000
Litter (2nd litter) [a]	0[a]	-	-	-
Tb.Th	**Estimate**	**SE**	**t**	***P*-value**
Intercept	0.147	0.004	34.945	0.000
Litter (1st litter)	0.023	0.005	4.883	0.000
Litter (2nd litter) [a]	0[a]	-	-	-
Tb.Sp	**Estimate**	**SE**	**t**	***P*-value**
Intercept	0.251	0.115	21.914	0.000
Litter (1st litter)	-0.050	0.014	-3.443	0.004
Litter (2nd litter) [a]	0[a]	-	-	-
SMI	**Estimate**	**SE**	**t**	***P*-value**
Intercept	1.454	0.310	4.696	0.000
Litter (1st litter)	-1.060	0.383	-2.769	0.015
Litter (2nd litter) [a]	0[a]	-	-	-

Table 4. *Linear mixed model maximum likelihood estimates of fixed factors. [a] Reference categories. SE, standard error; t, t-value.*

Discussion

The present study investigated the changes occurring in articular cartilage and subchondral bone from MCD-negative and MCD-positive Labrador retrievers, which originated from two litters with the dogs of the first litter being older and heavier than the dogs of the second litter. We found significant differences in the mean microCT attenuation of segmented articular cartilage at the different anatomical location, i.e. proximal, lateral and medial aspects of the MCP, as well as between dogs with and without MCD. The mean microCT attenuation was higher at the lateral aspect of the MCP than other anatomical locations and in MCD-positive group than MCD-negative group. Mean volume, surface area and thickness of segmented articular cartilage were all affected by different anatomical locations instead of MCP status. All these three parameters were highest at the proximal aspect of the MCP. Mean surface area was also affected by the bodyweight and the mean thickness by litter effect. All the parameters of subchondral bone micro-architecture were significantly different between the two litters.

The GAG content of cartilage changes during cartilage development, degeneration, and repair (Watrin et al., 2001; Williams et al., 2003), and its depletion contributes to one of the earliest signs of degenerative changes (Bashir et al., 1996; Piscaer et al., 2008b). The significant increase in mean microCT cartilage attenuation in the MCD group indicates that the GAG content of cartilage was already depleted in an early stage of MCD. In line with this, a reduced content of proteoglycan in the cartilage matrix was found in MCPs obtained from clinically lame dogs with MCD (Goldhammer et al., 2009). We found that this depletion starts very early in the disease process which is detected in a dog as young as 15 weeks old. The highest mean microCT attenuation of cartilage from the lateral aspect of the MCP is consistent with the observation that MCD lesions developed at the lateral aspect of MCP (Fig. 1b-d), an area in close contact with the proximal radial head (Preston et al., 2000). Radial incisure fragmentation has been described in a microCT study of clinical canine patients (Fitzpatrick et al., 2011) and was suggested to be due to abnormal torsional loading.

The significant differences in the morphological parameters of segmented articular cartilage i.e. mean volume, surface area and thickness at the different anatomical locations, with the highest at the proximal aspect of the MCP fit the anatomical and physiological facts. This proximal aspect at the humeral articular side all the time receives the vertical downward force from the humeral condyle (Cuddy et al., 2012). The litter- and weight-dependent changes in some aspects of articular cartilage morphology, mainly at the lateral and proximal aspects of the MCP, can be explained in terms of adaptation of articular cartilage to increasing maturation of cartilage and bone,

and increased load as the animal gets heavier with age (Shepherd and Seedhom, 1999; Xie et al., 2009; Yoo et al., 2011). The thickness of the articular cartilage at the lateral aspect of the MCP was significantly thinner in dogs from the first litter which were older and heavier than dogs from the second litter, which can be explained by changes in the mechanobiology of the cartilage/subchondral bone interface (Beaupré et al., 2000).

The precision of the measurements has been reported to have an error smaller than 3% in previous studies (Waarsing et al., 2004; Xie et al., 2009), in both articular cartilage and subchondral bone measurements. Although there were no supportive histological results to compare with the EPIC-microCT findings in our study, there is enough evidence from literature that this technique adequately reflects the GAG content of cartilage, and in addition it allows accurate study of the 3-D morphology of articular cartilage (Piscaer et al., 2008a; Xie et al., 2009; Benders et al., 2010; Xie et al., 2010). Before performing the EPIC-microCT study, we established from trials that 40% Hexabrix / 60% PBS solution with an immersion time of minimally 8 h provides optimal segmentation between cartilage and subchondral bone. The immersion time was slightly longer than that of another protocol (Xie et al., 2009) because the bones in our study were larger and fixed in formalin and it took longer for the contrast agent to diffuse and reach equilibrium. Its application for 3-D visualization of GAG in formalin fixed articular cartilage has been proofed to be reliable (Benders et al., 2010). X-ray attenuation is lower in formalin-fixed samples than in fresh samples, but this was not critical in our study because we were interested in the relative mean microCT attenuation of articular cartilage at different anatomical locations and all the samples were processed in the same way. In our study, we did not attempt to adjust the alpha level for multiple comparisons due to the fact that as a study in investigating the development of MCD in a longitudinal manner, our main objective is to explore and provide a new insight regarding the etiopathogenesis of this disease. With the animals being euthanized at different ages, normal physiological processes need to be taken into consideration while interpreting the outcome variables. Hence, the results must be interpreted with caution owing to the multiplicity of hypotheses.

MicroCT has been proved to be a precise tool to investigate the micro-architecture of the bone (Müller et al., 1998; Barou et al., 2002; Kuhn et al., 2005). Although short-term formalin fixation has been reported not to be associated with the changes in bone mineral density (Edmondston et al., 1994), we could not rule out completely its effect on the micro-architecture of the subchondral bone. The lack of significant differences (P>0.05) in the morphological parameters of subchondral bone between dogs with and without MCD was unexpected. Although the etiopathogenesis of MCD is still uncertain, changes in subchondral bone are believed to contribute to its development (Danielson et al., 2006; Temwichitr et al., 2010). Our findings are in contrast with an earlier report of an

increased porosity in dogs with MCD compared with dogs without MCD (Danielson et al., 2006). This discrepancy may be due to differences in the stage of the disease, as well as the methods of obtaining micro-architectural variables (3-D instead of 2-D methods) during the analysis. We analysed the 3-D structure of subchondral bone in an early stage of the disease. The changes in subchondral bone micro-architecture seen in different litters can be explained as adaptations to the increase in loading (Matsui et al., 1997; Nafei et al., 2000; Tanck et al., 2001; Wolschrijn and Weijs, 2005) since the dogs from the first litter were older and heavier than the dogs from the second litter. Not only was subchondral bone density and trabecular thickness increased, which reflect the greater loading, but there was also remodeling of subchondral bone, as evidenced by the decrease in bone surface area and the changes in SMI. The SMI findings showed that the rod-like structure of trabecular bone in the dogs from the second litter changed into a more plate-like structure in the dogs from the first litter, in order to absorb load more efficiently (Hildebrand and Rüegsegger, 1997).

Our study clearly demonstrated GAG depletion in early stages of MCD, and litter- and weight-related changes in the morphology of cartilage at the proximal and lateral aspects of the MCP. We cannot conclude that MCD develops as a result of changes in articular cartilage or that the GAG loss we observed was a consequence of MCD. This would necessitate histological investigation of the developing MCP. Even though fissures and fragmentation of the MCP were detected in the dogs with MCD, subchondral bone density and remodelling were not significantly affected in the early stages of the MCD. It is possible that the impaired compressive strength of articular cartilage ultimately leads to a failure to absorb load, leading to further micro-damage to subchondral bone. The etiopathogenesis of MCD can only be understood if the relationship between the mechanics and biology of the MCP is fully appreciated.

References

Barou, O., Valentin, D., Vico, L., Tirode, C., Barbier, A., Alexandre, C., Lafage-Proust, M.H., 2002. High-resolution three-dimensional micro-computed tomography detects bone loss and changes in trabecular architecture early: comparison with DEXA and bone histomorphometry in a rat model of disuse osteoporosis. Investigative Radiology 37, 40-46.

Bashir, A., Gray, M.L., Burstein, D., 1996. Gd-DTPA^{2-} as a measure of cartilage degradation. Magnetic Resonance in Medicine 36, 665-673.

Beaupré, G.S., Stevens, S.S., Carter, D.R., 2000. Mechanobiology in the development, maintenance, and degeneration of articular cartilage. Journal of Rehabilitation Research and Development 37, 145-152.

Benders, K.E.M., Malda, J., Saris, D.B.F., Dhert, W.J.A., Steck, R., Hutmacher, D.W., Klein, T.J., 2010. Formalin fixation affects equilibrium partitioning of an ionic contrast agent-microcomputed tomography (EPIC-microCT) imaging of osteochondral samples. Osteoarthritis and Cartilage 18, 1586-1591.

Botter, S.M., Van Osch, G., Waarsing, J.H., Day, J.S., Verhaar, J.A.N., Pols, H.A.P., Van Leeuwen, J., Weinans, H., 2006. Quantification of subchondral bone changes in a murine osteoarthritis model using micro-CT. Biorheology 43, 379-388.

Choudhury, A., 2009. Statistical Correlation. Retrieved 08 Jul. 2012 from Experiment Resources: http://www.experiment-resources.com/statistical-correlation.html

Cuddy, L.C., Lewis, D.D., Kim, S.E., Conrad, B.P., Banks, S.A., Horodyski, M.B., Fitzpatrick, N., Pozzi, A., 2012. Contact mechanics and three-dimensional alignment of normal dog elbows. Veterinary Surgery 41, 818-828.

Danielson, K.C., Fitzpatrick, N., Muir, P., Manley, P.A., 2006. Histomorphometry of fragmented medial coronoid process in dogs: a comparison of affected and normal coronoid processes. Veterinary Surgery 35, 501-509.

Edmondston, S., Singer, K., Day, R., Breidahl, P., Price, R., 1994. Formalin fixation effects on vertebral bone density and failure mechanics: an in-vitro study of human and sheep vertebrae. Clinical Biomechanics 9, 175-179.

Fitzpatrick, N., Smith, T.J., Evans, R.B., Yeadon, R., 2009. Radiographic and arthroscopic findings in the elbow joints of 263 dogs with medial coronoid disease. Veterinary Surgery 38, 213-223.

Fitzpatrick, N., Garcia-Nolen, T., Daryani, A., Watari, S., Hayashi, K., 2011. Structural analysis of canine medial coronoid disease by microCT: radial incisure versus tip fragmentation. In: Scientific Presentation Abstracts of American College of Veterinary Surgeons Veterinary Symposium, Chicago, Illinois, E26.

Goldhammer, M.A., Smith, S.H., Fitzpatrick, N., Clements, D.N., 2009. A comparison of radiographic, arthroscopic and histological measures of articular pathology in the canine elbow joint. The Veterinary Journal 186, 96-103.

Grøndalen J., Grøndalen T., 1981. Arthrosis in the elbow joint of young rapidly growing dogs. V. A pathoanatomical investigation. Nordisk Veterinaermedicin 33, 1-16.

Hazewinkel, H.A.W., Meij, B.P., Theyse, L.F.H., van Rijssen, B., 2009. Locomotor system. In: Medical History and Physical Examination in Companion Animals Second Ed. Elsevier Limited, Houten, NL, pp.136-148.

Hildebrand, T., Rüegsegger, P., 1997. Quantification of bone microarchitecture with the structure model index. Computer Methods in Biomechanics and Bio Medical Engineering 1, 15-23.

Hulse, D., Young, B., Beale, B., Kowaleski, M., Vannini, R., 2010. Relationship of the biceps-brachialis complex to the medial coronoid process of the canine ulna. Veterinary and Comparative Orthopaedics and Traumatology 23, 173-176.

Janutta, V., Hamann, H., Klein, S., Tellhelm, B., Distl, O., 2006. Genetic analysis of three different classification protocols for the evaluation of elbow dysplasia in German shepherd dogs. Journal of Small Animal Practice 47, 75-82.

Kirberger, R.M., Fourie, S.L., 1998. Elbow dysplasia in the dog: pathophysiology, diagnosis and control. Journal of the South African Veterinary Association 69, 43-54.

Kuhn, J., Goldstein, S., Feldkamp, L., Goulet, R., Jesion, G., 2005. Evaluation of a microcomputed tomography system to study trabecular bone structure. Journal of Orthopaedic Research 8, 833-842.

Lavrijsen, I.C., Heuven, H.C., Voorhout, G., Meij, B.P., Theyse, L.F., Leegwater, P.A., Hazewinkel, H.A., 2012. Phenotypic and genetic evaluation of elbow dysplasia in Dutch Labrador retrievers, Golden retrievers, and Bernese Mountain Dogs. The Veterinary Journal 193, 486-492.

Matsui, H., Shimizu, M., Tsuji, H., 1997. Cartilage and subchondral bone interaction in osteoarthrosis of human knee joint: a histological and histomorphometric study. Microscopy Research and Technique 37, 333-342.

Moores, A.P., Benigni, L., Lamb, C.R., 2008. Computed tomography versus arthroscopy for detection of canine elbow dysplasia lesions. Veterinary Surgery 37, 390-398.

Müller, R., Van Campenhout, H., Van Damme, B., Van Der Perre, G., Dequeker, J., Hildebrand, T., Rüegsegger, P., 1998. Morphometric analysis of human bone biopsies: a quantitative structural comparison of histological sections and micro-computed tomography. Bone 23, 59-66.

Nafei, A., Kabel, J., Odgaard, A., Linde, F., Hvid, I., 2000. Properties of growing trabecular ovine bone: part II: architectural and mechanical properties. Journal of Bone and Joint Surgery-British Volume 82-B, 921-927.

Olsson, S.-E., 1987. General and local [corrected] aetiologic factors in canine osteochondrosis. The Veterinary Quarterly 9, 268-278.

Palmer, A.W., Guldberg, R.E., Levenston, M.E., 2006. Analysis of cartilage matrix fixed charge density and three-dimensional morphology via contrast-enhanced micro-computed tomography. Proceedings of the National Academy of Sciences of the United States of America 103, 19255-19260.

Piscaer, T.M., van Osch, G., Verhaar, J.A.N., Weinans, H., 2008a. Imaging of experimental osteoarthritis in small animal models. Biorheology 45, 355-364.

Piscaer, T.M., Waarsing, J.H., Kops, N., Pavljasevic, P., Verhaar, J.A., van Osch, G.J., Weinans, H., 2008b. In vivo imaging of cartilage degeneration using microCT-arthrography. Osteoarthritis and Cartilage 16, 1011-1017.

Preston, C.A., Schulz, K.S., Kass, P.H., 2000. In vitro determination of contact areas in the normal elbow joint of dogs. American Journal of Veterinary Research 61, 1315-1321.

Preston, C.A., Schulz, K.S., Taylor, K.T., Kass, P.H., Hagan, C.E., Stover, S.M., 2001. In vitro experimental study of the effect of radial shortening and ulnar ostectomy on contact patterns in the elbow joint of dogs. American Journal of Veterinary Research 62, 1548-1556.

Sniekers, Y.H., Intema, F., Lafeber, F.P., van Osch, G.J., van Leeuwen, J.P., Weinans, H., Mastbergen, S.C., 2008. A role for subchondral bone changes in the process of osteoarthritis; a micro-CT study of two canine models. BMC Musculoskeletal Disorders 9, 20.

Shepherd, D.E., Seedhom, B.B., 1999. Thickness of human articular cartilage in joints of the lower limb. Annals of the Rheumatic Diseases 58, 27-34.

SkyScan, 2010. Manual for SkyScan CT-Analyser v.1.10. http://www.skyscan.be/next/CTan_UserManual.pdf

Tanck, E., Homminga, J., van Lenthe, G.H., Huiskes, R., 2001. Increase in bone volume fraction precedes architectural adaptation in growing bone. Bone 28, 650-654.

Temwichitr, J., Leegwater, P.A., Hazewinkel, H.A., 2010. Fragmented coronoid process in the dog: a heritable disease. The Veterinary Journal 185, 123-129.

Tirgari, M., 1980. Clinical, radiographical and pathological aspects of ununited medial coronoid process of the elbow joint in dogs. Journal of Small Animal Practice 21, 595-608.

van Ruijven, L.J., Giesen, E.B., Mulder, L., Farella, M., van Eijden, T.M., 2005. The effect of bone loss on rod-like and plate-like trabeculae in the cancellous bone of the mandibular condyle. Bone 36, 1078-1085.

Waarsing, J., Day, J., Van der Linden, J., Ederveen, A., Spanjers, C., De Clerck, N., Sasov, A., Verhaar, J., Weinans, H., 2004. Detecting and tracking local changes in the tibiae of individual rats: a novel method to analyse longitudinal in vivo micro-CT data. Bone 34, 163-169.

Watrin, A., Ruaud, J.P.B., Olivier, P.T.A., Guingamp, N.C., Gonord, P.D., Netter, P.A., Blum, A.G., Guillot, G.M., Gillet, P.M., Loeuille, D.H.J., 2001. T2 mapping of rat patellar cartilage. Radiology 219, 395-402.

Williams, A., Oppenheimer, R.A., Gray, M.L., Burstein, D., 2003. Differential recovery of glycosaminoglycan after IL-1-induced degradation of bovine articular cartilage depends on degree of degradation. Arthritis Research and Therapy 5, R97-105.

Wind, A.P., Packard, M.E., 1986. Elbow incongruity and developmental elbow diseases in the dog: part II. The Journal of American Animal Hospital Association 22, 725-730.

Wolschrijn, C.F., Weijs, W.A., 2004. Development of the trabecular structure within the ulnar medial coronoid process of young dogs. The Anatomical Record.Part A, Discoveries in molecular, cellular, and evolutionary biology 278, 514-519.

Wolschrijn, C.F., Weijs, W.A., 2005. Development of the subchondral bone layer of the medial coronoid process of the canine ulna. The Anatomical Record.Part A, Discoveries in molecular, cellular, and evolutionary biology 284, 439-445.

Xie, L., Lin, A.S., Levenston, M.E., Guldberg, R.E., 2009. Quantitative assessment of articular cartilage morphology via EPIC-microCT. Osteoarthritis and Cartilage 17, 313-320.

Xie, L., Lin, A.S., Guldberg, R.E., Levenston, M.E., 2010. Nondestructive assessment of sGAG content and distribution in normal and degraded rat articular cartilage via EPIC-microCT. Osteoarthritis and Cartilage 18, 65-72.

Yoo, W.J., Cheon, J.E., Lee, H.R., Cho, T.J., Choi, I.H., 2011. Physeal growth arrest by excessive compression: histological, biochemical, and micro-CT observations in rabbits. Clinics in Orthopedic Surgery 3, 309-314.

Zhao, C., Kurita, H., Kurashina, K., Hosoya, A., Arai, Y., Nakamura, H., 2010. Temporomandibular joint response to mandibular deviation in rabbits detected by 3D micro-CT imaging. Archives of Oral Biology 55, 929-937.

Chapter 7

Radiographic and computed tomographic assessment of the postnatal development of the antebrachia and elbow joints in Labrador retrievers with and without medial coronoid disease

S.F. Lau[1]; H.A.W. Hazewinkel[2]; G. Voorhout[1]

[1] Division of Diagnostic Imaging, Faculty of Veterinary Medicine, Utrecht University, Yalelaan 108, 3584CM, Utrecht, The Netherlands

[2] Department of Clinical Sciences of Companion Animals, Faculty of Veterinary Medicine, Utrecht University, Yalelaan 108, 3584CM, Utrecht, The Netherlands

Submitted to Veterinary Radiology & Ultrasound

Abstract

Objective:

To study the postnatal development of elbow joints

Methods:

Radiographic and computed tomographic (CT) images were taken every 2 weeks from purpose-bred Labrador retrievers (n=14 dogs) originating from MCD-positive dam and sires. The radial angulation, radioulnar length ratio, development of secondary ossification centers in the distal humerus and antebrachium, radioulnar joint congruency, and radioulnar angles were measured.

Results:

There were no significant differences in any of the variables measured in MCD-positive and MCD-negative dogs (all comparisons $P>0.05$).

Conclusion:

It is unlikely that the postnatal development of the elbow joints was associated with the development of MCD in these Labrador retrievers.

Introduction

The postnatal development of the canine radius, ulna, and humerus has been investigated in small and large breed dogs (Hare, 1961; Fox et al., 1983; Wind and Packard, 1986b; Guthrie et al., 1992; Voorhout et al., 1994; Breit et al., 2004; Wolschrijn and Weijs, 2004; Breit et al., 2005; Frazho et al., 2010). These bones grow lengthwise as a result of endochondral ossification, during which sequential changes occur, such as the reorganization of chondrocytes and the cartilage extracellular matrix, followed by gradual replacement of the cartilage matrix by bone (Wong and Carter, 1990; Mackie et al., 2008). Any disturbance of endochondral ossification may lead to abnormal skeletal development and maturation (Voorhout and Hazewinkel, 1987).

Medial coronoid disease (MCD), which includes both pathological lesions of cartilage and of subchondral bone of the medial coronoid process (MCP; Moores et al., 2008; Fitzpatrick et al., 2009), is postulated to be caused by a disturbance in endochondral ossification (Tirgari, 1974; Olsson, 1975), although radioulnar incongruency (RUI) is also a suggested cause (Sereda et al., 2009; Proks et al., 2011; Samoy et al., 2012). Despite the high incidence of MCD in Labrador retrievers and other breeds (Meyer-Lindenberg et al., 2002; Fitzpatrick et al., 2009; Seyrek-Intas et al., 2009), the etiopathogenesis of the disease has yet to be elucidated.

In a previous diagnostic imaging study of 14 Labrador retrievers purpose bred from MCD-affected dam and sires, MCD was detected by computed tomography (CT) in pups as young as 14 weeks of age (Lau et al., 2013). Thus abnormalities in the development and maturation of the elbow joint may occur during the first 3–4 months of life. The aim of this study was to compare the development, monitored by radiography and CT, of the antebrachium and elbow joint in dogs with healthy elbow joints and in dogs that developed MCD, in order to evaluate whether disturbances in postnatal antebrachial and elbow joint development lead to MCD.

Materials and methods

Data collection

Fourteen purpose-bred Labrador retrievers puppies (nine males, five females) originating from a MCD-positive dam and two MCD-positive sires were monitored by radiography and CT of the antebrachia and both elbow joints, from 6 (n=7) or 7 (n=7) weeks of age until euthanasia. All dogs were examined fortnightly with both diagnostic techniques, as described previously. Dogs were euthanized when a lesion of the MCP was suspected or as age- or weight- matched negative control. Elbows were grouped as MCD negative or

MCD positive, based on the combination of postmortem gross examination and histological study, as described previously (Lau et al., 2013). Of 28 elbows, 13 ulnas showed evidence of MCD; the remaining 15 ulnas were regarded as normal. Six dogs in the MCD-positive group were affected bilaterally and one female dog was affected unilaterally.

From the series of radiographs and CT images from 6 or 7 weeks until 16 or 17 weeks of age, including for two dogs from the second litter which were euthanized at the age of 15 weeks, the postnatal development of the antebrachia and elbow joints was assessed on the basis of the radial angulation, radioulnar length ratio, inter-relationship between the ulna and radius, development of secondary ossification centers (SOCs), and changes in radioulnar angle in the neutral position and during pronation and supination. All the measurements were performed by a single observer who was unaware of the MCP status of the dogs.

Center of Rotation of Angulation Methodology

Radial alignment quantification with the Center of Rotation of Angulation (CORA) method (Fox et al., 2006) was adapted to measure the normal alignment of the radius within the antebrachium. The physeal orientation lines in the frontal plane were determined on the craniocaudal (CrCd) radiographic projection, drawn along the proximal and distal growth plates of the radius (Fig. 1a). In this frontal plane, the radial anatomic axis was defined as the straight mid-diaphyseal line determined at points 25%, 50%, and 75% along the length of the radius. Then, physeal orientation angles for both the proximal and distal radius were determined by measuring the angles at the intersection of the physeal orientation lines and the anatomic axis, yielding the medial proximal radial angle (MPRA) and lateral distal radial angle (LDRA) (Fig. 1b). On the mediolateral (ML) radiographic projection, physeal orientation lines were drawn through the proximal and distal radial growth plates (Fig. 1c). Because of the natural cranial bowing of the radius in the sagittal plane, the sagittal radial anatomic axis was determined by drawing two separate straight mid-diaphyseal lines through the proximal and distal radial axis. Anatomic axes were determined by drawing the mid-diaphyseal points at the proximal half and distal half of each segment, respectively. Physeal orientation angles in the sagittal plane, namely, the proximal cranial radial angle (PCRA) and distal caudal radial angle (DCRA), were determined by measuring the angles of intersection of the anatomic axes and the parallel physeal orientation lines (Fig. 1d). The radial procurvatum angle (RPA) was measured at the point at which the two separate straight mid-diaphyseal lines intersected (Fig. 1d).

In order to detect any radial angular limb deformities during growth, MPRA, LDRA, PCRA, DCRA, and RPA were measured in all dogs from 6 or 7 weeks of age to 15 weeks of age (2 dogs) and to 16 or 17 weeks of age (12 dogs).

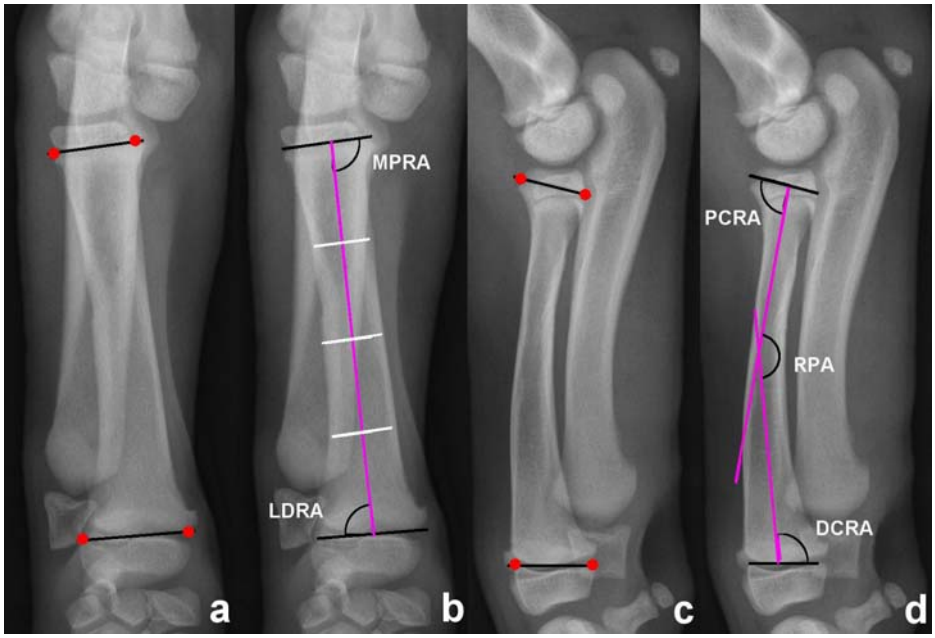

Fig. 1. *Right antebrachium of a normal dog at 9 weeks of age. (a) and (b) Craniocaudal radiograph; "physeal orientation lines" connect two points (Red) at the medial and lateral extent of the proximal and distal radial growth plate, respectively. Radial anatomic axis was drawn by connecting the mid-diaphyseal points along the length of the radius. (b) Medial proximal radial angle (MPRA) and lateral distal radial angle (LDRA), i.e. the angles of the anatomic axis with both physeal orientation lines. (c) and (d) Mediolateral radiograph; physeal orientation lines were drawn across the two points (red) at the cranial and caudal extent of proximal and distal radial growth plate, respectively. Radial anatomic axes were determined by connecting two mid-diaphyseal lines each for proximal half and distal half of the radial segments. Proximal cranial radial angle (PCRA) and distal caudal radial angle (DCRA) were determined by measuring the angles from intersecting anatomic axes and physeal reference lines. Radial procurvatum angle (RPA) was determined from the intersecting point of the two separate straight mid-diaphyseal lines.*

Radioulnar length ratio

The radioulnar (RU) length ratio was calculated using measurements from the serial ML radiographic projections, within the age range used as in the CORA method. The diaphyseal length of the radius was measured from the mid-point of the proximal radial growth plate to the mid-point of the distal radial growth plate along a straight line. The ulnar diaphyseal length was measured from the most proximal part of the ulnar metaphysis to the most distal part of the distal ulnar metaphysis along a straight line. The RU length ratio was calculated by dividing the length of the radius by the length of the ulna.

Secondary ossification centers

The ossification of SOCs of the olecranal apophysis (OA), medial humeral epicondyle (MHE), and ulnar styloid process (USP) was assessed on the radiographic serial images used in the CORA method. The stage of ossification and shape of the ossified bone were assessed as reported previously (Voorhout and Hazewinkel, 1987; Voorhout et al., 1994). Ossification of the anconeal process (AP) was assessed on serial CT images, and the stage of ossification was classified according to the shape: no evidence of ossification, irregular ossification, and proper anatomical shape.

Radioulnar joint congruence evaluation

Radioulnar joint congruence (RUC) was assessed from CT images as described before (Kramer et al., 2006). The RUC was measured three times on the reconstructed sagittal and dorsal CT images obtained from 12 or 13 weeks until 16 or 17 weeks of age, respectively (including for two dogs which were euthanized at the age of 15 weeks). In the sagittal plane reconstructed at the base of MCP at the junction with the trochlear notch (Fig. 2a), a circle was drawn along the ulnar trochlear notch (Fig. 2b). Joints were considered congruent when there was no step defect between the most proximal epiphyseal border of the radius with the circle. Otherwise, the distance of the step defect was measured. In both dorsal planes reconstructed at mid and apex of the MCP (Fig. 2a), the distance between the most proximal ulnar surface and the most proximomedial aspect of radial head was measured (Fig. 2c and d).

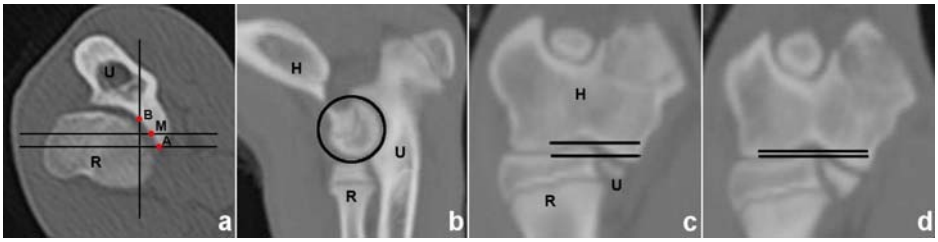

Fig. 2. *Computed tomographic images obtained from the right elbow joint of a dog at 17 weeks of age. (a) Transverse computed tomographic slice demonstrates the orientation of reformatted images. Sagittal plane was reconstructed at the region of the base (B) of the medial coronoid process (MCP). Two dorsal planes were reconstructed at the mid (M), and apex (A) of the MCP. (b) In sagittal plane, a circle was drawn along the ulnar trochlear notch to detect the step defect in the radioulnar joint. In dorsal planes reconstructed at (c) Apex and (d) Mid of the MCP with the distance measured in between the most proximal ulnar surface with the most proximomedial aspect of radial head. U, Ulna; R, Radius; H, Humerus.*

Radioulnar angles in neutral position and during pronation and supination

As for RUC evaluation, the CT images obtained from 12 or 13 weeks until 16 or 17 weeks of age (including for two dogs which were euthanized at the age of 15 weeks) were used for RU angle measurements. RU angles were measured on the transverse views of the CT at the level of the apex of the MCP obtained in neutral position and during pronation and supination. At the ulna, a line was drawn across the longest axis from the apex of the MCP through the most caudolateral part of the ulnar cortex. Subsequently, another line was drawn along the more or less straight lateral edge of the radius and the RU angle was measured at the intersection of the two lines (Fig. 3).

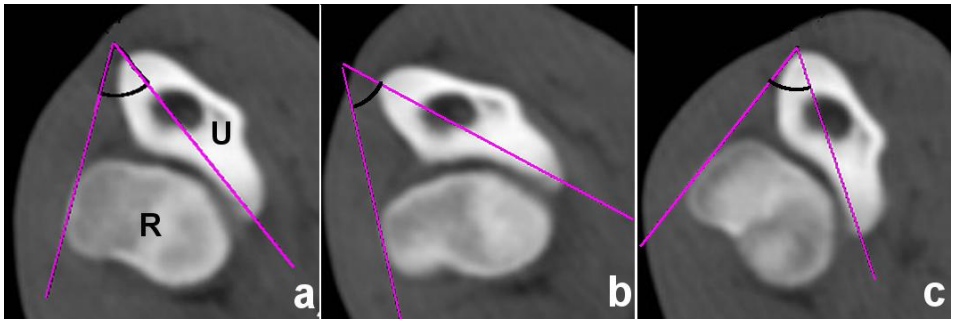

Fig. 3. *Computed tomographic images obtained from the right elbow joint of a dog at 17 weeks of age. Radioulnar (RU) angles were measured on the transverse views of the CT obtained during (a) neutral, (b) pronation, and (c) supination positions.*

Statistical analysis

Statistical analyses were performed using SPSS (SPSS version 20.0, SPSS Inc.). Linear mixed models containing both fixed and random effects were used to analyze the MPRA, LDRA, PCRA, DCRA, RPA, RU length ratio, RUC evaluation, and RU angles. Model selection was based on the Akaike Information Criterion (AIC). Conditions for the use of mixed models, including the normal distribution of the data, were assessed by analyzing the residuals (PP and QQ plots) of the acquired models; no violations of these conditions were observed. Data are expressed as mean ± SD (Table 1 and 2), and differences were considered statistically significant at $P<0.05$. Non-parametric Kruskal-Willis test was used to analyze the data of the SOCs study because the dependent outcome was an ordinal score; differences were considered statistically significant at $P<0.05$.

Results

Center of Rotation of Angulation Methodology

The MPRA, LDRA, PCRA, DCRA, and RPA are shown in Tables 1 and 2, by age and MCP status. MPRA, LDRA, and DCRA increased with age ($P \leq 0.001$), whereas PCRA ($P=0.14$) and RPA ($P=0.58$) did not (Table 1 and 2). MPRA, LDRA, PCRA, DCRA, and RPA were not significantly different in MCD-positive and MCD-negative dogs ($P=0.17$-0.67). There was no interaction effect between age and MCP status.

Radioulnar length ratio

The mean (± SD) RU length ratio for the canine antebrachia is shown in Tables 1 and 2. The RU length ratio increased significantly with age ($P<0.001$) but was not affected by MCP status ($P=0.06$). There was no interaction effect between age and MCP status.

	Age in weeks					
	6-7	8-9	10-11	12-13	14-15	16-17
Center of Rotation of Angulation Methodology, mean (SD)						
MPRA (°)	90.5 (2.5)	91.2 (2.2)	92.2 (2.7)	91.9 (2.2)	91.9 (2.0)	92.8 (2.3)
LDRA (°)	86.1 (3.0)	87.4 (2.3)	87.9 (2.1)	87.7 (2.2)	87.5 (2.2)	87.9 (2.0)
PCRA (°)	95.2 (2.2)	95.5 (2.0)	95.4 (2.2)	94.4 (1.5)	95.1 (1.8)	95.0 (2.3)
DCRA (°)	85.7 (3.1)	85.9 (2.8)	85.4 (2.5)	86.1 (2.8)	87.8 (2.7)	87.5 (2.7)
RPA (°)	168.3(0.4)	168.4(0.5)	168.3(0.3)	168.3(0.4)	168.4(0.5)	168.2(0.4)
Radioulnar length ratio, mean (SD)						
RU (ratio)	0.778 (0.01)	0.784 (0.01)	0.783 (0.01)	0.784 (0.01)	0.788 (0.01)	0.791 (0.01)
Radioulnar congruence, mean(SD)						
Apex (mm)	-	-	-	1.58 (0.18)	1.52 (0.17)	1.53 (0.18)
Mid (mm)	-	-	-	0.86 (0.02)	0.87 (0.02)	0.86 (0.02)
Radioulnar angles, mean(SD)						
Neutral	-	-	-	52.8 (4.1)	50.8 (4.1)	50.3 (3.9)
Pronation	-	-	-	41.7 (4.8)	40.9 (4.8)	43.2 (3.4)
Supination	-	-	-	62.1 (3.0)	60.7 (2.7)	61.7 (3.1)

Table 1. *Different measurements used to investigate the postnatal development of the antebrachia and elbow joints at different ages (in weeks). SD, standard deviation; MPRA, medial proximal radial angle; LDRA, lateral distal radial angle; PCRA, proximal cranial radial angle; DCRA, distal caudal radial angle; RPA, radial procurvatum angle; RU, radioulnar.*

	Medial coronoid process status	
	MCD negative	MCD positive
Center of Rotation of Angulation Methodology, mean (SD)		
MPRA (°)	91.2 (2.2)	92.3(2.5)
LDRA (°)	87.5 (2.3)	87.3 (2.4)
PCRA (°)	95.6 (2.0)	94.7 (2.0)
DCRA (°)	85.7 (2.9)	87.1 (2.7)
RPA (°)	168.3 (0.4)	168.4 (0.4)
Radioulnar length ratio, mean (SD)		
RU (ratio)	0.786(0.01)	0.783(0.01)
Radioulnar congruence evaluation, mean(SD)		
Apex (mm)	1.54 (0.16)	1.51 (0.13)
Mid (mm)	0.86 (0.02)	0.86 (0.02)
Radioulnar angles, mean(SD)		
Neutral	52.0 (3.8)	49.6 (3.8)
Pronation	41.9 (4.8)	41.9 (4.0)
Supination	61.8 (3.0)	60.2 (2.6)

Table 2. *Different measurements used to investigate the postnatal development of the antebrachia and elbow joints of dogs with a different medial coronoid process status. MCD, medial coronoid disease; SD, standard deviation; MPRA, medial proximal radial angle; LDRA, lateral distal radial angle; PCRA, proximal cranial radial angle; DCRA, distal caudal radial angle; RPA, radial procurvatum angle; RU, radioulnar.*

Secondary ossification centers

The OA was absent in nine dogs but was visible as an ill-defined area of ossification in five dogs at 6 or 7 weeks of age. It was detectable in all dogs at 8 or 9 weeks of age. The structure was well delineated with a rounded edge at 10 or 11 weeks of age in all dogs. The OA attained its proper anatomical shape at 14 or 15 weeks of age. With regard to ossification of the MHE, the SOCs were either ill-defined areas of ossification (six dogs) or round (eight dogs) at 6 or 7 weeks of age. In all dogs, the MHE attained its rounded edges by 10 or 11 weeks of age and acquired its proper anatomical shape in the subsequent weeks.

At 6 or 7 weeks of age, the appearance of the USP was either an irregular area of ossification (eight dogs) or had a rectangular shape with the width larger than the height (six dogs). Thereafter, the USP ossified gradually into a cone shape with irregular ossification at the apex of the processes by 14 or 15 weeks of age. The apex of the USP was well defined and delineated at 16 or 17 weeks of age (Fig. 4). The earliest age at which a small area of irregular ossification in the region of the AP could be detected was 11 weeks, and this area of ossification was connected with the rest of the ulna (Fig. 5b). None of the dogs had evidence of a separate ossification center in the AP, and by 15 or 16 weeks of age all APs had attained their proper anatomic shape (Fig. 5c). Statistically, the ossification of

SOCs differed significantly with age (P<0.001) but not with MCD-positive or negative status (P=0.66-0.82). There was no interaction effect between age and MCP status.

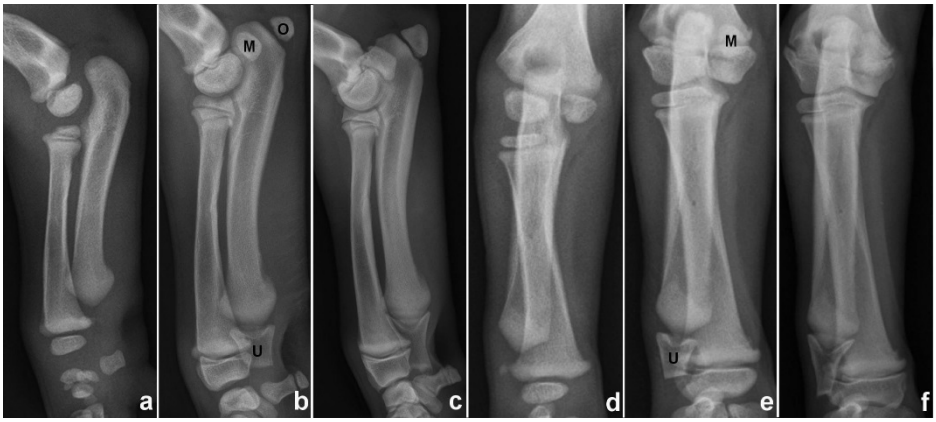

Fig. 4. *Radiographic images of the right antebrachium of the same Labrador retriever diagnosed negative for medial coronoid disease taken at different ages. (a) Mediolateral (ML) view taken at the age of 6 weeks, absence of the olecranal apophysis (OA), ill-defined secondary ossification center (SOC) of the medial humeral epicondyle (MHE), and irregular SOC of the ulnar styloid process (USP) can be observed. (b) ML view taken at the age of 10 weeks, well delineated and rounded OA and MHE, rectangular shaped of the USP (width equal to height) can be observed. (c) ML view taken at the age of 14 weeks, all the SOCs reached their proper anatomical shape, but did not fuse with the diaphysis yet. Irregular ossification can still be observed at the apex of the USP. Craniocaudal view of the same dog taken at (d) 6 weeks of age, (e) 10 weeks of age, and (f) 14 weeks of age. O, olecranal apophysis; M, medial humeral epicondyle; U, ulnar styloid process.*

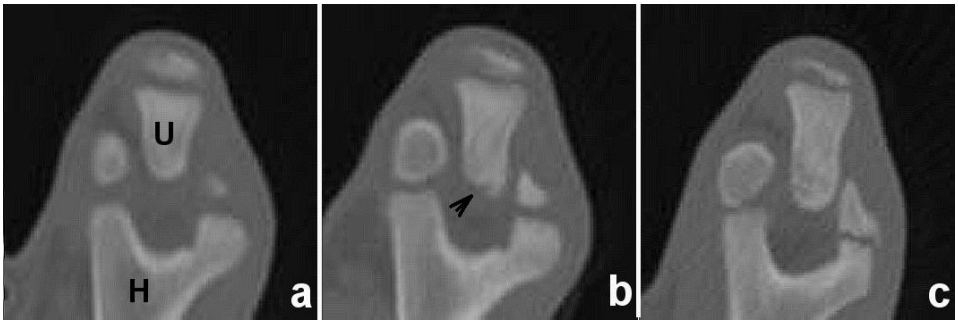

Fig. 5. *Transverse slice of the computed tomographic images of the left elbow obtained from dogs at different ages showing the ossification of the anconeal process (AP). (a) 10 weeks of age with absence of the ossification of AP, (b) 12 weeks of age with incomplete ossified AP without separation line with the ulnar diaphysis (arrow), (c) 14 weeks of age with proper anatomical shape of AP. U; ulnar; H, humerus.*

Radioulnar congruence evaluation

In neutral position, RUI was not detected from 12 or 13 weeks until 16 or 17 weeks of age in any dog, including two dogs that were euthanized at 15 weeks of age. No step defect was observed. The mean ± SD distance between the most proximal ulnar surface and the most proximomedial aspect of radial head is given in Tables 1 and 2. The distance was not affected significantly by age (*P*=0.22-0.67) or MCD-positive or negative status (*P*=0.57-0.89). There was no interaction effect between age and MCP status.

Radioulnar angles in neutral position and during pronation and supination

The mean ± SD RU angles in different limb positions are shown in Tables 1 and 2. The angles did not change significantly with increasing age (*P*=0.18-0.63) or by MCD-positive and -negative status (*P*=0.19-0.84). There was no interaction effect between age and MCP status.

Discussion

For all the parameters, i.e., MPRA, LDRA, PCRA, DCRA, RPA, RU length ratio, ossification of SOCs, RUC evaluation, and RU angles, there was no significant difference in the postnatal development of the antebrachia and elbow joints of dogs positive or negative for MCD. This may be because the incidence of RUI and radius angular deformities is lower in Labrador retrievers than in Bernese Mountain Dogs (Ubbink et al., 1999; Wind, 1986a) and Bouviers des Flandres (Temwichitr et al., 2010). Even though some investigators consider that radiographic findings regarding the structural anatomy of the bones are not accurate before 16 weeks of age due to incomplete ossification (Wind and Packard, 1986b; Breit et al., 2005), it is crucial to investigate the development of the elbow joints since MCD can occur as early as 14 weeks of age (Lau et al., 2013).

We modified the CORA method (Fox et al., 2006) by using physeal orientation lines instead of joint orientation lines, because the dogs in our study were very young and the SOCs were not completely developed, and the orientation of the proximal and distal articular surfaces of the radius could not be accurately assessed. We drew orientation lines based on the proximal and distal radial growth plates. There was no evidence of radius angular deformities during growth. The RU length ratio changed significantly with age, but was not different in MCD-positive and MCD-negative dogs.

Although SOCs development showed some variation among the 14 pairs of elbow joints studied, the proper anatomical shape was attained in all elbows by 16 or 17 weeks of age. SOCs of the OA, HME, and USP were not fully fused with the diaphysis at the age of 16 or 17 weeks. The ossification of the AP in Labrador retrievers differs from that in Great Danes (Voorhout and Hazewinkel, 1987; Voorhout et al., 1994). Unlike Great Danes,

Labrador retrievers do not have a clearly distinguishable, distinct SOC in the AP. Ossification started from the base and was completed within 2 weeks. SOCs development was not significantly different in MCD-positive and MCD-negative dogs.

RUC evaluation and RU angles were not different in dogs with and without MCD. We conclude that joint incongruity does not play a role in the development of MCD in Labrador retrievers. We evaluated the RUC and measured RU angles from the age of 12-13 weeks onward because the large joint space before the age of 12 weeks made measurements inaccurate. Bones had almost achieved their proper anatomic shape by 12 weeks even though they were still undergoing remodeling. All measurements should be interpreted with caution because radiographs and CT images are not able to visualize the cartilage layer. Although CT is considered a gold standard to detect RUI (De Rycke et al., 2002), mild radioulnar incongruency may be missed on CT due to partial volume effects. Furthermore, we cannot rule out the dynamic RU longitudinal incongruency as proposed (Fitzpatrick and Yeadon, 2009) by using the static radiography.

We monitored the growth of Labrador retrievers during a period of active growth, and the absence of periarticular osteophytosis in all images enabled us to identify the bony edges and landmarks accurately. On the basis of our findings, we conclude that it is unlikely that the postnatal growth of the radius and ulna, as well as the development of SOCs, are related with the development of the MCD in these Labrador retrievers.

References

Breit, S., Künzel, W., Seiler, S., 2004. Variation in the ossification process of the anconeal and medial coronoid processes of the canine ulna. Research in Veterinary Science 77, 9-16.

Breit, S., Kunzel, W., Seiler, S., 2005. Postnatal modelling of the humeroantebrachial contact areas of radius and ulna in dogs. Anatomia Histologia Embryologia 34, 258-264.

De Rycke L.M., Gielen I.M., van Bree H., Simoens P.J., 2002. Computed tomography of the elbow joint in clinically normal dogs. American Journal of Veterinary Research 63, 1400-1407.

Fitzpatrick, N., Smith, T.J., Evans, R.B., Yeadon, R., 2009. Radiographic and arthroscopic findings in the elbow joints of 263 dogs with medial coronoid disease. Veterinary Surgery 38, 213-223.

Fitzpatrick, N., Yeadon, R., 2009. Working algorithm for treatment decision making for developmental disease of the medial compartment of the elbow in dogs. Veterinary Surgery 38, 285-300.

Fox D.B., Tomlinson J.L., Cook J.L., Breshears L.M., 2006. Principles of uniapical and biapical radial deformity correction using dome osteotomies and the center of rotation of angulation methodology in dogs. Veterinary Surgery 35, 67-77.

Fox S.M., Bloomberg M.S., Bright R.M., 1983. Developmental anomalies of the canine elbow. Journal of the American Animal Hospital Association 19, 605-615.

Frazho J.K., Graham J., Peck J.N., De Haan J.J., 2010. Radiographic evaluation of the anconeal process in skeletally immature dogs. Veterinary Surgery 39, 829-832.

Guthrie, S., Plummer, J.M., Vaughan, L.C., 1992. Post natal development of the canine elbow joint: a light and electron microscopical study. Research in Veterinary Science 52, 67-71.

Hare W.C., 1961. The ages at which the centers of ossification appear roentgenographically in the limb bones of the dog. American Journal of Veterinary Research 22, 825-835.

Kramer, A., Holsworth, I.G., Wisner, E.R., Kass, P.H., Schulz, K.S., 2006. Computed tomographic evaluation of canine radioulnar incongruence in vivo. Veterinary Surgery 35, 24-29.

Lau S.F., Wolschrijn C.F., Hazewinkel H.A.W., Siebelt M., Voorhout G., 2013. The early development of medial coronoid disease (MCD) in growing Labrador retrievers: Radiographic, computed tomographic, necropsy and micro-computed tomographic findings. The Veterinary Journal (Final revision).

Mackie E., Ahmed Y., Tatarczuch L., Chen K.S., Mirams M., 2008. Endochondral ossification: How cartilage is converted into bone in the developing skeleton. The International Journal of Biochemistry & Cell Biology 40, 46-62.

Meyer-Lindenberg, A., Langhann, A., Fehr, M., Nolte, I., 2002. Prevalence of fragmented medial coronoid process of the ulna in lame adult dogs. The Veterinary Record 151, 230-234.

Moores, A.P., Benigni, L., Lamb, C.R., 2008. Computed tomography versus arthroscopy for detection of canine elbow dysplasia lesions. Veterinary Surgery 37, 390-398.

Olsson, S.-E., 1975. Lameness in the dog: A review of lesions causing osteoarthrosis of the shoulder, elbow, hip, stifle and hock joints. Journal of the American Animal Hospital Association 1, 363.

Proks P., Necas A., Stehlik L., Srnec R., Griffon D.J., 2011. Quantification of humeroulnar incongruity in Labrador retrievers with and without medial coronoid disease. Veterinary Surgery 40, 981-986.

Samoy Y., Van Vynckt D., Gielen I., van Bree H., Duchateau L., Van Ryssen B., 2012. Arthroscopic findings in 32 joints affected by severe elbow incongruity with concomitant fragmented medial coronoid process. Veterinary Surgery 41, 355-361.

Sereda C.W., Lewis D.D., Radasch R.M., Bruce C.W., Kirkby K.A., 2009. Descriptive report of antebrachial growth deformity correction in 17 dogs from 1999 to 2007, using hybrid linear-circular external fixator constructs. The Canadian Veterinary Journal 50, 723-732.

Seyrek-Intas, D., Michele, U., Tacke, S., Kramer, M., Gerwing, M., 2009. Accuracy of ultrasonography in detecting fragmentation of the medial coronoid process in dogs. Journal of the American Veterinary Medical Association 234, 480-485.

Temwichitr J., Leegwater P.A.J., Auriemma E., van't Veld E.M., Zijlstra C., Voorhout G., Hazewinkel H.A.W., 2010. Evaluation of radiographic and genetic aspects of hereditary subluxation of the radial head in Bouviers des Flandres. American Journal of Veterinary Research 71, 884-890.

Tirgari M., 1974. Clinical radiographical and pathological aspects of arthritis of the elbow joint in dogs. Journal of Small Animal Practice 15, 671-679.

Ubbink G.J., Hazewinkel H.A.W., van de Broek J., Rothuizen J., 1999. Familial clustering and risk analysis for fragmented coronoid process and elbow joint incongruity in Bernese Mountain dogs in the Netherlands. American Journal of Veterinary Research 60, 1082-1087.

Voorhout, G., Hazewinkel, H.A.W., 1987. Radiographic evaluation of the canine elbow joint with special reference to the medial humeral condyle and the medial coronoid process. Veterinary Radiology 28, 158-165.

Voorhout G., Nap R.C., Hazewinkel H.A.W., 1994. A radiographic study on the development of the antebrachium in Great Dane pups, raised under standardized conditions. Veterinary Radiology & Ultrasound 35, 271-276.

Wind, A.P., 1986a. Elbow incongruity and developmental elbow diseases in the dog: part I. Journal of the American Veterinary Medical Association 22, 711-724.

Wind, A.P., Packard, M.E., 1986b. Elbow incongruity and developmental elbow diseases in the dog: part II. Journal of the American Veterinary Medical Association 22, 725-730.

Wolschrijn, C.F., Weijs, W.A., 2004. Development of the trabecular structure within the ulnar medial coronoid process of young dogs. The Anatomical Record. Part A, Discoveries in Molecular, Cellular, and Evolutionary Biology 278, 514-519.

Wong M., Carter D.R., 1990. A theoretical model of endochondral ossification and bonearchitectural construction in long bone ontogeny. Anatomy Embryology 181, 523-532.

Chapter 8

Delayed endochondral ossification in early medial coronoid disease: A morphological and immunohistochemical evaluation in growing Labrador retrievers

S.F. Lau[1], H.A.W. Hazewinkel[2], G.C.M. Grinwis[3], C.F. Wolschrijn[4], M. Siebelt[5], J.C.M. Vernooij[6], G. Voorhout[1], M.A. Tryfonidou[2]

[1] Division of Diagnostic Imaging, Faculty of Veterinary Medicine, Utrecht University, Yalelaan 108, 3584CM, Utrecht, The Netherlands

[2] Department of Clinical Sciences of Companion Animals, Faculty of Veterinary Medicine, Utrecht University, Yalelaan 108, 3584CM, Utrecht, The Netherlands

[3] Department of Pathobiology, Pathology Division, Faculty of Veterinary Medicine, Utrecht University, Yalelaan 1, 3584CL, Utrecht, The Netherlands

[4] Department of Pathobiology, Division of Anatomy and Physiology, Faculty of Veterinary Medicine, Utrecht University, Yalelaan 1, 3584CL, Utrecht, The Netherlands

[5] Department of Orthopedic Surgery, Erasmus Medical Center, Rotterdam, The Netherlands

[6] Department of Farm Animal Health, Faculty of Veterinary Medicine, Utrecht University, Yalelaan 7, 3584CL, Utrecht, The Netherlands

Adapted from The Veterinary Journal, 2013

http://dx.doi.org/10.1016/j.tvjl.2013.04.021

Abstract

Objective:

To investigate the early micromorphological changes occurring in articular cartilage during the development of medial coronoid disease (MCD) and to describe the postnatal development of the medial coronoid process (MCP) before MCD develops.

Methods:

Three litters of MCD-prone young Labrador retrievers were purpose-bred from a dam and two sires with MCD. Elbow joints were collected immediately after euthanasia and the joints were examined macroscopically before being examined by micro-computed tomography. Histological and immunohistochemical studies were performed accordingly.

Results:

By comparing the micromorphological appearance of the MCPs in MCD-negative and MCD-positive joints, it was demonstrated that MCD was initially associated with a disturbance of endochondral ossification, namely a delay in calcification of the calcifying zone, without concurrent abnormalities in the superficial layers of the joint cartilage. Cartilage canals containing patent blood vessels were only detected in dogs <12 weeks.

Conclusion:

MCD development occurred due to a disturbance of endochondral ossification, and in particular delayed calcification in the calcifying zone. The retained hyaline cartilage could ultimately ossify during MCD progression, but weaker points might also develop into cracks between the retained hyaline cartilage and the subchondral bone. Increased pressure or shearing forces during joint movement will lead to detachment of the coronoid process.

Introduction

Medial coronoid disease (MCD) is the most commonly recognized heritable, developmental orthopaedic disease in large-breed dogs (Grøndalen and Grøndalen, 1981; Boulay, 1998; Janutta and Distl, 2008; Temwichitr et al., 2010). The term has been introduced as being more representative than fragmented medial coronoid process (MCP), since it encompasses the entire range of lesions, both of cartilage and subchondral bone, of the MCP (Moores et al., 2008; Fitzpatrick et al., 2009).

Different theories have been postulated regarding the etiopathogenesis of MCD. Osteochondrosis, which is characterized by a disturbance of endochondral ossification that leads to an area of retained cartilage (Reiland et al., 1978), was originally thought to contribute to MCD (Tirgari, 1974; Olsson, 1981), with the retained cartilage acting as a starting point for fissures (Olsson, 1981; Ekman and Carlson, 1998; Ytrehus et al., 2007). This theory was disagreed in histological studies of MCPs from dogs with clinical signs of disease, in which retained cartilage was not detected in 34 diseased MCPs (Crouch et al., 2000), and suggests that MCD is due to fatigue-induced microdamage of subchondral bone rather than osteochondrosis (Danielson et al., 2006). Other postulated causes or factors contributing to MCD include different distribution of loading or forces within the joint, such as tensile forces originating from the annular ligament (Wolschrijn and Weijs, 2004) and shear stress between the contact area of the proximal radial head and axial border of the MCP during pronation and supination (Hulse, 2010). Mechanical overloading of the ulnar surface due to joint incongruity with a shortened radius (Preston et al., 2001) or underdevelopment of the ulnar trochlear notch (Wind, 1986a; Wind and Packard, 1986b) has also been suggested to cause or contribute to the disease. Although there is evidence that the etiopathogenesis of MCD is multifactorial, a causative relationship between MCD and one of these factors has not yet been established.

Most of the reported findings were obtained from dogs with clinical disease, and hence are mostly related to an advanced stage of MCD (Fitzpatrick et al., 2009; Lavrijsen et al., 2012). This means that both regenerative and degenerative secondary changes could have influenced the clinical, radiological, and pathological manifestations of the disease. In order to elucidate the pathogenesis of MCD, in this study we investigated the histology of normal and abnormal MCPs samples obtained from 23 growing Labrador retrievers. The study was divided into two parts: in study I, we investigated early micromorphological changes of articular cartilage, and in study II we investigated the modelling of articular cartilage and subchondral bone before structural maturity and the onset of MCD.

Materials and methods

Specimen collection

This study had been approved by the Ethics Committee of the Utrecht University as required by Dutch legislation (D.E.C. 2009.III.06.050). In total, 46 elbows were collected from 23 purpose-bred Labrador retrievers, originating from three litters with eight, six, and nine puppies, respectively, from one MCD-affected dam and two MCD-affected sires. Elbow joints were collected immediately after euthanasia and until further processing fixed in 4% buffered formaldehyde (Gebufferde Formaldehyde, Klinipath BV). The joints were examined macroscopically before being examined by micro-computed tomography.

Study I: Early micromorphological changes of the medial coronoid process in dogs with medial coronoid disease

Fourteen pups from the first two litters were examined by radiography and computed tomography (CT) every 2 weeks from the age of 6 (*n*=7) or 7 weeks (*n*=7) until euthanasia was performed with an IV overdose of barbiturate when there was a suspicion of MCD lesion (*n*=7), based on radiographic or CT studies. MCD-negative dogs (*n*=3) were euthanased as an age- and weight-matched negative control or at the end of the investigation period (*n*=4; 27 weeks).

Study II: Postnatal development of the medial coronoid process

On the basis of the results from study I, animals from the third litter (*n*=9) were euthanized at 5 (*n*=2), 7 (*n*=2), 9 (*n*=2), and 12 weeks of age (*n*=3), before MCD could be detected by radiography or CT, in order to study the postnatal development of the MCP.

Micro-computed tomography

In both study I and II, micro-computed tomography (microCT) was performed to visualise the MCP. In study I, 28 ulnas were scanned in a microCT system (SkyScan 1076, Skyscan) from 2 cm proximal of the MCP to 2 cm distal of the MCP, using 60 kV and 170 µA, an exposure time of 948 ms, and a pixel size of 36 µm. In study II, 18 ulnas were scanned in a microCT system (Scanco microCT 80, Scanco Medical) from 2 cm proximal of the MCP to 2 cm distal of the MCP, using 55 kV, 145 mA, an exposure time of 1 s, and a pixel size of 36.9 µm. MicroCT images were reconstructed in three dimensions (3-D; Fig. 1) to depict the subchondral bone structures of the MCP and to identify the exact anatomical location of fissures or fragments. The MCP was considered "MCD positive" if fissures or fragmentation were detected. Fissures were identified as incomplete detachment of the MCP from the rest of the process, and fragmentation was characterised by the complete separation of

calcified bone from adjacent bone (Fig. 2). Depending on the definitive diagnosis, joints in study I were grouped into MCD-negative and MCD-positive groups, and by bodyweight (<20 kg, 20-25 kg and >25 kg), in order to investigate whether the changes in the MCP were due to pathological remodelling or physiological adaptive process.

Histological studies of the medial coronoid process

In both studies, bones were decalcified in 10% ethylenediaminetetraacetic acid (EDTA, Sigma-Aldrich) for 1-3 months. After decalcification, the whole MCP was dissected from the ulna caudal to the base of the coronoid process, approximately 1 cm in length from the apex of the coronoid process (Fig. 1a). MCPs were routinely embedded in paraffin. Sections of 4 µm were cut in the vertical plane and collected on microscopic slides (KP Plus Slides, Klinipath) and stained with haematoxylin and eosin (H&E) or safranin-O (SO). Adjacent tissue sections were used for immunohistochemistry, as described below. A veterinary pathologist (G.G.) examined the sections for histopathological changes in the articular cartilage and subchondral bone. In study I, the sections were examined for evidence of a secondary ossification centre, a nidus of hypertrophic chondrocytes nourished by cartilage canals and which ultimately ossifies (Kugler et al., 1979); thickening and fissuring of the articular cartilage; and diffuse damage and micro-cracks of subchondral bone, especially on the lateral aspect of MCP (latMCP; Fig. 1d). In study II, the morphological changes with age were studied.

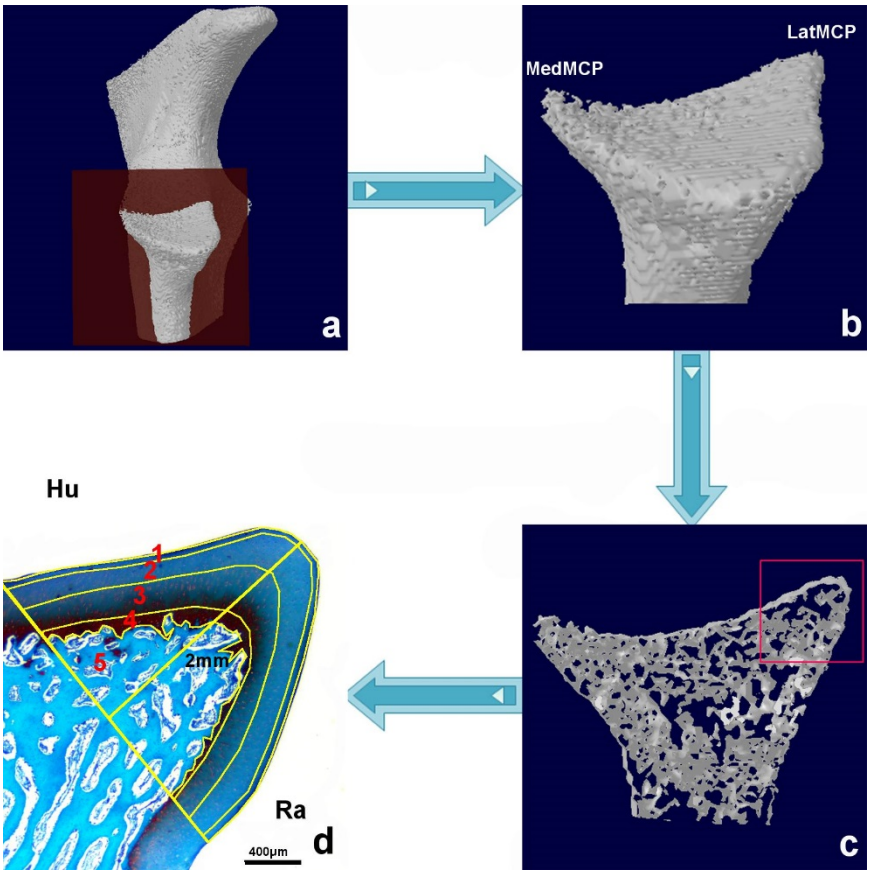

Fig. 1. *Explanatory diagram of the work flow for obtaining the region of interest (ROI) for histomorphometrical analysis of the medial coronoid process (MCP) by using a 3-D reconstructed micro-computed tomography (microCT) image to represent real bone. (a) 3-D reconstructed microCT image of the proximal part of the ulna, MCP was dissected from the rest of the ulna at the base of the MCP (red plane). (b) 3-D reconstructed microCT of the dissected MCP. MedMCP, medial aspect of the MCP; LatMCP, lateral aspect of the MCP. (c) MicroCT image of the dissected MCP in vertical plane. The area for histopathological evaluation is indicated by the red square. (d) Safranin O-stained latMCP. The ROI was a triangular area, 2-mm from the tip of the latMCP. The surface area of different zones in articular cartilage both at the humeral contact surface (Hu) and radial contact surface (Ra) within the ROI was calculated. Different zones were identified based on the different morphological appearance of chondrocytes and their alignment. (1). Tangential zone; (2) Transitional zone; (3) Radial zone; (4) Calcifying zone; (5) Bone.*

Histomorphometrical analysis of the medial coronoid process

In study I, the zonal distribution of articular cartilage was analysed in the latMCP, where lesions were located according to 3-D reconstructed microCT images (Fig. 2). On each histological section of the latMCP, a 2-mm line was drawn from the tip of latMCP and the whole triangular area with 2-mm height was selected as region of interest (ROI; Fig. 1d). Four different zones as defined by Recht and Resnick were identified in articular cartilage, i.e. tangential, transitional, radial, and calcifying cartilage zone, based on the morphological appearance of chondrocytes and their alignment (Recht and Resnick, 1994). The surface area of zones within the ROI was calculated as the average of three measurements, using the open source software, ImageJ v1.47b (ImageJ, NIH).

Immunohistochemical studies of the medial coronoid process

Tissue sections were stained for type X collagen to identify chondrocytes in the radial and calcifying zones, and for von Willebrand factor (vWF) to identify vascular endothelial cells in articular cartilage. After deparaffinisation and rehydration in xylene and a graded series of ethanol, antigen retrieval and blocking of endogenous peroxidase were performed (Table 1). After incubation with 10% normal goat serum (NGS, Sigma-Aldrich) in PBS/T for 30 min at room temperature, the sections were incubated with primary antibody overnight at 4 °C (Table 1). Thereafter, sections were treated with peroxidase-labelled polymer (EnVision, Dako) for 30 min at room temperature. Type X collagen and vWF were visualised using the DAB chromogen system (DAB, Dako). Sections were counterstained with haematoxylin solution (Hematoxylin QS, Vector) and mounted in permanent mounting medium (VectaMount, Vector). To diminish variability, all slides were stained in one batch for each specific stain. In the negative controls, the primary antibody was replaced by normal mouse IgG_1 (Normal mouse IgG_1, Santa Cruz) at concentration of 5 µg/ml (similar with the concentration used in primary antibody for type X collagen) in PBS/T. Costal growth plate cartilage served as positive control for type X collagen staining.

In both studies, the presence of type X collagen was determined in triplicate by calculating the absolute and relative surface area positive for type X collagen expression within the ROI. A special plug-in of ImageJ v1.47b(Colour Convolution, NIH) was used to quantify the DAB-stained area (Ruifrok and Johnston, 2001). vWF staining was used to identify the presence of a vascular network within the cartilage canals of the latMCP and medial aspect of MCP (medMCP) in both study I and II. MedMCP is defined as the articular cartilage at the medial border of the MCP (Fig. 1b).

Protocols	Type X collagen	von Willebrand factor
Antigen retrieval	0.5% pepsin [1], 20 min in 37 °C. Addition of 1.6% hyarulonidase [2], incubation for 30 min in 37 °C	10 mM citrate buffer solution, pH 6, 60 min in a water bath at 70 °C (modified protocol from Tryfonidou et al., 2010)
Endogenous peroxidase activity	Peroxidase block [3], 5 min at room temperature	Peroxidase block [3], 15 min in room temperature
Primary antibody	Monoclonal antibody to Type X [4], 1:50 in PBS/T	Polyclonal Rabbit Anti-Human Von Willebrand factor [5], 1:1000 in PBS

Table 1. *Antigen retrieval, endogenous peroxidase activity blocking, and primary antibody incubation protocols used in Type X collagen and von Willebrand factor.*

[1] Pepsin, Dako

[2] Hyarulonidase from bovine testes, Sigma-Aldrich

[3] Dual endogenous Enzyme Block, Dako

[4] Collagen Type X, Quartett

[5] vWF, Dako

Terminal deoxynucleotidyl Transferase dUTP nick end labelling (TUNEL)

In study I, the commercial TUNEL assay (ApopTag Plus Peroxidase In-Situ Apoptosis Detection Kit, #S7101 Chemicon International) was used according to the manufacturer's instruction to assist the detection of the apoptotic cells in the retained hyaline cartilage.

Statistical analysis

All statistical analyses were conducted using SPSS (SPSS version 20.0, SPSS Inc.). In study I, multivariate analysis of covariance (MANOVA) was used to compare the main effects of MCP status and bodyweight as fixed factors and the relative surface area of the four different zones as dependent outcomes. Interactions between the fixed factors were determined using a costumed model. A full-factorial model excluding interaction was selected because there was no interaction effect. The results are expressed as means ± SD. Multivariate binary logistic regression with backward stepwise (likelihood ratio) was used to investigate the relationship between MCP status, bodyweight and binary type X collagen outcome. Statistical significance was set at 5% (P<0.05).

Results

Study I: Early micromorphological changes in the medial coronoid process of dogs with medial coronoid disease

Twenty-eight ulnas were collected from 14 Labrador retrievers (nine males and five females) aged 15-27 weeks with mean ± SD bodyweight of 23.1 ± 5.8 kg. Detailed individual data are given in the Table 1 (Chapter 4). During the necropsy examination, fissures at the articular cartilage were only found in MCD-positive joints obtained from dogs >17 weeks of age.

Micro-computed tomography findings

Thirteen out of 28 ulnas were diagnosed with MCD (bilaterally in six dogs and unilaterally in one dog), based on lesions detected on microCT. The youngest dog diagnosed with MCD was 15 weeks old. The MCPs from the MCD-positive group showed either an incomplete fissure at the lat*MCP* (*n*=5 MCPs) or fragmentation across the base to the apex of the MCP (*n*=8 MCPs; Fig. 2).

Histological studies of the medial coronoid process

The absence of lesions in the microCT images was confirmed histologically by the presence of normal hyaline cartilage (Fig. 2) with distinct tangential, transitional, radial, and calcifying zones in the normal MCPs. In the section from the youngest dog (15 weeks of age), we could no longer detect the presence of clustered hypertrophic cartilage cells.

In contrast, the articular cartilage of MCPs obtained from MCD-positive joints had a different morphological appearance, with a large area of hyaline cartilage with focal areas of empty lacunae being found in the calcifying zone of the lat*MCP* (Fig. 3) at the site where ossified trabecular bone was found in normal dogs. The morphological appearance of the three most superficial zones (tangential, transitional, and radial zones) was not different from that seen in MCD-negative joints.

There seemed to be a progression in the appearance of retained hyaline cartilage with increasing age in the MCD positive group illustrated in Figure 2. Abnormal MCP from the youngest dogs showed retained hyaline cartilage in the lat*MCP*, but in older dogs (17 and 18 weeks of age) an island of trabecular bone was visible within the area of retained hyaline cartilage. A cleft separating retained hyaline cartilage from underlying bone was clearly present. In abnormal MCPs obtained from dogs older than 18 weeks, lesions were characterised by the presence of trabecular bone in the area of retained hyaline cartilage. Cleft formation with active granulation tissue in the adjacent medullar area was also prominent in the older animals. None of the sections from either group of dogs showed a secondary ossification centre or cartilage canals in articular cartilage.

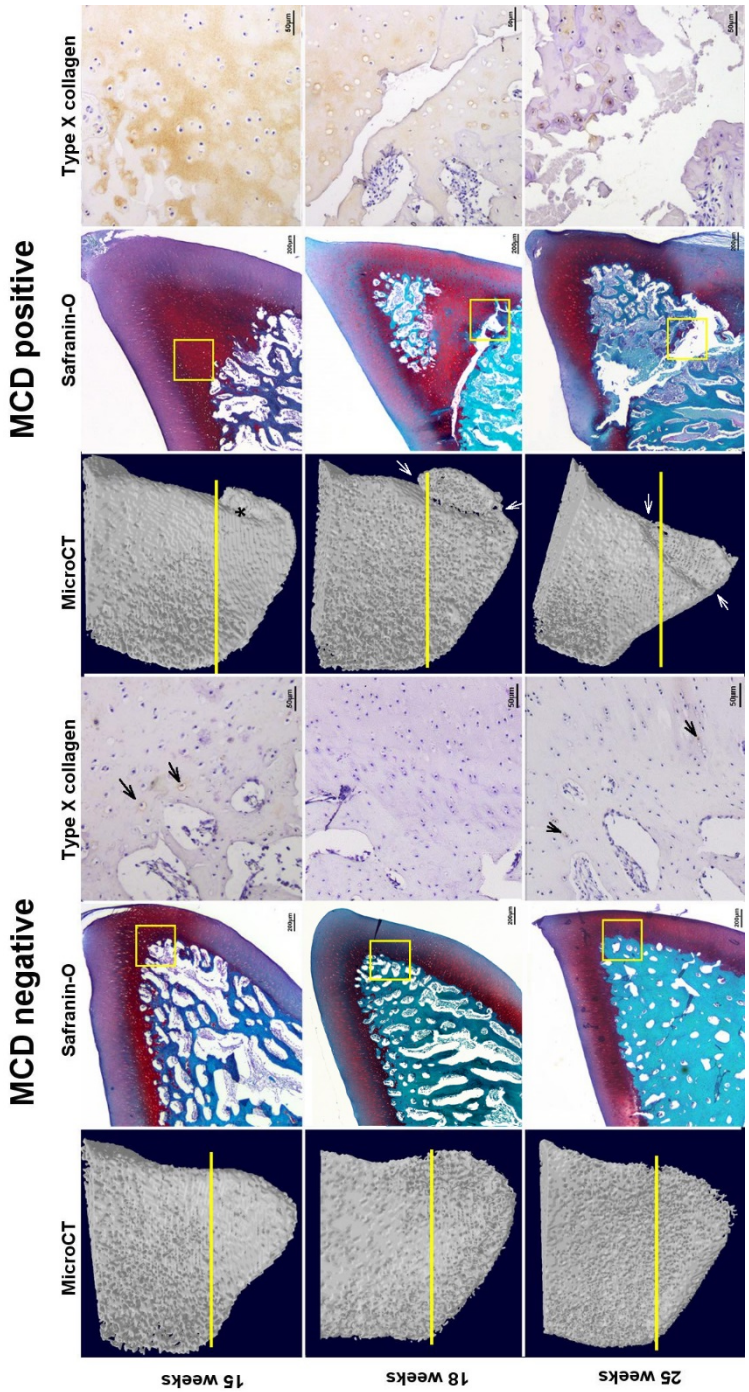
MCD positive
MCD negative
Type X collagen
Safranin-O
MicroCT
Type X collagen
Safranin-O
MicroCT
15 weeks
18 weeks
25 weeks

Fig. 2. *Comparison of the proximal view of 3-D reconstructed micro-computed tomography (microCT) images of the medial coronoid process (MCP) with corresponding (cut at yellow line) safranin-O and type X collagen staining in medial coronoid disease (MCD)- negative and -positive joints obtained from dogs aged 15, 18 and 25 weeks.*

Typical examples: In the MCD-negative group, histologically, the lateral aspect of the medial coronoid process (latMCP) of dogs at 15, 18 and 25 weeks of age had a normal appearance, with articular cartilage covering the subchondral bone layer. In the MCD positive group, MCP from a 15-week-old dog showing a "fissure" (*) incompletely dividing the MCP from the rest of the process. MCP from 18- and 25-week old dogs showing "fragmentation" that separated the MCP from the rest of the process (white arrows). Histologically, the latMCP of a 15-week-old dog showing evidence of retained hyaline cartilage and of an 18-week-old dog showing an island of trabecular bone within the area of retained hyaline cartilage and a cleft separating the retained hyaline cartilage from the underlying bone. The latMCP of a 25-week-old dog showing a cleft separating the trabecules from the rest of the bone. In the MCD-negative group, type X collagen staining from the area in the yellow box was found at the calcifying zone and stained in pericellular pattern (arrows) in 15- and 25-week-old dogs. Type X collagen was not detected in the 18-week-old dog. In the MCD-positive group, type X collagen showed a pericellular and intercellular staining pattern; the retained hyaline cartilage and cartilage along the cleft stained also positive for type X collagen.

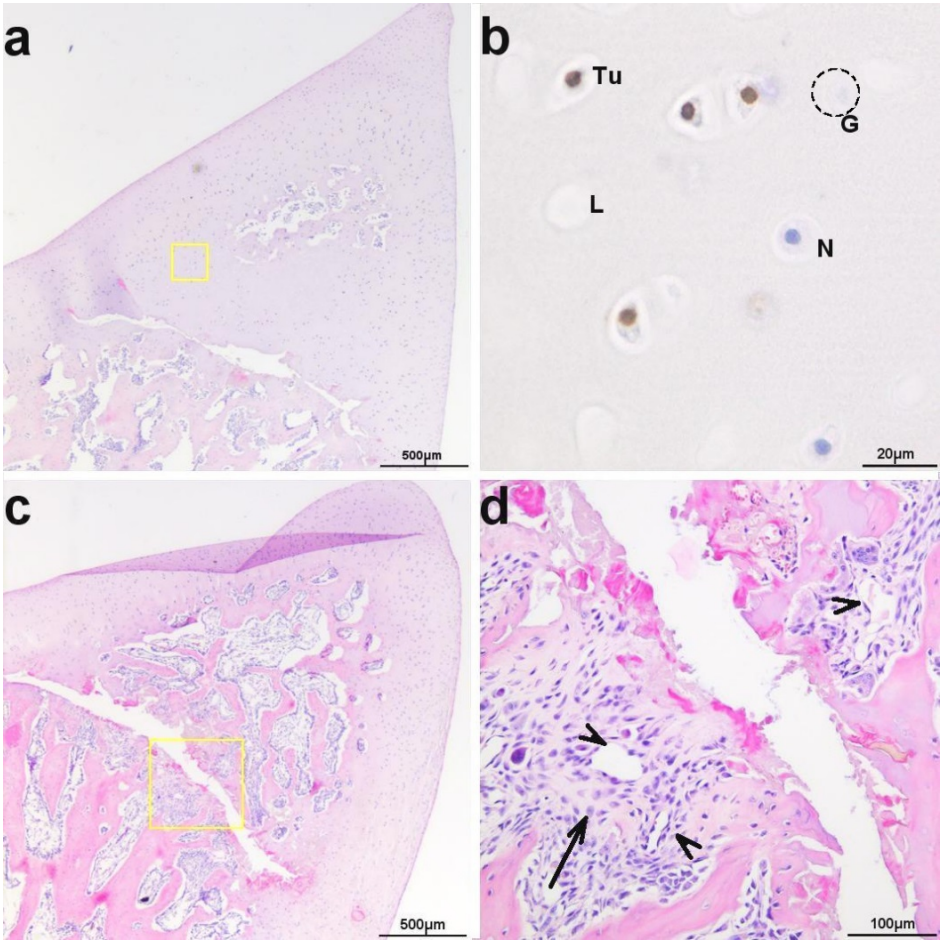

Fig. 3. *Haematoxylin and Eosin staining of the medial coronoid process (MCP) from dogs with medial coronoid disease (MCD). (a) The lateral aspect of the medial coronoid process (latMCP) from an 18-week-old dog showing an increased hypocellular area of hyaline cartilage at the site where in normal dogs ossified trabecular bone is found, with a cleft separating the retained hyaline cartilage from underlying bone. (b) magnification of the yellow box in a, showing empty lacunae (L), chondronecrotic-like "ghost cells" (dead cells; G), TUNEL-positive chondrocytes indicative of DNA fragmentation (Tu) and normal appearance of single chondrocytes (N). (c) The latMCP from a 25-week-old dog showing a cleft and proliferation of granulation tissue in the adjacent bone marrow (yellow box), and (d) on higher magnification the granulation tissue is seen with blood vessels (arrow heads) and activated mesenchymal cells (arrow).*

Histomorphometrical analysis of the medial coronoid process

The relative surface area of the tangential and transitional zones was significantly smaller in the MCD-positive joints than in the MCD-negative joints (*P*=0.01 and 0.02, respectively). The relative surface area of the radial zone was also smaller, but this difference was not statistically significant. In contrast, the relative surface area of the calcifying zone was two-fold larger (*P*<0.001) in the MCD-positive joints than in the MCD-negative joints (Table 2). The relative surface area of all four zones was not significantly influenced by bodyweight (*P*=0.12-0.45).

	Mean ± SD, Relative (Absolute value, mm²)		
Zones	Normal group (*n*=15)	MCD group (*n*=13)	*P* value
Tangential	9.8 ± 2.3 (0.2 ± 0.1)	7.4 ± 1.7 (0.2 ± 0.0)	0.01
Transitional	36.8 ± 8.4 (0.7 ± 0.2)	27.4 ± 5.5 (0.7 ± 0.1)	0.02
Radial	40.6 ± 6.7 (0.8 ± 0.2)	34.6 ± 7.9 (0.9 ± 0.2)	0.08
Calcifying	12.8 ± 3.9 (0.3 ± 0.1)	30.7 ± 11.5 (0.8 ± 0.4)	<0.001
Col X,	0.3 ± 0.7 (0.04 ± 0.1)	3.7 ± 4.6 (0.10 ± 0.1)	0.001

Table 2. *Surface area (relative and absolute value) of different zones and type X collagen staining in the articular cartilage of growing Labrador retrievers with and without medial coronoid disease (MCD). n, number of medial coronoid processes; MCD, medial coronoid disease; Col X, Type X collagen; SD, standard deviation. Note that type X collagen was mainly expressed in the calcifying zone of articular cartilage.*

Type X collagen

Type X collagen was distributed either pericellularly or more diffusely within the intercellular matrix in both groups of dogs. In the MCD-negative group, type X collagen was found only in the calcifying zone and appeared at or just above the tidemark. In contrast, in the MCD-positive group type X collagen was found in the calcifying zone, including the retained hyaline cartilage, as well as in the matrix along the cleft (Fig. 2). The positively stained surface area (mean ± SD, in %) was 0.3 ± 0.7% in the MCD-negative group and 3.7 ± 4.6% in the MCD-positive group (Fig. 4). Type X collagen stained surface area was significantly associated with MCP status (*P*=0.001), despite the high variability within the two groups, but not with bodyweight (*P*=0.09). Type X collagen was not found in the ROI of the latMCP in one of the MCD-positive MCPs and in seven of the MCD-negative MCPs (Fig. 4).

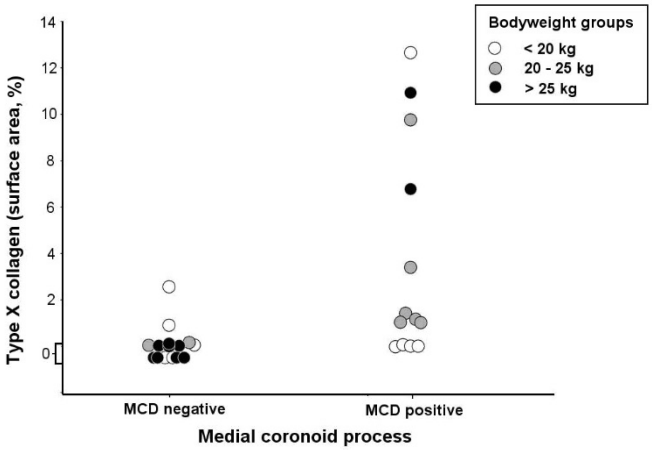

Fig. 4. *Type X collagen distribution in dogs negative and positive for medial coronoid disease (MCD) by bodyweight.*

Von Willebrand factor (vWF)

Cartilage canals in the articular cartilage of MCPs were not detected in either group. In the MCD-negative group, vWF-positive endothelial cells were not detected along the osteochondral junction, whereas in the MCD-positive group numerous vWF-positive vascular endothelial cells were seen in the inter-trabecular medullary area contained by the retained hyaline cartilage and at the edges of clefts.

Terminal deoxynucleotidyl transferase dUTP nick end labeling (TUNEL)

Chondrocytes in the retained hyaline cartilage of the MCD-positive group stained positive for TUNEL, indicating DNA fragmentation (Fig. 3b).

Study II: Postnatal development of the medial coronoid process

Eighteen ulnas were collected from nine Labrador retrievers (five males and four females) aged 5-12 weeks with mean ± SD bodyweight 7.2 ± 3.7 kg. There was no articular cartilage lesion of the MCP observed during necropsy examination.

Micro-computed tomographic findings

There were no signs of MCD in any of the 18 ulnas, based on microCT

Histological studies of the medial coronoid process

The morphology and alignment of chondrocytes in articular cartilage changed with increasing age (Fig. 5). At the age of 5 weeks, the tangential zone comprised elongated single cells lying parallel to the articular cartilage, followed by chondrocytes in the transitional zone, mostly single cells and some in pairs. In the next layer, the radial zone, larger vacuole-shaped chondrocytes were seen arranged in columns oriented perpendicularly to the joint surface. At the age of 12 weeks, the hypertrophic chondrocytes in the radial zone had lost their growth plate-like stacked columnar appearance and were arranged in randomly distributed clusters of three or four chondrocytes. There was no distinguishable calcifying zone (Fig. 5).

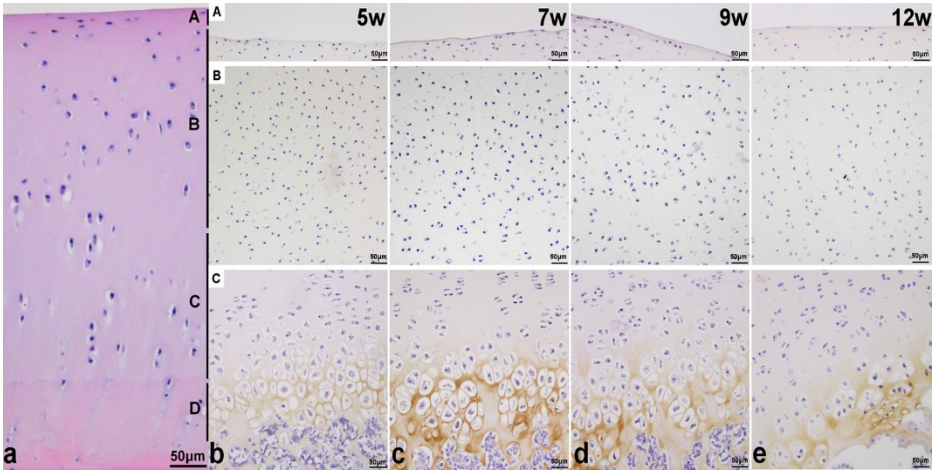

Fig. 5. *Morphology and alignment of chondrocytes in articular cartilage. (a) Articular cartilage of a 25-week-old dog (MCD-negative) showing four distinct zones (haematoxylin and eosin stained). (A). Tangential zone, the chondrocytes are flattened lying parallel to the joint surface; (B) Transitional zone, the rounded chondrocytes are individually located; (C) Radial zone, the chondrocytes appear to be paired and oriented perpendicular to the joint surface; (D) Calcifying zone, the single chondrocytes are distributed randomly. Morphological appearance of the articular cartilage in tangential, transitional, and radial zones in the articular cartilage of dogs of (b) 5 weeks of age; (c) 7 weeks of age; (d) 9 weeks of age; and (e) 12 weeks of age displaying type X collagen expression surrounding hypertrophic chondrocytes. No evidence of calcifying zone in the period of 5-12 weeks of age. (Type X and haematoxylin counterstained)*

Type X collagen

Type X collagen was observed surrounding the hypertrophic chondrocytes in pericellular and intercellular patterns (Fig. 5). The proportion of the surface area staining positive for

type X collagen ranged from 0% to 9.1% (Table 3). Four of 18 MCPs (bilateral from two dogs at 5 and 12 weeks of age) were negative for type X collagen, even though the positive control originating from the same animals, i.e. the costal growth plate, stained for type X collagen in the hypertrophic zone.

Age of animals (weeks)	Type X collagen (Mean surface area ± SD, %)	Range (Range, %)
5 (n=2)	3.6 ± 4.5	0.0 - 9.1
7 (n=2)	7.3 ± 0.8	6.4 - 8.1
9 (n=2)	3.9 ± 0.9	2.7 - 4.5
12 (n=3)	2.3 ± 3.0	0.0 - 7.1

Table 3. *Surface area of articular cartilage staining positive for type X collagen in study II. n, number of dogs; SD, standard deviation*

Von Willebrand factor (vWF)

Cartilage canals were observed in both the latMCP and medMCP at 5 and 7 weeks of age only (Figs. 6a, 6b, 6e, and 6f) and were present in the latMCP only at 9 weeks (Fig. 6c). These canals were no longer present in dogs at and older than 12 weeks (Figs. 6d and 6h).

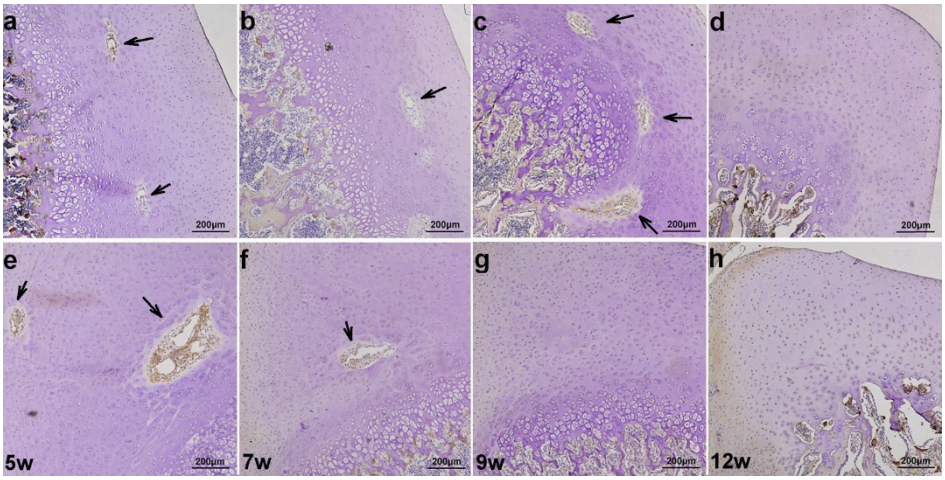

Fig. 6. *Cartilage canals disappear during the development of the medial coronoid process at an early age. (a - d) The lateral aspect of the medial coronoid process (latMCP) from dogs of 5, 7, 9 and 12 weeks of age, showing the presence of cartilage canals (arrow/s) that were no longer detected at 12 weeks of age. (e - h) The medial aspect of the medial coronoid process (medMCP) from dogs of 5, 7, 9 and 12 weeks of age showing the presence of cartilage canals (arrow/s) until 7 weeks of age and no longer can be detected at 9 and 12 weeks of age. (von Willebrand factor and haematoxylin counterstained).*

Discussion

MCD is a multifactorial disease, most studies to date have investigated elbows with clinical signs of the disease, and hence findings are mostly for advanced stages of MCD. This makes it difficult to establish whether reported findings are the cause or consequence of MCD. For this reason, we attempted to study the development of MCD in its early stages, before it becomes clinically manifest. We purpose-bred Labrador retrievers, which have a high clinical prevalence of MCD (11-50%; Meyer-Lindenberg et al., 2002; Fitzpatrick et al., 2009), from an MCD-affected dam and MCD-affected sires. We used microCT to visualise the latMCP, and in combination with histopathological analysis we provide evidence that a disturbance of endochondral ossification is involved in MCD development.

CT findings were confirmed by the microCT studies indicating that signs of MCD developed as early as 15 weeks in the Labrador retrievers. Combination of necropsy and microCT findings indicated that MCD solely involved subchondral bone and did not affect joint cartilage in dogs younger than 18 weeks of age. Histological studies revealed that MCD is initiated in the deeper layer of the articular cartilage, i.e. in the calcifying zone. The presence of clustered hypertrophic cartilage cells, which had been reported to be present in Golden retriever at the age of 13 weeks (Wolschrijn et al., 2008), could no longer be detected in the section from the youngest dog (15 weeks of age).

The histological findings suggest that MCP modelling, especially of the latMCP, might underlie the development of MCD in this breed. The relative surface area of the calcifying cartilage zone was approximately two-fold larger ($P<0.001$) in MCD-positive joints than in MCD-negative joints. We used type X collagen as a specific marker of the matrix produced by hypertrophic chondrocytes (Von der Mark et al., 1992; Shen, 2005) and found extensive type X collagen staining in MCD-positive joints (3.7 ± 4.6%) compared with MCD-negative joints (0.3 ± 0.7%; Fig. 4). The retained hyaline cartilage stained positive for collagen type X in the MCD-positive joints, which is suggestive of a localized delay in endochondral ossification, mainly in the calcifying zone as the three most superficial cartilage layers were not affected. The persistence of cartilage could give rise to cleft formation as a result of physiological or abnormal biomechanical forces, followed by secondary changes in articular cartilage.

The persistence of cartilage canals containing a vascular network has previously been related to osteochondrosis lesions in pigs (Woodard et al., 1987); however, these canals were not seen in articular cartilage (study I). Regression of the cartilage canals had already occurred before 12 weeks of age (study II), i.e. at least 3 weeks before the earliest radiographical manifestation of MCD. The presence of an extensive vascular network in the retained hyaline cartilage and edges of clefts in the MCD-positive group is suggestive of a

healing process. It should be stressed that the presence of active granulation tissue indicates that the clefts are physiological and not due to an artefact.

The cross-sectional character of study I enabled us to study MCD development over the period 15-27 weeks of age, and findings imply that there is modelling of the diseased MCP in growing Labrador retrievers. MicroCT and histological findings (Fig. 2) suggest that the retained hyaline cartilage within the MCD lesion ultimately ossifies, giving rise to the typical histological appearance of MCD specimens obtained from dogs with clinical disease (Crouch et al 2000, Danielson et al., 2006; Goldhammer et al., 2009).

As we identified MCD lesions with microCT at 15 weeks, we investigated the development of MCD before the appearance of fissures and fragmentation of the MCP in dogs aged 5, 7, 9, and 12 weeks. However, macroscopic evaluation, microCT, and histomorphometric analysis of MCPs from animals younger than 15 weeks of age revealed no clear-cut criteria that could distinguish dogs that would develop MCD from those that would not. Thus early lesions of MCD could not be detected in dogs younger than 12 weeks.

Cartilage canals containing vascular networks were no longer present in articular cartilage in 12-week-old dogs. This finding is consistent with previous publications reporting the regression of cartilage canals from articular cartilage before 13 weeks of age in a MCD-free population of dogs (Guthrie et al., 1992; Wolschrijn et al., 2008). The absence of positive type X collagen staining in the entire MCP in two of nine affected dogs was unexpected, especially because cartilage of the costal growth plate from the same dogs was positive for type X collagen. We cannot explain this finding, but cannot exclude that it was due to technical limitations.

References

Boulay, J.P., 1998. Fragmented medial coronoid process of the ulna in the dog. Veterinary Clinics of North America: Small Animal Practice 28, 51-74.

Crouch, D.T., Cook, J.L., Lewis, D.D., Kreeger, J.M., Tomlinson, J.L., 2000. The presence of collagen types II and X in medical coronoid processes of 21 dogs. Veterinary and Comparative Orthopaedics and Traumatology 13, 178-184.

Danielson, K.C., Fitzpatrick, N., Muir, P., Manley, P.A., 2006. Histomorphometry of fragmented medial coronoid process in dogs: a comparison of affected and normal coronoid processes. Veterinary Surgery 35, 501-509.

Ekman, S., Carlson, C.S., 1998. The pathophysiology of osteochondrosis. Veterinary Clinics of North America: Small Animal Practice 28, 17-32.

Fitzpatrick, N., Smith, T.J., Evans, R.B., Yeadon, R., 2009. Radiographic and arthroscopic findings in the elbow joints of 263 dogs with medial coronoid disease. Veterinary Surgery 38, 213-223.

Goldhammer, M.A., Smith, S.H., Fitzpatrick, N., Clements, D.N., 2009. A comparison of radiographic, arthroscopic and histological measures of articular pathology in the canine elbow joint. The Veterinary Journal 186, 96-103.

Grøndalen, J., Grøndalen, T., 1981. Arthrosis in the elbow joint of young rapidly growing dogs. V. A pathoanatomical investigation. Nordisk Veterinaermedicin 33, 1-16.

Guthrie, S., Plummer, J.M., Vaughan, L.C., 1992. Post natal development of the canine elbow joint: a light and electron microscopical study. Research in Veterinary Science 52, 67-71.

Hulse, D., Young, B., Beale, B., Kowaleski, M., Vannini, R., 2010. Relationship of the biceps-brachialis complex to the medial coronoid process of the canine ulna. Veterinary and Comparative Orthopaedics and Traumatology 23, 173-176.

Janutta, V., Distl, O., 2008. Review on canine elbow dysplasia: pathogenesis, diagnosis, prevalence and genetic aspects. Deutsche Tierarztliche Wochenschrift 115, 172-181.

Kugler, J.H., Tomlinson, A., Wagstaff, A., Ward, S.M., 1979. The role of cartilage canals in the formation of secondary centres of ossification. Journal of Anatomy 129, 493-506.

Lavrijsen, I.C., Heuven, H.C., Voorhout, G., Meij, B.P., Theyse, L.F., Leegwater, P.A., Hazewinkel, H.A., 2012. Phenotypic and genetic evaluation of elbow dysplasia in Dutch Labrador retrievers, Golden retrievers, and Bernese Mountain Dogs. The Veterinary Journal 193, 486-492.

Meyer-Lindenberg, A., Langhann, A., Fehr, M., Nolte, I., 2003. Arthrotomy versus arthroscopy in the treatment of the fragmented medial coronoid process of the ulna (FCP) in 421 dogs. Veterinary and Comparative Orthopaedics and Traumatology 16, 204-210.

Moores, A.P., Benigni, L., Lamb, C.R., 2008. Computed tomography versus arthroscopy for detection of canine elbow dysplasia lesions. Veterinary Surgery 37, 390-398.

Olsson, S.-E., 1981. Pathophysiology morphology, and clinical signs of osteochondrosis in the dog. In: Bojrab, M.J. (Ed), Pathophysiology in Small Animal Surgery, First Ed. Lea & Febiger, Philadelphia, USA, pp. 604-617.

Preston, C.A., Schulz, K.S., Taylor, K.T., Kass, P.H., Hagan, C.E., Stover, S.M., 2001. In vitro experimental study of the effect of radial shortening and ulnar ostectomy on contact patterns in the elbow joint of dogs. American Journal of Veterinary Research 62, 1548-1556.

Recht, M.P., Resnick, D., 1994. MR imaging of articular cartilage: current status and future directions. American Journal of Roentgenology 163, 283-290.

Reiland, S., Ordell, N., Lundeheim, N., Olsson, S.-E., 1978. Heredity of osteochondrosis, body constitution and leg weakness in the pig. A correlative investigation using progeny testing. Acta Radiologica. Supplementum 358, 123-137.

Ruifrok, A.C., Johnston, D.A., 2001. Quantification of histochemical staining by color deconvolution. Analytical and Quantitative Cytology and Histology 23, 291-299.

Shen, G., 2005. The role of type X collagen in facilitating and regulating endochondral ossification of articular cartilage. Orthodontics & Craniofacial Research 8, 11-17.

Temwichitr, J., Leegwater, P.A., Hazewinkel, H.A., 2010. Fragmented coronoid process in the dog: a heritable disease. The Veterinary Journal 185, 123-129.

Tirgari, M., 1974. Clinical radiographical and pathological aspects of arthritis of the elbow joint in dogs. Journal of Small Animal Practice 15, 671-679.

Tryfonidou, M.A., Hazewinkel, H.A., Riemers, F.M., Brinkhof, B., Penning, L.C., Karperien, M., 2010. Intraspecies disparity in growth rate is associated with differences in expression of local growth plate regulators. American Journal of Physiology - Endocrinology and Metabolism 299, E1044-1052.

Von der Mark, K., Kirsch, T., Nerlich, A., Kuss, A., Weseloh, G., Glückert, K., Stöss, H., 1992. Type X collagen synthesis in human osteoarthritic cartilage. Indication of chondrocyte hypertrophy. Arthritis & Rheumatism 35, 806-811.

Wind, A.P., 1986a. Elbow incongruity and developmental elbow diseases in the dog: part I. Journal of the American Veterinary Medical Association 22, 711-724.

Wind, A.P., Packard, M.E., 1986b. Elbow incongruity and developmental elbow diseases in the dog: part II. Journal of the American Veterinary Medical Association 22, 725-730.

Wolschrijn, C.F., Gruys, E., van der Wiel, C.W., Weijs, W.A., 2008. Cartilage canals in the medial coronoid process of young Golden retrievers. The Veterinary Journal 176, 333-337.

Wolschrijn, C.F., Weijs, W.A., 2004. Development of the trabecular structure within the ulnar medial coronoid process of young dogs. The Anatomical Record. Part A, Discoveries in Molecular, Cellular, and Evolutionary Biology 278, 514-519.

Woodard, J.C., Becker, H.N., Poulos, P.W., 1987. Articular cartilage blood vessels in swine osteochondrosis. Veterinary Pathology 24, 118-123.

Ytrehus, B., Carlson, C.S., Ekman, S., 2007. Etiology and pathogenesis of osteochondrosis. Veterinary Pathology 44, 429-448.

Chapter 9

General discussion

General discussion

Medial coronoid disease (MCD), previously known as ununited or fragmented medial coronoid process (MCP), appears to be the most common component of elbow dysplasia in Labrador retrievers (Lavrijsen et al., 2012). This despite the implementation of breeding selection programs to exclude affected animals from breeding stocks. Due to the late manifestation of the disease, the pathological findings obtained from clinical patients are usually complicated by degenerative and regenerative changes, with uncertainty whether the findings are causes by or consequences of MCD. To elucidate the pathogenesis of this disease, longitudinal studies were designed to follow the development of the normal and diseased MCP. The purpose of this thesis was to investigate, in depth, the diagnostic features at the early stage and the etiopathogenesis of MCD.

In Chapter 2, a literature review is presented on canine MCD, to obtain insight into the background and current knowledge of this disease, the normal postnatal development of the MCP, the disease manifestations of MCD, commonly accepted hypotheses regarding the etiopathogeneses of the MCD, and diagnostic techniques used. This information was used in designing the studies as described in this thesis. Currently, the widely accepted theory regarding the development of the MCP is that it develops through endochondral ossification from the base to the apex with the ossification occurring at the axial border first, then followed by the abaxial borders, without the evidence of a secondary ossification center (Fox et al., 1983; Guthrie et al., 1992; Breit et al., 2004; Wolschrijn and Weijs, 2004; Breit et al., 2005; Wolschrijn and Weijs, 2005; Breit et al., 2006; Wolschrijn et al., 2008).

The ossification of the MCP is completed later in large breed dogs (approximately 20 weeks of age) than in smaller dogs (approximately 16 weeks of age) suggesting that the cartilage maturation and ossification of the MCP might play a role in the development of MCD (Breit et al., 2004; Breit et al., 2006). In addition to the impairment of the development of either articular cartilage (Tirgari, 1974; Grøndalen and Grøndalen, 1981; Olsson, 1981) or subchondral bone (Danielson et al., 2006; Goldhammer et al., 2009; Temwichitr et al., 2009), inter-bones and musculoskeletal relationships are believed to contribute to development of MCD (Wind, 1986a; Wind and Packard, 1986b; Murphy et al., 1998; Preston et al., 2001; Wolschrijn and Weijs, 2004; Fitzpatrick and Yeadon, 2009; Hulse et al., 2010; Cuddy et al., 2012). All these proposed etiologies were each supported with either histological, radiographical, computed tomographical, or surgical findings. However, whether or not the findings were primary causes or consequences of MCD remained to be solved, since most of the data from those studies were obtained from MCD affected animals with secondary degenerative changes.

MCD is an important ailment in veterinary medicine, and despite all the efforts to diagnose MCD at an early stage, the ideal diagnostic approach for consistently and accurately determining the presence of MCD has not been established. Radiography has been used as the first line diagnostic modality to diagnose MCD, but most of the time, secondary changes, such as osteophytosis, ulnar subtrochlear sclerosis (STS), and blunting or blurring of the cranial edge of the MCP, have been used to determine the likelihood of MCD (Keller et al., 1997; Hornof et al., 2000; Mason et al., 2002). The use of computed tomography (CT) alleviates the problems of superimposition, which improves the examination of the lateral aspect of the MCP. A wide spectrum of CT findings has been reported in dogs with MCD (Reichle and Snaps, 1999; Reichle et al., 2000; Gemmill, 2004; Holsworth et al., 2005; Gemmill et al., 2006; Kramer et al., 2006; Samoy et al., 2006; Wagner et al., 2007). However, the use of CT has been restricted by the fact that animals have to be anesthetized for the examination. In addition, other modalities such as MRI and scintigraphy have been implied.

The discussion of the studies reported in this thesis is discussed into two major parts: the diagnostic aspect and the etiopathogenesis aspect.

Diagnostic aspect

In this thesis, we provide new breed-specific information regarding MCD from the diagnostic point of view. The radiographic, CT, and arthroscopic findings in Labrador retrievers diagnosed with MCD in different age groups were described in Chapter 3. Radiographically, STS and blurring of the cranial edge of the medial coronoid process were common findings in our patient groups (≤ and >12 months of age during the first complaint of lameness). Meanwhile, fragmentation of the MCP was the most common finding on computed tomography in both age groups. Our findings showed the less severe disease manifestations (e.g. ulnar subtrochlear sclerosis) in the Labrador retrievers referred at an age >12 months in comparison with Labrador retrievers referred at an age ≤12 months, and these findings were in agreement with previous publications (Meyer-Lindenberg et al., 2002; van Bruggen et al., 2010). Furthermore, arthroscopically, osteochondromalacia was the most common finding in dogs >12 months of age in comparison with displaced fragment in dogs ≤12 months of age. Thus, we are tempted to conclude that different manifestations of MCD might have occurred in dogs at different age stages. In the same chapter, radiographic evaluated ulnar STS was strongly correlated with CT measured ulnar STS and we demonstrated the sclerosis of the intramedullary bone cavity by comparing ulnas with and without sclerosis and without interference from periarticular osteophytosis.

In Chapter 4, we followed the postnatal development of the elbow joints of the

Labrador retrievers with radiography and computed tomography with incipient MCD. In contrast with the advanced clinical cases, radiography failed to detect any changes (0% sensitivity). The earliest signs of MCD were found with CT at the age of 14 weeks with a mineralized bone fragment at the base of the MCP, not extending towards the apex of the MCP. This finding differed from the commonly reported CT findings, where the fragmentation of the MCP is distinctly separated from the rest of the subchondral bone at the level of the apex of the MCP (Reichle et al., 2000; Moores et al., 2008; Groth et al., 2009; Lappalainen et al., 2009). In our longitudinal study, there was absence of both blurring and blunting of the cranial edge of MCP and of ulnar STS. Therefore, both findings should be regarded as a consequence of MCD and not as the primary cause.

Different from the findings obtained from clinical patients in Chapter 3, ulnar STS was not detected in the young Labrador retrievers in Chapter 4. In human osteoarthritic research (Dequeker et al., 1995; Felson and Neogi, 2004), it has been speculated that subchondral bone sclerosis may be the primary cause triggering osteoarthritis. In parallel, it was suggested that MCD is caused by inappropriate thickened and more rigid subchondral bone which in combination with repetitive microtrauma during the joint movement eventually lead to cartilage lesion (Temwichitr et al., 2010). We found the different scenario in our longitudinal study in MCD-prone Labrador retrievers showing the development of MCD. Most likely, ulnar STS detected in the intramedullary bone cavity was the consequence of the disease and bone remodeling, as a product of structural-functional relationship which aims at repairing the micro-damage by removing the damaged bone and replacing it with new bone deposition (Kawcak et al., 2001). Histologically, subchondral bone density has been characterized as increasing subchondral plate thickness and demonstrated as a progressive osteoarthritis changes after the anterior cruciate ligament transection in the dog (Brandt et al., 1991). One might argue that the change in subchondral bone might be beyond the detection threshold of radiography and CT because the assessment of ulnar STS was done subjectively. However, in the micro-computed tomographic (microCT) study in Chapter 6, we found no evidence of subchondral bone osteoporosis or osteosclerosis at the MCP in the same group of young Labrador retrievers. The combination of the results in Chapter 4 and 6 indicates that sclerosis is a repair mechanism instead of causing the MCD.

In Chapter 4, both radiography and CT failed to show signs of radioulnar joint incongruity (RUI). Before proceeding with the necropsy examination, two intramedullary pins were inserted horizontally across the radius and ulna in order to secure the forelimb in a position resembling the normal standing angle (135°), before soaking the specimen in the formalin solution. During necropsy examination, we found an atypical appearance of RUI in one of the radioulnar joints in a 15-week-old dog, which clearly showed a step of

approximately 1.5 mm, with a steeper downward slope of the MCP against the proximal radius, resulting in a loss of contact between the base of the MCP and the radial head. This particular joint was diagnosed MCD negative with radiography and CT. The appearance of RUI in this dog differed from that described in earlier reports, which stated that RUI is more likely to be present at the apex of the MCP rather than at the base of MCP (Gemmill et al., 2005).

The combination of necropsy and microCT findings of the MCP in Chapter 4 revealed that in dogs younger than 18 weeks MCD was only manifest as a lesion of the subchondral bone. This indicates that MCD started in the deeper layer of the articular cartilage or even in the subchondral bone, as suggested before (Danielson et al., 2006) rather than in the superficial articular cartilage layer. This finding was confirmed in the histological study as described in Chapter 8. In addition, we observed the consistent close contact between the base of the MCP and the radial head in the apparent congruent radioulnar joints. Its importance will be highlighted and discussed together with the findings presented in Chapter 8.

As was shown in the study described in Chapter 4, radiography is not an optimal tool to diagnose incipient MCD, in which the secondary changes are absent. Fissures and fragmentation of the MCP can occur without significant lameness and abnormal findings during physical examination. Hence, it is difficult to diagnose incipient MCD. However, the recognition of incipient MCD is possible with CT.

With the high incidence of MCD in Labrador retrievers, there is a need to develop a non-invasive test which is easy to perform and has a high sensitivity in an early stage of the disease. Referring to previous studies (Hayashi et al., 2009; Prink et al., 2010), we investigated the potential of a biomarker, namely, Col2-3/4C$_{long\ mono}$ in the plasma and synovial fluid from elbow joints of Labrador puppies to diagnose incipient MCD. Our results, as described in Chapter 5, revealed that this biomarker is not clinical useful in detecting incipient MCD in growing dogs. MCD is a developmental skeletal disease that occurs in animals still in their active growth phase, with the articular cartilage and subchondral bone in an active modeling stage. Type II collagen denaturation and cleavage is present in case of pathological degeneration of joint cartilage, but also in case of normal skeletal modeling (Donabédian et al., 2008). In the same chapter, we demonstrated that there was no influence of dietary cartilage food supply on the type II collagen cleavage in the plasma and urine.

In dogs, MCD is often diagnosed at the advanced stage. It is important to accurately screen the elbow joints and to detect the problem at the early stage of the disease before it progresses into severe osteoarthritis. In humans, CT and MRI following the intra-articular administration of contrast medium have been described for the examination

of joints (Waldt et al., 2005; Siebelt et al., 2011), but the smaller size of the joints in dogs and the thinner cartilage make these techniques less applicable in dogs. We attempted to diagnose fragmentation of the MCP using CT-arthrography but was not successful due to inadequate distribution of contrast medium in the joint space between the humeral trochlea and the MCP (Personal communication, Prof. H. van Bree). Better results might be obtained with high field (≥ 3 Tesla) MRI scanners (Wucherer et al., 2012).

Etiopathogenic aspect

The studies in Chapter 6, 7 and 8 were designed in an attempt to investigate, in depth, the possible pathogeneses of MCD. In Chapter 6 by using the non-destructive equilibrium partitioning of an ionic contrast agent with microCT, we showed the early degeneration of articular cartilage in dogs with incipient MCD, without changes in MCP's subchondral bone density or remodeling. A reduced content of glycosaminoglycan (GAG) in the cartilage matrix has been reported in MCPs obtained from clinically lame, mature dogs with MCD (Goldhammer et al., 2009). In our study, we demonstrated that a reduced GAG content of cartilage occurs in a very early stage of MCD, even without evidence of clinical signs or abnormalities during orthopaedic examination. Due to the fact that this study was performed at a single time point after euthanasia, we cannot conclude that MCD develops primarily as a result of changes in articular cartilage, or that the GAG loss we demonstrated was a consequence of MCD.

In the EPIC-microCT study, we did not observe any parameters of subchondral bone micro-architecture affected by MCD. All the changes in the studied parameters, namely, the ratio of bone volume over tissue volume (BV/TV), bone surface density (BS/TV), bone surface to volume ratio (BS/BV), trabecular thickness (Tb.Th; mm), size of marrow cavities described by trabecular spacing (Tb.Sp; mm), and structural model index (SMI), were only age- and weight- dependent. Osteoporosis has been suggested as one of the etiopathogeneses leading to MCD with the weaker axial border of the MCP being predisposed to the development of the microcracks (Burton et al., 2010) and this has been reported on basis of histological examination of diseased MCPs by others (Danielson et al., 2006; Goldhammer et al., 2009). The different findings in our study can be explained by the difference in the stage of the disease and we analysed the MCP as a whole structure rather than dividing it into an axial and abaxial part. As stated in the diagnostic point of view, combined with the absence of ulnar STS noticed radiographically as described in Chapter 4, we conclude that it is unlikely that abnormalities in the subchondral bone are the primary cause of the MCD.

Although elbow joint disparity and limb angular deformities are more common in

other breeds, it had been reported in Labrador retrievers with MCD (Ubbink et al., 1999; Malm et al., 2008; Lavrijsen et al., 2012; Samoy et al., 2012). The results in Chapter 7 demonstrated that there were no significant differences regarding radial alignment quantification with the Center of Rotation of Angulation Methodology (CORA), radioulnar length ratio and development of secondary ossification centers in the elbow joints in dogs with and without MCD during the active growth period between 6 and 17 weeks of age. Therefore, we conclude that it is unlikely that the postnatal development of the antebrachium and of the elbow joints in Labrador retrievers is related to the development of the MCD. Furthermore, with radiography and CT, no radioulnar incongruity (RUI) during the growth period was demonstrated, despite the fact that one of the elbow joints proved to be false negative during necropsy examination and showed atypical RUI. However, there were several limitations in this study that should be considered. Both radiography and CT used in this study were unable to assess cartilage integrity. In addition, the animals were not in weight bearing position during the radiographical and CT examination (De Rycke et al., 2002; Mason et al., 2002). Therefore, pathological changes in the articular cartilage layer could not be assessed, nor could the physiological incongruity of the elbow joints during movement. It is possible that the step defect or length differences between the radius and ulna were too small and beyond the detection threshold of radiography and CT, and thus could not be detected.

In study I of Chapter 8, the results of the histological examination provided convincing evidence that delayed endochondral ossification plays a role in the development of MCD, by demonstrating the retained cartilage at the lateral aspect of the MCP (latMCP) at the level of the base of the MCP. There was a relatively large area of hyaline cartilage with focal areas of empty lacunae, consistent with cell death at the site where in normal dogs ossified trabecular bone was found, at the calcifying cartilage zone of the latMCP. Notably, a cleft separating the retained hyaline cartilage from underlying subchondral bones was present. Cleft formation was prominent in dogs older than 18 weeks, with active granulation tissue in the adjacent cleft region. The presence of extensive vascular distribution at the retained hyaline cartilage and edges of clefts in the MCD positive group indicates the involvement of a healing process. Based on the chondrocytes morphology, findings in Chapter 8 indicate a delay in the calcification process, rather than a disturbance in differentiation of the proliferating chondrocytes (transitional zone) into hypertrophic chondrocytes (radial zone). The persistence of retained cartilage provides a weak point at the cartilage-bone interface, which forms the initiation of cleft formation due to biomechanical forces.

Disturbance of endochondral ossification has been widely described under an umbrella term, osteochondrosis (OC), which is generally referring to the lesions at the

articular cartilage and physeal growth plate in many species, including cattle (Wegener and Heje, 1992), horse (Olstad et al., 2008; Van Grevenhof et al., 2009; Olstad et al., 2011), pigs (Hill et al., 1984; Ytrehus et al., 2004), and dogs (Tirgari, 1974; Grøndalen and Grøndalen, 1981; Olsson, 1981; Goedegebuure and Hazewinkel, 1986; Tryfonidou et al., 2003; Kuroki et al., 2005; Wolschrijn et al., 2005; Mathis et al., 2009). Our findings were, however, different from the described OC findings reported in other species. The lesion does not seem to appear at the articular cartilage and proceed into the deeper subchondral bone layer as reported, but rather originates at the deeper layer of the articular cartilage at the calcifying zone. In horses, a variety of histological lesions has been reported, mainly describing the disrupting transition of the chondrocytes in the proliferating zone into hypertrophic chondrocytes and presence of a chondronecrotic area predominantly in the hypertrophic zones (Henson et al., 1997). Similar histological description also applied to the OC lesions in cattle and pigs (Wegener and Heje, 1992; Ytrehus et al., 2004). Instead of these described lesions in *osteochondrosis latens*, which is characterised by focal disturbance of endochondral ossification confined to the lesion at the epiphyseal cartilage (Ytrehus et al., 2007), our findings shared certain degree of similarities to *osteochondrosis manifesta* lesions, where an area of cartilage necrosis has been found surrounded by subchondral bone. In a previous study in four to six months old pigs (Reiland, 1978), the osteochondrotic articular cartilage had a degenerative appearance at the basal layers of the cartilage (calcifying zone) with a large defect into the subchondral bone. In slightly older animals (more than 6 months of age) crack formation was found in the osteochondral junction at the degenerated region that extended into the cartilage surface. Our findings in Labrador retrievers at different ages resembled the described morphological findings in pigs (Reiland, 1978).

The first available histological findings of MCD related the disease to OC was reported in 1974 in a bone fragment removed from an abnormal MCP. The histological result showed a mass homogenous substance without the presence of chondrocytes at the articular cartilage layer and the underlying subchondral bone had a necrotic appearance, with reduced size of osteoblastic cells and pyknotic nuclei (Tirgari, 1974). However, this information was only available in writing without any histological figures. Thus, comparison with our findings is not possible. Grøndalen and Grøndalen (1981) and Wolschrijn et al. (2005) described OC lesions in the MCP as degenerated hyaline cartilage found at both edges of the fissure line and degeneration of the deeper layer of the joint cartilage at the humeral contact surface, which is not exactly at the latMCP as we found. Our findings were representative of the incipient MCD since all the diseased MCPs were free from the evidence of secondary degenerative changes and the dogs showed no lameness, nor abnormalities during the orthopaedic examination. With the help of the high resolution

microCT, we had the advantage to be able to identify the lesions before cutting at the microtome and slice the specimen at the more accurate site for the histological study.

In the study II of Chapter 8, we reported that cartilage canals containing vascular networks were no longer present in the articular cartilage at the age of 12 weeks and older in MCD positive and negative dogs. A relationship has been reported between the regression of the cartilage canals and the development of OC (Carlson et al., 1991; Carlson et al., 1995; Ekman and Carlson, 1998; Ytrehus et al., 2004; Ytrehus et al., 2007; Olstad et al., 2008). The widely accepted theory is that with the chondrification, areas of articular cartilage receive inadequate blood supply which subsequently leads to the formation of an area of ischemic necrotic cartilage. In our study, the time lag between the chondrification of the cartilage canals till the first detectable MCD lesions on CT was at least two weeks and whether or not the chondrification process contributed to MCD is still unclear.

Despite of the extensive research in OC, its pathogenic mechanism still remains uncertain. It is known to be complex and multifactorial, and from our studies, it is unlikely that the gross lesions of canine MCD are arising from solely one pathogenic mechanism. In Chapter 7, we demonstrated from the quantitative radiographical and CT studies that it is unlikely that the postnatal development of the antebrachium and of the elbow joints in Labrador retrievers is related to the development of MCD. Although it remains unclear whether the depletion of GAG as described in Chapter 6 was a cause or a consequence of MCD, GAG loss definitely affects the proper compressive and friction properties of the articular cartilage. The dysfunction of the articular cartilage might eventually lead to crack formation in the osteochondral junction at the latMCP. Although the concrete evidence of delayed endochondral ossification involvement in the development of MCD as reported in Chapter 8, further investigation of the pathogenesis of this disturbance is warranted. From the necropsy examination in Chapter 4, it appears that the consistent close contact between the base of the MCP and the radial head in the apparent congruent radioulnar joint might be the cornerstone in the development of MCD. Carter and Wong (1988) proposed a theory associating the intermittently applied shear stresses promoting endochondral ossification, and intermittent applied hydrostatic compression inhibiting or preventing cartilage degeneration and ossification, by using the finite elements analysis on a computed model. Further biomechanical studies in the elbow joint should focus on the cause of the delayed endochondral ossification of the latMCP.

Main findings of this thesis

The main findings of the research conducted can be summarized as follows:

- Out of the 14 purpose bred Labrador retrievers from the MCD affected dam and sires, 50% were considered as MCD positive based on the combined results of the necropsy and microCT examination; 86% (six out of seven dogs) of the MCD positive dogs were affected bilaterally.

- Incipient MCD could be detected on CT, before the clinical signs manifest, as early as 14 weeks of age with a mineralized bone fragment at the base of the MCP, not extending towards the apex of the MCP. Computed tomography proved to be more sensitive (30.8%) than radiography (0%) in detecting early MCD.

- Ulnar subtrochlear sclerosis (STS) is most likely the consequence of MCD and not the primary cause. The remodeling of the intramedullary cavity might be related to new bone deposition. The absence of ulnar STS on radiograph should not exclude MCD. A thorough physical examination and history remain essential to the diagnosis.

- In the advanced stage of MCD, the radiographic diagnosis of MCD is mainly based on the secondary regenerative and degenerative changes such as ulnar STS, blurring or blunting of the cranial edge of the medial coronoid process, and formation of periarticular osteophytes. At the same time, recognition of the primary lesion i.e., fragmentation of the MCP, was the main finding on computed tomography. Manifestations of MCD may be different in different age groups and more severe in dogs presented with lameness at an age ≤12 months than dogs that first show lameness at an age >12 months.

- There was a significant depletion of GAG from articular cartilage in an early stage of MCD as reflected in the mean microCT x-ray attenuation of segmented articular cartilage, without significant changes in the MCP's subchondral bone density and remodelling. The latter was shown as an age- and weight- dependency process. Lack of significant changes in MCP's subchondral bone density between MCD positive and MCD negative dogs suggested that MCD might have started at the deeper layer of the articular cartilage and proceed towards the underlying subchondral bone.

- MCD in Labrador retrievers is most likely the product of delayed endochondral ossification at the lateral aspect of the MCP (latMCP) at the level of the base of the MCP, with focus on the delay in calcification of the calcifying zone without there being concurrent abnormalities in the superficial layers of the joint cartilage. The persistence of retained cartilage provides a weak point at the cartilage-bone interface, where biomechanical forces may initiate cleft formation.

- Cartilage canals containing vascular networks were no longer present in articular cartilage in all dogs of 12 weeks and older. However, from our studies no conclusions can be drawn on the role of this chondrification process in the development of MCD.

References

Brandt, K.D., Myers, S.L., Burr, D., Albrecht, M., 1991. Osteoarthritic changes in canine articular cartilage, subchondral bone, and synovium fifty-four months after transection of the anterior cruciate ligament. Arthritis & Rheumatism 34, 1560-1570.

Breit, S., Künzel, W., Seiler, S., 2004. Variation in the ossification process of the anconeal and medial coronoid processes of the canine ulna. Research in Veterinary Science 77, 9-16.

Breit, S., Kunzel, W., Seiler, S., 2005. Postnatal modelling of the humeroantebrachial contact areas of radius and ulna in dogs. Anatomia Histologia Embryologia 34, 258-64.

Breit, S., Kunzel, W., Seiler, S., 2006. On the weight-bearing function of the medial coronoid process in dogs. Anatomia Histologia Embryologia 35, 7-12.

Burton, N.J., Perry, M.J., Fitzpatrick, N., Owen, M.R., 2010. Comparison of bone mineral density in medial coronoid processes of dogs with and without medial coronoid process fragmentation. American Journal of Veterinary Research 71, 41-46.

Carlson, C.S., Cullins, L.D., Meuten, D.J., 1995. Osteochondrosis of the articular-epiphyseal cartilage complex in young horses: evidence for a defect in cartilage canal blood supply. Veterinary Pathology 32, 641-647.

Carlson, C.S., Meuten, D.J., Richardson, D.C., 1991. Ischemic necrosis of cartilage in spontaneous and experimental lesions of osteochondrosis. Journal of Orthopaedic Research 9, 317-329.

Carter, D.R., Wong, M., 1988. Mechanical stresses and endochondral ossification in the chondroepiphysis. Journal of Orthopaedic Research 6, 148-154.

Cuddy, L.C., Lewis, D.D., Kim, S.E., Conrad, B.P., Banks, S.A., Horodyski, M.B., Fitzpatrick, N., Pozzi, A., 2012. Contact mechanics and three-dimensional alignment of normal dog elbows. Veterinary Surgery 41, 818-828.

Danielson, K.C., Fitzpatrick, N., Muir, P., Manley, P.A., 2006. Histomorphometry of fragmented medial coronoid process in dogs: a comparison of affected and normal coronoid processes. Veterinary Surgery 35, 501-509.

De Rycke, L.M., Gielen, I.M., van Bree, H., Simoens, P.J., 2002. Computed tomography of the elbow joint in clinically normal dogs. American Journal of Veterinary Research 63, 1400-1407.

Dequeker, J., Mokassa, L., Aerssens, J., 1995. Bone density and osteoarthritis. The Journal of Rheumatology.Supplement 43, 98-100.

Donabédian, M., Weeren, P.R., Perona, G., Fleurance, G., Robert, C., Léger, S., Bergero, D., Lepage, O., Martin-Rosset, W., 2008. Early changes in biomarkers of skeletal metabolism and their association to the occurrence of osteochondrosis (OC) in the horse. Equine Veterinary Journal 40, 253-259.

Ekman, S., Carlson, C.S., 1998. The pathophysiology of osteochondrosis. Veterinary Clinics of North America: Small Animal Practice 28, 17-32.

Felson, D.T., Neogi, T., 2004. Osteoarthritis: is it a disease of cartilage or of bone? Arthritis & Rheumatism 50, 341-344.

Fitzpatrick, N., Yeadon, R., 2009. Working algorithm for treatment decision making for developmental disease of the medial compartment of the elbow in dogs. Veterinary Surgery 38, 285-300.

Fox, S.M., Bloomberg, M.S., Bright, R.M., 1983. Developmental anomalies of the canine elbow. The Journal of the American Animal Hospital Association 19, 605-615.

Gemmill, T., 2004. Completing the picture: use of CT to investigate elbow dysplasia. Journal of Small Animal Practice 45, 429-430.

Gemmill, T.J., Hammond, G., Mellor, D., Sullivan, M., Bennett, D., Carmichael, S., 2006. Use of reconstructed computed tomography for the assessment of joint spaces in the canine elbow. Journal of Small Animal Practice 47, 66-74.

Gemmill, T.J., Mellor, D.J., Clements, D.N., Clarke, S.P., Farrell, M., Bennett, D., Carmichael, S., 2005. Evaluation of elbow incongruency using reconstructed CT in dogs suffering fragmented coronoid process. Journal of Small Animal Practice 46, 327-333.

Goedegebuure, S., Hazewinkel, H., 1986. Morphological findings in young dogs chronically fed a diet containing excess calcium. Veterinary Pathology 23, 594-605.

Goldhammer, M.A., Smith, S.H., Fitzpatrick, N., Clements, D.N., 2009. A comparison of radiographic, arthroscopic and histological measures of articular pathology in the canine elbow joint. The Veterinary Journal 186, 96-103.

Grøndalen, J., Grøndalen, T., 1981. Arthrosis in the elbow joint of young rapidly growing dogs. V. A pathoanatomical investigation. Nordisk Veterinaermedicin 33, 1-16.

Groth, A.M., Benigni, L., Moores, A.P., Lamb, C.R., 2009. Spectrum of computed tomographic findings in 58 canine elbows with fragmentation of the medial coronoid process. Journal of Small Animal Practice 50, 15-22.

Guthrie, S., Plummer, J.M., Vaughan, L.C., 1992. Post natal development of the canine elbow joint: a light and electron microscopical study. Research in Veterinary Science 52, 67-71.

Hayashi, K., Kim, S.U.N.Y., Lansdowne, J.L., Kapatkin, A., Dejardin, L.M., 2009. Evaluation of a collagenase generated osteoarthritis biomarker in naturally occurring canine cruciate disease. Veterinary Surgery 38, 117-121.

Henson, F., Davies, M., Jeffcott, L., 1997. Equine dyschondroplasia (osteochondrosis)-histological findings and type VI collagen localization. The Veterinary Journal 154, 53-62.

Hill, M.A., Ruth, G.R., Hilley, H.D., Hansgen, D.C., 1984. Dyschondroplasias, including osteochondrosis, in boars between 25 and 169 days of age: histologic changes. American Journal of Veterinary Research 45, 903-916.

Holsworth, I.G., Wisner, E.R., Scherrer, W.E., Filipowitz, D., Kass, P.H., Pooya, H., Larson, R.F., Schulz, K.S., 2005. Accuracy of computerized tomographic evaluation of canine radio-ulnar incongruence in vitro. Veterinary Surgery 34, 108-113.

Hornof, W.J., Wind, A.P., Wallack, S.T., Schulz, K.S., 2000. Canine elbow dysplasia. The early radiographic detection of fragmentation of the coronoid process. Veterinary Clinics of North America: Small Animal Practice 30, 257-266.

Hulse, D., Young, B., Beale, B., Kowaleski, M., Vannini, R., 2010. Relationship of the biceps-brachialis complex to the medial coronoid process of the canine ulna. Veterinary and Comparative Orthopaedics and Traumatology 23, 173-176.

Janarv, P., Hesser, U., Hirsch, G., 1997. Osteochondral lesions in the radiocapitellar joint in the skeletally immature: radiographic, MRI, and arthroscopic findings in 13 consecutive cases. Journal of Pediatric Orthopaedics 17, 311-314.

Kawcak, C.E., McIlwraith, C.W., Norrdin, R., Park, R., James, S., 2001. The role of subchondral bone in joint disease: a review. Equine Veterinary Journal 33, 120-126.

Keller, G.G., Kreeger, J.M., Mann, F.A., Lattimer, J.C., 1997. Correlation of radiographic, necropsy and histologic findings in 8 dogs with elbow dysplasia. Veterinary Radiology & Ultrasound 38, 272-276.

Kramer, A., Holsworth, I.G., Wisner, E.R., Kass, P.H., Schulz, K.S., 2006. Computed tomographic evaluation of canine radioulnar incongruence in vivo. Veterinary Surgery 35, 24-29.

Kuroki, K., Cook, J.L., Stoker, A.M., Turnquist, S.E., Kreeger, J.M., Tomlinson, J.L., 2005. Characterizing osteochondrosis in the dog: potential roles for matrix metalloproteinases and mechanical load in pathogenesis and disease progression. Osteoarthritis and Cartilage 13, 225-234.

Lappalainen, A.K., Molsa, S., Liman, A., Laitinen-Vapaavuori, O., Snellman, M., 2009. Radiographic and computed tomography findings in Belgian shepherd dogs with mild elbow dysplasia. Veterinary Radiology & Ultrasound 50, 364-369.

Lavrijsen, I.C., Heuven, H.C., Voorhout, G., Meij, B.P., Theyse, L.F., Leegwater, P.A., Hazewinkel, H.A., 2012. Phenotypic and genetic evaluation of elbow dysplasia in Dutch Labrador retrievers, Golden retrievers, and Bernese Mountain Dogs. The Veterinary Journal 193, 486-492.

Malm, S., Fikse, W.F., Danell, B., Strandberg, E., 2008. Genetic variation and genetic trends in hip and elbow dysplasia in Swedish Rottweiler and Bernese Mountain Dog. Journal of Animal Breeding and Genetics 125, 403-412.

Mason, D.R., Schulz, K.S., Samii, V.F., Fujita, Y., Hornof, W.J., Herrgesell, E.J., Long, C.D., Morgan, J.P., Kass, P.H., 2002. Sensitivity of radiographic evaluation of radio-ulnar incongruence in the dog in vitro. Veterinary Surgery 31, 125-132.

Mathis, K.R., Havlicek, M., Beck, J.B., Eaton-Wells, R.D., Park, F.M., 2009. Sacral osteochondrosis in two German Shepherd Dogs. Australian Veterinary Journal 87, 249-252.

Meyer-Lindenberg, A., Langhann, A., Fehr, M., Nolte, I., 2002. Prevalence of fragmented medial coronoid process of the ulna in lame adult dogs. The Veterinary Record 151, 230-234.

Moores, A.P., Benigni, L., Lamb, C.R., 2008. Computed tomography versus arthroscopy for detection of canine elbow dysplasia lesions. Veterinary Surgery 37, 390-398.

Murphy, S.T., Lewis, D.D., Shiroma, J.T., Neuwirth, L.A., Parker, R.B., Kubilis, P.S., 1998. Effect of radiographic positioning on interpretation of cubital joint congruity in dogs. American Journal of Veterinary Research 59, 1351-1357.

Olsson, S.-E., 1981. Pathophysiology morphology, and clinical signs of osteochondrosis in the dog. In: Pathophysiology in Small Animal Surgery, First Ed. Lea & Febiger, Philadelphia, USA, pp. 604-617.

Olstad, K., Cnudde, V., Masschaele, B., Thomassen, R., Dolvik, N.I., 2008. Micro-computed tomography of early lesions of osteochondrosis in the tarsus of foals. Bone 43, 574-583.

Olstad, K., Ytrehus, B., Ekman, S., Carlson, C.S., Dolvik, N.I., 2008. Epiphyseal cartilage canal blood supply to the tarsus of foals and relationship to osteochondrosis. Equine Veterinary Journal 40, 30-39.

Olstad, K., Ytrehus, B., Ekman, S., Carlson, C.S., Dolvik, N.I., 2011. Early lesions of articular osteochondrosis in the distal femur of foals. Veterinary Pathology 48, 1165-1175.

Preston, C.A., Schulz, K.S., Taylor, K.T., Kass, P.H., Hagan, C.E., Stover, S.M., 2001. In vitro experimental study of the effect of radial shortening and ulnar ostectomy on contact patterns in the elbow joint of dogs. American Journal of Veterinary Research 62, 1548-1556.

Prink, A., Hayashi, K., KIM, S.U.N.Y., Kim, J., Kapatkin, A., 2010. Evaluation of a collagenase generated osteoarthritis biomarker in the synovial fluid from elbow joints of dogs with medial coronoid disease and unaffected dogs. Veterinary Surgery 39, 65-70.

Reichle, J.K., Park, R.D., Bahr, A.M., 2000. Computed tomographic findings of dogs with cubital joint lameness. Veterinary Radiology & Ultrasound 41, 125-130.

Reichle, J.K., Snaps, F., 1999. The elbow. Clinical Techniques in Small Animal Practice 14, 177-186.

Reiland, S., 1978. Morphology of osteochondrosis and sequelae in pigs. Acta Radiologica.Supplementum 358, 45-90.

Samoy, Y., Van Vynckt, D., Gielen, I., van Bree, H., Duchateau, L., Van Ryssen, B., 2012. Arthroscopic findings in 32 joints affected by severe elbow incongruity with concomitant fragmented medial coronoid process. Veterinary Surgery 41, 355-361.

Samoy, Y., Van Ryssen, B., Gielen, I., Walschot, N., van Bree, H., 2006. Review of the literature: elbow incongruity in the dog. Veterinary and Comparative Orthopaedics and Traumatology 19, 1-8.

Siebelt, M., van Tiel, J., Waarsing, J., Piscaer, T., van Straten, M., Booij, R., Dijkshoorn, M., Kleinrensink, G., Verhaar, J., Krestin, G., 2011. Clinically applied CT arthrography to measure the sulphated glycosaminoglycan content of cartilage. Osteoarthritis and Cartilage 19, 1183-1189.

Temwichitr, J., Leegwater, P.A., Hazewinkel, H.A., 2009. Fragmented coronoid process in the dog: A heritable disease. The Veterinary Journal 185, 123-129 .

Tirgari, M., 1974. Clinical radiographical and pathological aspects of arthritis of the elbow joint in dogs. Journal of Small Animal Practice 15, 671-679.

Tryfonidou, M.A., Holl, M.S., Vastenburg, M., Oosterlaken-Dijksterhuis, M.A., Birkenhager-Frenkel, D.H., van den Brom, W.E., Hazewinkel, H.A., 2003. Hormonal regulation of calcium homeostasis in two breeds of dogs during growth at different rates. Journal of Animal Science 81, 1568-1580.

Ubbink, G., Hazewinkel, H., Van de Broek, J., Rothuizen, J., 1999. Familial clustering and risk analysis for fragmented coronoid process and elbow joint incongruity in Bernese Mountain Dogs in The Netherlands. American Journal of Veterinary Research 60, 1082-1087.

van Bruggen, L.W., Hazewinkel, H.A., Wolschrijn, C.F., Voorhout, G., Pollak, Y.W., Barthez, P.Y., 2010. Bone scintigraphy for the diagnosis of an abnormal medial coronoid process in dogs. Veterinary Radiology & Ultrasound 51, 344-348.

Van Grevenhof, E.M., Ducro, B.J., Van Weeren, P.R., Van Tartwijk, J.M., Van den Belt, A.J., Bijma, P., 2009. Prevalence of various radiographic manifestations of osteochondrosis and their correlations between and within joints in Dutch warmblood horses. Equine Veterinary Journal 41, 11-16.

Vermote, K.A., Bergenhuyzen, A.L., Gielen, I., van Bree, H., Duchateau, L., Van Ryssen, B., 2009. Elbow lameness in dogs of six years and older. Veterinary and Comparative Orthopaedics and Traumatology 23, 43-50.

Wagner, K., Griffon, D.J., Thomas, M.W., Schaeffer, D.J., Schulz, K., Samii, V.F., Necas, A., 2007. Radiographic, computed tomographic, and arthroscopic evaluation of experimental radio-ulnar incongruence in the dog. Veterinary Surgery 36, 691-698.

Waldt, S., Bruegel, M., Ganter, K., Kuhn, V., Link, T., Rummeny, E., Woertler, K., 2005. Comparison of multislice CT arthrography and MR arthrography for the detection of articular cartilage lesions of the elbow. European Radiology 15, 784-791.

Wegener, K.M., Heje, N.I., 1992. Dyschondroplasia (osteochondrosis) in articular-epiphyseal cartilage complexes of three calves from 24 to 103 days of age. Veterinary Pathology 29, 562-563.

Wind, A., 1986a. Elbow incongruity and developmental elbow diseases in the dog: part I. Journal of the American Animal Hospital Association 22, 711-724.

Wind, A.P., Packard, M.E., 1986b. Elbow incongruity and developmental elbow diseases in the dog: part II. Journal of the American Veterinary Medical Association 22, 725-730.

Wolschrijn, C.F., Gruys, E., van der Wiel, C.W., Weijs, W.A., 2008. Cartilage canals in the medial coronoid process of young Golden retrievers. The Veterinary Journal 176, 333-337.

Wolschrijn, C.F., Gruys, E., Weijs, W.A., 2005. Microcomputed tomography and histology of a fragmented medial coronoid process in a 20-week-old golden retriever. Veterinary Surgery 157, 383-386.

Wolschrijn, C.F., Weijs, W.A., 2004. Development of the trabecular structure within the ulnar medial coronoid process of young dogs. The Anatomical Record. Part A, Discoveries in Molecular, Cellular, and Evolutionary Biology 278, 514-519.

Wolschrijn, C.F., Weijs, W.A., 2005. Development of the subchondral bone layer of the medial coronoid process of the canine ulna. The Anatomical Record. Part A, Discoveries in Molecular, Cellular, and Evolutionary Biology 284, 439-445.

Wucherer, K.L., Ober, C.P., Conzemius, M.G., 2012. The use of delayed gadolinium enhanced magnetic resonance imaging of cartilage and T2 mapping to evaluate articular cartilage in the normal canine elbow. Veterinary Radiology & Ultrasound 53, 57-63.

Ytrehus, B., Carlson, C.S., Ekman, S., 2007. Etiology and pathogenesis of osteochondrosis. Veterinary Pathology 44, 429-448.

Ytrehus, B., Ekman, S., Carlson, C.S., Teige, J., Reinholt, F.P., 2004. Focal changes in blood supply during normal epiphyseal growth are central in the pathogenesis of osteochondrosis in pigs. Bone 35, 1294-1306.

Chapter 10

Summary, Samenvatting & Ringkasan

Summary

Medial coronoid disease (MCD), the most frequently diagnosed component of elbow dysplasia in Labrador retrievers, has been the subject of many publications over the past four decades. The first signs of lameness related to MCD can occur as early as three months of age, as late as six years, or even older. The most commonly presented clinical signs are lameness, a stiff or stilted gait due to shortened steps, and slight supination and abduction of the affected forelimb. During orthopaedic examination, joint effusion, crepitus, and pain reaction during joint manipulation can be observed. In the Labrador retriever, the main breed for guide dogs for the blind and assistance dogs for the disabled, MCD is a heritable disease of major concern.

Different aspects of MCD are reviewed in **Chapter 2**, such as the normal postnatal development of the medial coronoid process (MCP), the different disease manifestations of MCD, commonly accepted hypotheses regarding the etiopathogenesis of MCD, and techniques used to diagnose MCD. Despite extensive research, there is no diagnostic tool to definitively diagnose or exclude MCD yet, and its etiopathogenesis has still to be elucidated.

The first aim of this thesis was to study breed-specific features of advanced and incipient MCD in Labrador retrievers using radiography, computed tomography (CT), and examination at surgery or necropsy.

In the studies described in **Chapter 3,** a group of 31 Labrador retrievers, suffering from advanced MCD, was investigated. In this stage the radiographic diagnosis is usually based on secondary regenerative and degenerative changes such as ulnar subtrochlear sclerosis, blurring or blunting of the cranial edge of the MCP, and peri-articular osteophytes. Fragmentation of the MCP was the most common CT finding. In dogs with the first complaints of lameness at a young age, i.e. ≤12 months, a displaced fragment of the MCP was the most common arthroscopic finding. Osteochondromalacia was the most common arthroscopic finding in dogs with the first complaints of lameness starting at a mature age, i.e. >12 months. There were distinctly different disease manifestations of MCD in these two age groups and without knowing the exact etiopathogenesis, the possibility that there are two different disease mechanisms involved in these age groups cannot be excluded. Ulnar subtrochlear sclerosis is most likely the result and not the cause of MCD, and is based on an increased bone density in the medullary cavity of the ulna. Absence of this sclerosis cannot

be used to exclude MCD. A thorough physical examination and history remain essential to the diagnosis.

In **Chapter 4,** the development of MCD in two litters of purpose bred Labrador retrievers, originating from MCD-affected dam and sires, was studied longitudinally. Fifty per cent of this offspring (7 out of 14 dogs) were considered to be MCD positive based on the combined results of necropsy and microCT examination. Eighty-six per cent (six out of seven dogs) of the MCD positive dogs were affected bilaterally. Results demonstrated that radiography has no value in the diagnosis of incipient MCD, without presence of secondary degenerative joint changes. CT is a more reliable tool to detect the disease, and MCD was diagnosed as early as 14 weeks of age. On CT, incipient MCD was found at the base of the MCP without extending towards the apex of the MCP. Ulnar subtrochlear sclerosis, one of the most important indicators for MCD, must be regarded as a secondary degenerative change since none of the MCD-positive dogs in this longitudinal study (till the age of 27 weeks) showed evidence of ulnar subtrochlear sclerosis.

The studies in **Chapter 5** explored the diagnostic value of the plasma and synovial collagenase-generated biomarker of cartilage, i.e. Col2-3/4C$_{\text{long mono}}$ (C2C), as an early marker of incipient MCD. The results of these studies indicated that this biomarker is not sensitive enough to detect incipient MCD. In the same chapter, studies showed that cartilage constituents in the daily ration given to dogs did not affect the results of the C2C biomarker in plasma and urine.

The second aim of this thesis was to try to elucidate the pathogenesis of MCD to provide a foundation for the interpretation of the molecular genetic studies performed by others.

The studies described in **Chapter 6** aimed to assess both the articular cartilage and subchondral bone of the MCP by using the non-destructive equilibrium partitioning of an ionic contrast agent with microCT. There was a significant depletion of glycosaminoglycan (GAG) in articular cartilage in dogs with incipient MCD, as reflected by the mean radiodensity measured with microCT, of the segmented articular cartilage, without concurrent evidence of an osteoporotic or osteosclerotic MCP. The lack of significant differences in denstity of the subchondrol bone between dogs with MCD and dogs with a normal MCP, suggests that MCD starts in the deeper layers of the articular cartilage and expands to the underlying subchondral bone. Whether or not the depletion of GAG is the key to the development of MCD, however, could not be concluded due to the fact that this study was performed at a single time point.

In **Chapter 7,** the postnatal development of the antebrachia and elbow joints was investigated. From the age of 6 or 7 weeks till 16 or 17 weeks radiography and CT were performed every two weeks. There was no difference between the MCD-affected and MCD-negative dogs in this study in the rate of ossification of secondary ossification centers. There was no evidence that radial angular deformities or joint incongruity played a role in the development of MCD in these dogs.

The studies in **Chapter 8** describe the evidence of delayed endochondral ossification in the development of MCD in Labrador retrievers, and in particular delayed calcification in the calcifying zone. The retained hyaline cartilage may ultimately ossify during MCD progression, but weaker points might also develop into cracks between the retained hyaline cartilage and the subchondral bone. Increased pressure or shearing forces during joint movement might lead to detachment of the lateral aspect of the MCP. In the same chapter, the reorganization of articular cartilage and subchondral bone was studied in Labrador retrievers before the age of 14 weeks and the results showed that cartilage canals containing vascular networks were no longer present in articular cartilage in 12-week-old dogs.

Conclusion

In dogs where secondary joint changes due to MCD have not yet developed, CT is a much more reliable diagnostic tool than radiography. In the population of purpose bred Labrador retrievers the lesion commenced at the base of the MCP. It is very well imaginable that contact or shear forces in the radioulnar joint may advance or initiate the lesion. Histologically a delay of endochondral ossification was demonstrated in the subchondral bone at the base of the MCP. The GAG-content in the articular cartilage, covering the subchondral bone with delayed mineralisation was diminished, which may be the cause or the consequence of MCD. Whether delayed mineralisation is in concordance with a lack of cartilage GAG-content should be subject for further studies.

Samenvatting

Het afwijkend processus coronoideus medialis van de ulna, de meest voorkomende vorm van elleboogdysplasie bij Labrador retrievers, is de afgelopen 40 jaar onderwerp geweest van veel publicaties. De eerste tekenen van kreupelheid ten gevolge van deze aandoening kunnen al op een leeftijd van drie maanden optreden, maar ook pas op een leeftijd van zes jaar of zelfs ouder. De meest voorkomende klinische verschijnselen die bij het afwijkend mediaal coronoïd optreden zijn kreupelheid, een stijve gang ten gevolge van een verkorte staplengte en geringe supinatie en abductie van de betreffende voorpoot. Tijdens het orthopedisch onderzoek kan een overvuld ellebooggewricht worden waargenomen dat crepiteert en pijnlijk is tijdens passieve bewegingen van dat gewricht. Bij de Labrador retriever, het ras dat het meest gebruikt wordt voor blindengeleide- of hulphond, is het afwijkend mediaal coronoïd als erfelijke afwijking een bron van grote zorg.

In een overzicht worden in **hoofdstuk 2** verschillende aspecten van het afwijkend mediaal coronoïd belicht, zoals de normale postnatale ontwikkeling van het processus coronoideus medialis ulnaris, de verschillende vormen van afwijkend mediaal coronoïd, de gangbare hypothesen met betrekking tot de etiopathogenese van het afwijkend mediaal coronoïd en de technieken om de diagnose afwijkend mediaal coronoïd te kunnen stellen. Ondanks uitgebreid onderzoek naar deze aandoening is er geen diagnostische techniek waarmee een afwijkend mediaal coronoïd definitief kan worden aangetoond of uitgesloten, en de etiopathogenese is nog niet opgehelderd.

De eerste doelstelling van dit promotieonderzoek was het bestuderen van rasspecifieke kenmerken van het gevorderde en beginnende afwijkend mediaal coronoïd bij Labrador retrievers met behulp van röntgenologisch en computertomografisch (CT) onderzoek en bij onderzoek tijdens operatie of bij sectie.

In **hoofdstuk 3** worden studies beschreven die werden uitgevoerd bij een groep van 31 Labrador retrievers die leden aan een gevorderd stadium van het afwijkend mediaal coronoïd. In dit stadium is de röntgenologische diagnose meestal gebaseerd op de secundaire regeneratieve en degeneratieve veranderingen zoals sclerose van het subtrochleare gebied van de ulna, een vage belijning van de voorrand of een stompe vorm van het processus coronoideus medialis en de vorming van periarticulaire osteofyten. Fragmentatie van het processus coronoideus medialis was de meest voorkomende bevinding bij CT. Bij honden die voor het eerst kreupelheid vertoonden op een leeftijd van 12 maanden of jonger, werd bij artroscopisch onderzoek vooral een verplaatst los

fragment van het processus coronoideus medialis gevonden. Honden waarbij de eerste kreupelheid op volwassen leeftijd (ouder dan 12 maanden) optrad, vertoonden bij artroscopisch onderzoek het meest frequent abnormaal zacht bot en kraakbeen (*osteochondromalacie*) van het processus coronoideus medialis. Er waren duidelijk verschillende verschijningsvormen van het afwijkend mediaal coronoïd in de twee leeftijdsgroepen en aangezien de etiopathogenese van deze aandoening niet precies bekend is, kan de mogelijkheid dat hier sprake is van twee verschillende ziektemechanismen bij deze leeftijdsgroepen niet worden uitgesloten. Sclerose van het subtrochleare gebied van de ulna is hoogstwaarschijnlijk een gevolg en niet de oorzaak van een afwijkend mediaal coronoïd en berust op een toegenomen botdichtheid van de mergholte van de ulna. De afwezigheid van sclerose van het subtrochleare gebied van de ulna kan niet worden gebruikt om een afwijkend mediaal coronoïd uit te sluiten. Een gedegen lichamelijk onderzoek en anamnese blijven essentieel voor het stellen van de juiste diagnose.

In **hoofdstuk 4** worden de resultaten beschreven van het longitudinaal onderzoek van twee nesten Labrador retrievers die speciaal voor dit onderzoek gefokt werden uit ouderdieren met een afwijkend mediaal coronoïd. Vijftig procent van de gefokte pups (7 van de 14 honden) werd als positief voor een afwijkend mediaal coronoïd beoordeeld op basis van de resultaten van microCT en histologisch onderzoek. Zesentachtig procent (6 van 7 honden) van de honden met een afwijkend mediaal coronoïd was beiderzijds aangedaan. Röntgenologisch onderzoek was voor de diagnostiek van het afwijkend mediaal coronoïd in een zeer vroeg stadium, waarbij er nog geen secundaire degeneratieve gewrichtsafwijkingen zichtbaar zijn, van geen waarde. CT is een meer betrouwbare onderzoeksmethode om het afwijkend mediaal coronoïd vast te stellen: het afwijkend mediaal coronoïd kon al op de leeftijd van 14 weken worden aangetoond. Met CT werd in het beginstadium van het afwijkend mediaal coronoïd een gemineraliseerd botfragment aan de basis van het processus coronoideus medialis gezien, dat zich niet uitstrekte tot de punt van het processus coronoideus medialis. Sclerose van de mergholte van de ulna, één van de belangrijkste indicatoren voor de aanwezigheid van het afwijkend mediaal coronoïd, moet als secundaire degeneratieve verandering beschouwd worden, want het werd bij geen van de pups met afwijkend mediaal coronoïd in deze longitudinale studie (van de leeftijd van 6 tot 17 weken) aangetroffen.

In **hoofdstuk 5** wordt het onderzoek beschreven naar de diagnostische waarde van de bepaling van Col2-3/4C$_{long\ mono}$ (C2C), een biologische indicator van kraakbeenafbraak, in bloedplasma en in gewrichtsvloeistof, als detectiemethode van het beginnend afwijkend

mediaal coronoïd. De resultaten van deze studie toonden aan dat de biomarker niet met voldoende gevoeligheid een beginnende vorm van afwijkend mediaal coronoïd kon detecteren. In deze studie werd aangetoond dat kraakbeen in de voeding van honden de resultaten van concentratie van Col2-3/4$C_{long\ mono}$ in plasma en urine van deze honden niet beïnvloedt.

De tweede doelstelling van dit promotieonderzoek was het ophelderen van de pathogenese van het afwijkend mediaal coronoïd om zo een basis te leggen voor de interpretatie van moleculair genetisch onderzoek dat elders wordt verricht naar het afwijkend mediaal coronoïd.

Het onderzoek dat in **hoofdstuk 6** wordt beschreven, behelst een studie van het gewrichtskraakbeen en het onderliggend bot van het processus coronoideus medialis, waarbij gebruik werd gemaakt van de niet-destructieve evenwichtstoestand van een ionische contrastvloeistof in het kraakbeen die zichtbaar gemaakt werd met behulp van microCT. Er was een significante afname van glycosaminoglycanen (GAG) in het gewrichtskraakbeen bij beginnend afwijkend mediaal coronoïd, zoals weerspiegeld in de gemiddelde röntgendichtheid, gemeten met microCT, van het gesegmenteerde gewrichtskraakbeen, zonder significante veranderingen van de dichtheid en remodellering van het subchondrale bot van het processus coronoideus medialis. Het ontbreken van significante verschillen in de dichtheid van het subchondrale bot tussen honden met een afwijkend mediaal coronoïd en honden met een normaal mediaal coronoïd wekt de suggestie dat een afwijkend mediaal coronoïd begint in de diepere lagen van het gewrichtskraakbeen en zich uitbreidt naar het onderliggende subchondrale bot. Omdat de ellebogen slechts op één tijdstip onderzocht konden worden, kon niet worden vastgesteld of de afgenomen GAG concentratie in het gewrichtskraakbeen een sleutelrol speelt in het ontstaan van het afwijkend mediaal coronoïd.

In **hoofdstuk 7** wordt de postnatale ontwikkeling van de antebrachia en de ellebooggewrichten beschreven. Vanaf de leeftijd van 6 of 7 weken tot de leeftijd van 16 of 17 weken werd elke twee weken röntgenologisch en CT-onderzoek verricht. Er bleek tussen de honden met en die zonder het afwijkend mediaal coronoïd geen verschil te zijn in de ontwikkelingssnelheid van de secundaire ossificatiecentra. Er waren geen aanwijzingen dat standsafwijkingen van het antebrachium of incongruenties van het ellebooggewricht een rol speelden in de ontwikkeling van het afwijkend mediaal coronoïd bij deze honden.

In **hoofdstuk 8** worden de studies beschreven die het bewijs leverden dat een vertraagde endochondrale ossificatie een rol speelt in de ontwikkeling van het afwijkend mediaal coronoïd bij Labrador retrievers, waarbij in het bijzonder een vertraagde calcificatie optreedt van het gebied van de mineralisatiezone van het kraakbeen. Het niet-gemineraliseerde kraakbeen kan gedurende de ontwikkeling van het afwijkend mediaal coronoïd uiteindelijk verbenen, maar op zwakke plaatsen zouden zich scheurtjes kunnen vormen tussen het achtergebleven kraakbeen en het onderliggend subchondrale bot. Verhoogde druk- of schuifkrachten gedurende gewrichtsbeweging zouden kunnen leiden tot loslaten van het laterale vlak van het processus coronoideus medialis. In hetzelfde hoofdstuk werd de reorganisatie van het gewrichtskraakbeen en het subchondrale bot bestudeerd bij Labrador retrievers tot een leeftijd van 14 weken en de resultaten toonden aan dat de kraakbeenkanaaltjes, waarin bloedvaten verlopen tijdens de vroege ontwikkeling, niet meer aanwezig waren in het gewrichtskraakbeen van 12 weken oude pups.

Conclusie

Bij honden waarbij secundaire gewrichtsveranderingen ten gevolge van het afwijkend mediaal cornoïd nog niet ontstaan zijn is CT een meer waardevolle diagnostische techniek dan röntgenologisch onderzoek. In de populatie van speciaal voor dit onderzoek gefokte Labrador retrievers begon de laesie aan de basis van het processus coronoideus medialis. Het is heel goed voorstelbaar dat contact of schuifkrachten in het radio-ulnaire gewricht de laesie kan doen toenemen of doen ontstaan. Histologisch werd een vertraagde endochondrale ossificatie in het subchondrale bot aan de basis van het processus coronoideus medialis aangetoond. Het GAG-gehalte in het gewrichtskraakbeen dat het subchondrale bot bedekt waarvan de mineralisatie was vertraagd, was afgenomen. Of de vertraagde endochondrale mineralisatie verband houdt met een gebrek aan GAG in het kraakbeen moet nog nader worden onderzocht.

Ringkasan

Penyakit medial koronoid, merupakan komponen penyakit siku yang paling kerap didiagnosis dalam baka anjing Labrador retrievers dan telah menjadi subjek penerbitan dalam tempoh empat dekad yang lalu. Tanda-tanda pertama kepincangan yang berkaitan dengan penyakit medial koronoid boleh berlaku seawal-awalnya semasa berumur tiga bulan, atau selewat-lewatnya berumur lebih tua daripada enam tahun. Tanda-tanda klinikal yang paling kerap dibentangkan adalah kepincangan, gaya berjalan yang keras atau kaku disebabkan pergerakan langkah yang pendek, dan supinasi dan abduksi kaki hadapan yang terjejas. Semasa pemeriksaan ortopedik, cairan sendi, crepitus, dan tindak balas kesakitan semasa manipulasi sendi boleh diperhatikan. Labrador retriever merupakan baka utama yang digunakan sebagai anjing panduan untuk orang buta dan anjing bantuan untuk orang kurang berupaya, maka penyakit medial koronoid adalah penyakit warisan yang menjadi kebimbangan utama.

Pelbagai aspek penyakit medial koronoid dikaji di dalam **Bab ke-2**, seperti perkembangan medial cuaran koronoid yang normal selepas dilahirkan, manifestasi penyakit yang berbeza daripada penyakit medial koronoid, hipotesis mengenai etiopathogenesis daripada penyakit medial koronoid yang diterima umum, dan teknik-teknik yang digunakan untuk mendiagnosis penyakit medial koronoid. Walaupun penyelidikan yang banyak sudah dilaksanakan, tidak ada alat diagnostik untuk mendiagnosis penyakit medial koronoid secara muktamad, dan etiopathogenesis masih perlu dijelaskan.

Matlamat utama projek ini adalah untuk mengkaji ciri-ciri tertentu untuk baka Labrador retriever dengan menggunakan radiografi, tomografi berkomputer (CT), dan pemeriksaan semasa pembedahan atau bangkai.

Dalam kajian yang dinyatakan di dalam **Bab ke-3**, sebanyak 31 Labrador retrievers yang mengalami penyakit medial koronoid telah dikaji. Pada peringkat ini, diagnosis radiografi kebiasaannya berdasarkan perubahan degeneratif dan regeneratif seperti ulnar subtrochlear sclerosis, kabur pada pinggir MCP, dan osteophytes dekat peri-artikular. Pemecahan medial cuaran koronoid adalah keputusan CT yang paling kerap. Penemuan anjing dengan tanda awal kepincangan pada usia muda, iaitu ≤12 bulan, serpihan medial cuaran koronoid adalah penemuan yang paling kerap dengan menggunakan artroskopi. "Osteochondromalacia" adalah keputusan artroskopi yang paling lazim ditemui pada anjing dengan aduan pertama kepincangan bermula pada usia yang matang, iaitu >12 bulan. Manifestasi penyakit penyakit medial koronoid jelas berbeza di antara kedua-dua

kumpulan umur dan tanpa mengetahui etiopathogenesis yang tepat, kemungkinan bahawa terdapat dua mekanisme penyakit yang berbeza yang terlibat dalam kumpulan umur yang berbeza tidak boleh dikecualikan. Ulnar subtrochlear sclerosis kemungkinan besar adalah disebabkan oleh penyakit medial koronoid dan bukan punca penyakit medial koronoid, dan berdasarkan kepada kepadatan tulang yang meningkat dalam sumsum ulna. Ketiadaan ulnar subtrochlear sclerosis tidak boleh digunakan untuk mengecualikan penyakit medial koronoid. Pemeriksaan fizikal yang menyeluruh dan sejarah pesakit kekal penting bagi tujuan diagnosis.

Dalam **Bab ke-4**, kejadian penyakit medial koronoid dalam dua seperindukan Labrador retrievers, yang lahir dari baka induk yang mengalami penyakit medial koronoid telah dikaji. Lima puluh peratus daripada anak-anak anjing ini (7 daripada 14) telah dianggap sebagai penyakit medial koronoid positif berdasarkan gabungan keputusan pemeriksaan bangkai dan pemeriksaan microCT. Lapan puluh enam peratus (enam daripada tujuh) anak anjing yang positif penyakit medial koronoid didapati terjejas dua kaki hadapan. Keputusan menunjukkan bahawa radiografi tidak mempunyai nilai dalam mendiagnosis penyakit medial koronoid pada peringkat awal, tanpa sebarang kehadiran perubahan degeneratif. CT adalah alat yang lebih dipercayai untuk mengesan penyakit, dan penyakit medial koronoid boleh didiagnosis seawal-awalnya pada umur 14 minggu. Untuk CT, penyakit medial koronoid pada peringkat awal ditemui di pangkal MCP tanpa ke arah puncak medial cuaran koronoid. Ulnar subtrochlear sclerosis, merupakan salah satu petunjuk yang paling penting untuk penyakit medial koronoid, dan sepatutnya dianggap sebagai perubahan degeneratif memandangkan tiada anjing-anjing yang positif penyakit medial koronoid di dalam kajian ini (sehingga umur 27 minggu) yang menunjukkan tanda-tanda/bukti sclerosis pada ulnar subtrochlear.

Kajian dalam **Bab ke-5** adalah mengenai nilai diagnostik biomarker collagenase dalam plasma dan sinovia, iaitu Col2-3/4Clong mono (C2C), sebagai petanda awal penyakit medial koronoid. Keputusan kajian ini menunjukkan bahawa penanda biomarker ini tidak cukup sensitif untuk mengesan penyakit medial koronoid pada peringkat awal. Di dalam bab yang sama, kajian juga menunjukkan bahawa tambahan rawan dalam makanan harian yang diberikan kepada anjing tidak menjejaskan keputusan C2C dalam plasma dan air kencing.

Kajian yang dinyatakan dalam **Bab ke-6** adalah bertujuan untuk menilai kedua-dua rawan artikular dan tulang subchondral daripada medial cuaran koronoid dengan menggunakan microCT. Terdapat kekurangan glycosaminoglycan (GAG) dalam rawan

artikular pada anjing yang dijejas/mengidap penyakit medial koronoid pada peringkat awal, seperti yang ditunjukkan oleh radiodensity min yang diukur dengan microCT, tanpa bukti yang serentak daripada medial cuaran koronoid osteoporosis atau osteosclerotic. Kekurangan perbezaan yang signifikan dalam ketumpatan mineral tulang subchondrol antara anjing dengan penyakit medial koronoid dan anjing dengan medial cuaran koronoid normal, menunjukkan bahawa penyakit medial koronoid bermula pada lapisan rawan artikular dan mengembang ke tulang subchondral asas. Sama ada atau tidak kekurangan GAG adalah kunci kepada kejadian penyakit medial koronoid, kesimpulan tidak dapat dibuat memandangkan kajian ini telah dilakukan pada satu titik masa tunggal.

Dalam **Bab ke-7**, pertumbuhan antebrachia dan sendi siku selepas dilahirkan telah dikaji. Dari umur 6 atau 7 minggu sehingga 16 atau 17 minggu, radiografi dan CT telah dijalankan setiap dua minggu. Tiada perbezaan didapati di antara anijng yang dijejaskan oleh penyakit medial koronoid dan anjing yang negatif penyakit medial koronoid dalam kajian ini, samada pada kadar osifikasi atau pertumbuhan pusat osifikasi. Tiada bukti bahawa kecacatan sudut jejari atau kejanggalan tulang memainkan peranan dalam kejadian penyakit medial koronoid dalam anjing.

Kajian dalam **Bab ke-8** menerangkan bukti pembentukan osifikasi yang lambat dalam kejadian penyakit medial koronoid pada Labrador retrievers, dan khususnya kalsifikasi lambat dalam zon calcifying. Rawan yang terjejas akhirnya boleh menjadi tulang semasa kejadian penyakit medial koronoid, tetapi titik/tempat yang lemah juga berupaya untuk retak di antara rawan dan tulang subchondral. Peningkatan tekanan semasa pergerakan sendi mungkin membawa kepada pemisahan medial cuaran koronoid. Di dalam bab yang sama, penyusunan semula rawan artikular dan tulang subchondral telah dikaji pada Labrador retrievers sebelum umur 14 minggu dan keputusan menunjukkan bahawa canal rawan tidak lagi mengandungi rangkaian vaskular pada anjing berumur 12 minggu.

Kesimpulan

Pada anjing yang terjejas penyakit medial koronoid pada peringkat awal, CT adalah alat yang lebih dipercayai daripada diagnostik radiografi. Pada baka Labrador retrievers penyakit bermula di pangkal medial cuaran koronoid. Ia adalah sangat mudah untuk dibayangkan bahawa hubungan atau daya ricih di dalam sendi radioulnar boleh mencepatkan atau memulakan penyakit. Histologi kelewatan osifikasi endokondral ditunjukkan dalam tulang subchondral di dasar medial cuaran koronoid. Kandungan GAG di lapisan rawan artikular, yang meliputi tulang subchondral dengan kadar mineralisasi

yang lambat adalah berkurangan, juga boleh menjadi punca atau akibat daripada penyakit medial koronoid. Sama ada kadar mineralisasi subchondral yang lambat adalah dalam konkordans dengan kekurangan kandungan-GAG pada rawan haruslah tertakluk untuk kajian selanjutnya.

Acknowledgements & Curriculum vitae

Acknowledgements

In order to make this dissertation possible, many people have contributed to its production. I owe my gratitude to all of you and because of you, my graduate experience has been one that I will cherish forever.

I would like to express the deepest appreciation to my promoters, Prof. dr. G.Voorhout and Prof. dr. H.A.W. Hazewinkel. I have been extremely fortunate to have both of you for giving me the freedom to explore on my own, taught me how to question critically and express ideas. Your patience and support helped me to overcome many obstacles. I would like to thank Dr. C.F. Wolschrijn and Dr. M.A. Tryfonidou as well for your kindness and support. Your insightful comments, remarks and advices inspired me through these years. Without your persistent help and guidance, completion of the studies in this thesis would not have been possible.

Susanne, AJ, Eldo, Stephanie, Leonie, Kim, Martijn, Federico, Elise, Monique, Joris, Joost, Chantal, Marjolijn, Anke, Hans, Marieke and everyone in the Division of Diagnostic Imaging. Thank you for your encouragements and technical support these years. The positive and cheerful energy in the division guided me through my saddest moments and difficult times. I appreciate every short discussions and sharing that we had. Harry, Zwanie, Inge and Hans, i appreciate your help during my studies.

Ronald, Annette, Guy, Henk, and everyone from the Department of Pathobiology of the Faculty of Veterinary Medicine. Thank you for your suggestion/input and help during my histological studies. I have been privileged enough to work with all of you and it was indeed a wonderful experience. Rob, Joop and Lindsay, thank you for helping me in taking nice pictures for my manuscripts. Hans, i am grateful that your door was always open to discuss statistical problems. Thank you for leading me in solving the problems and making the publications possible.

Furthermore I would also like to acknowledge with much appreciation the crucial role of everyone in the Department of Orthopedic Surgery, Erasmus Medical Center, Rotterdam, and Eindhoven University of Technology who provided me an excellent technical and moral support. I appreciate that you gave me the permission to use all required equipment and the necessary materials to complete all my studies.

A special thanks goes to my friends and office mates, who help me to assemble the parts

and gave suggestion whenever I have lost myself. Ineke, Chalika, Ja, Ronald, Luc, HJ, Niklas, Frank, Kim, Jeannette, Adri and everyone, thank you for your sharing and caring these years. Last but not least, many thanks go to the staff of the Bureau of International Contacten (BIC) for your help. Dr. Paling, Rosita, Adja, and Marian, I got a very warm welcome during my stay in The Netherlands.

Most importantly, none of this would have been possible without the love and patience of my family and friends in Malaysia. Your support and care helped me overcome setbacks and stay focused on my graduate study. I deeply appreciate your belief in me.

Special thanks also go to Prof. Zamri, Prof. Bashir, Prof. Hair, Dr. Hassan, Dr. Rosnina, Dr. Jalila, and Dr. Gurmeet from the Faculty of Veterinary Medicine, UPM, who has supported me in persuaing my graduate study. Finally, I appreciate the financial support from the Ministry of Higher Education and Universiti Putra Malaysia that funded my graduate study in The Netherlands.

My apologies if I have forgotten to mention someone, I truly appreciate all of you.

"Without you nothing is possible.
With you, nothing is impossible."

Curriculum vitae

The author was born on 22 December 1979, in Sarikei, Malaysia. She attended secondary school at S.M.K. Simanggang, Sri Aman and graduated in 1996. She studied Veterinary Medicine in Faculty of Veterinary Medicine, Universiti Putra Malaysia (UPM) and graduated in 2003. After graduated from the veterinary school, she worked as a small animal practitioner in a private clinic. In 2005, she joined the University Veterinary Hospital (UVH), UPM, as a veterinary officer for 4 years before she was assigned to be a staff member of the Department of Veterinary Clinical Studies, Faculty of Veterinary Medicine, UPM in 2009. She was then granted the scholarship from the Ministry of Higher Education, Malaysia in 2009 and began her journey as a PhD candidate in the Department of Clinical Sciences of Companion Animal of the Faculty of Veterinary Medicine, Utrecht University.

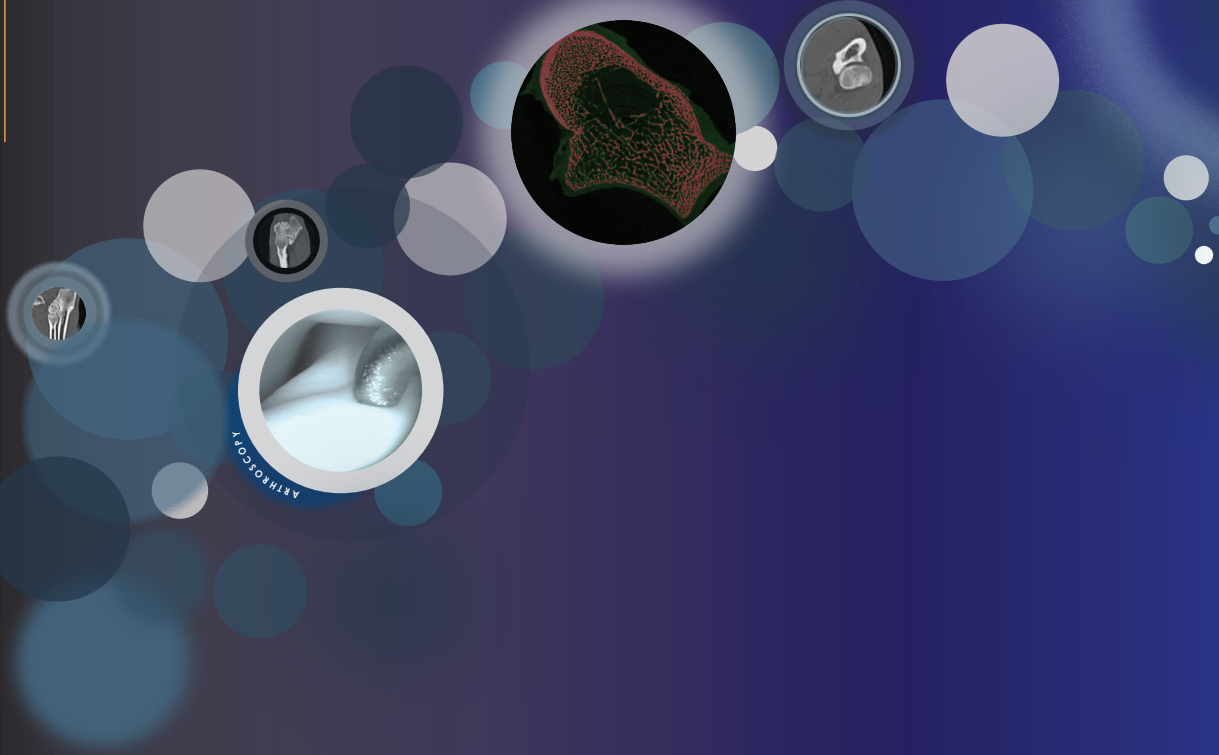
ARTHROSCOPY